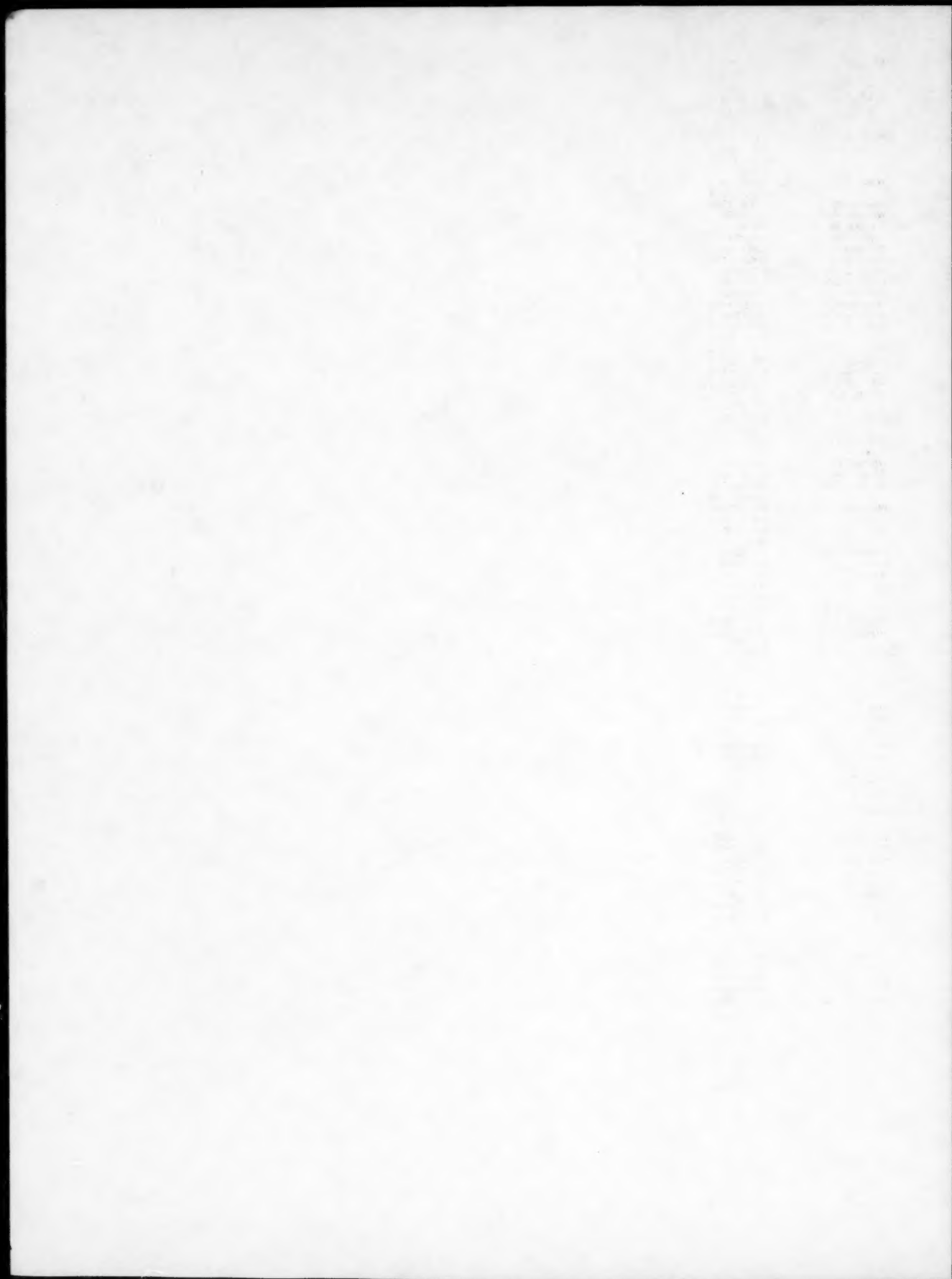






Vivès, Ch.	227-235B
Voice, W.E.	377-384B
Voorhees, P.W.	511-520A
	337-347A
Wade, H.	1479-1490A
	815-822B
	1355-1357A
	303-312B
Wade, T.	109-114A
	1355-1357A
Wadsworth, J.	2319-2332A
Wagoner, R.H.	421-425A
Wallace, W.	2068A
Walls, H.A.	267-274A
Walqui, H.	339-344B
Wang, J.-W.	1663-1670A
Wang, Z.	873-880A
Warren, G.W.	715-724B
Was, G.S.	349-359A
Waterstrat, R.M.	1943-1949A
Watkinson, A.P.	763-774B
Wayman, C.M.	1567-1579A
	1581-1597A
Weatherly, G.C.	1363-1369A
Weber, D.-J.	263-275B
Weertman, J.	2231-2236A
Wei, R.P.	2039-2050A
Weinberg, F.	355-357B
	367-375B
	823-829B
	595-604B
Welsch, G.	1831-1834A
West, R.	693A
White, C.L.	651-660A
Wiese, J.W.	203-209B
Williams, D.B.	686-690A
	1203-1211A
Williams, J.C.	1983-1995A
	739-751A
	753-760A
	987A
Williams, R.O.	929-933A
Wilson, R.D.	847-849B
Won, S.	163-168B
	645-662B
	831-839B
Woodward, R.L.	2031-2037A
Woychik, C.G.	1353-1354A
Wright, R.N.	881-890A
	891-895A
Wynnyckyj, J.R.	345-353B
Xiang, C.	785-792B
Xue, T.	455-463B
Yan, B.	1151-1157A
Yanagisawa, O.	667-673A
Yang, A.J.	471-474A
Yang, D.Z.	1385-1392A
Yang, S.	785-792B
Yang, S.W.	661-665A
Yank, D.Z.	1523-1526A
Yao, P.C.	41-46B
Yerebakan, M.	1687-1689A
Yi, J.J.	1237-1245A
Yoo, M.H.	651-660A
Yoon, D.N.	923-928A
Yoon, G.W.	2072-2073A
Yörük, S.	425-432B
Yu, J.	1325-1331A
	1671-1681A
Zaiken, E.	1467-1477A
Zevin, L.	167-171A
Zhang, T.-Y.	1649-1653A
	1655-1662A
Ziaai-Mosayyed, A.A.	1069-1076A





## Combined Subject Index

- Absorbance**  
See Absorptivity
- Absorbing**  
See Absorptivity
- Absorbance**  
See Absorptivity
- Absorption (energy)**  
Absorption of CO<sub>2</sub> Laser Beam by AISI 4340 Steel. 853-856B
- Absorption (material)**  
The Kinetics of the Nitrogen Reaction With Liquid Iron—Sulfur Alloys. 551-559B
- Absorption coefficient**  
See Absorption (energy)
- Absorptivity, Coating effects**  
The Use of Palladium to Obtain Reproducible Boundary Conditions for Permeability Measurements Using Galvanostatic Charging. 715-719A
- Accelerated tests**  
See Huey test
- Acid cleaning**  
Studies on the Analysis of Hydrogen in High Strength Steels. 1694-1695A
- Acid leaching**  
See also Sulfuric acid leaching  
The Leaching of Hematite in Acid Solutions. 23-30B  
The Kinetics of Dissolution of Sphalerite in Ferric Chloride Solution. 413-424B  
Water and Solute Activities of H<sub>2</sub>SO<sub>4</sub>—Fe<sub>2</sub>(SO<sub>4</sub>)<sub>3</sub>—H<sub>2</sub>O and HCl—FeCl<sub>3</sub>—H<sub>2</sub>O Solution Systems: I.—Activities of Water. 433-439B
- Acid resistance tests**  
See Huey test
- Acids (inorganic)**  
See Inorganic acids
- Actinide metals**  
See Uranium
- Activation energy**  
Mobility of Martensitic Interfaces. 1713-1722A  
Mobility of the  $\beta_1/\gamma_1$  Martensitic Interface in Cu—Al—Ni. I.—Experimental Measurements. 1723-1734A
- Activity (chemical)**  
Activities of Arsenic, Antimony, Bismuth and Lead in Copper Matrices. 129-141B  
Effect of Arsenic on the Activity of Oxygen Dissolved in Dilute Liquid Copper Solutions. 339-344B
- Activity (chemical), Composition effects**  
Thermodynamic Properties of S—Fe—Co—Ni and Fe—Co—Ni Systems. 907-911A
- Activity coefficients**  
See Activity (chemical)
- Additives**  
See Master alloys
- Adhesion, Alloying effects**  
Reactive Element—Sulfur Interaction and Oxide Scale Adherence. 1164-1166A
- Adhesivity**  
See Adhesion
- Age hardening**  
See Precipitation hardening
- Age hardening steels**  
See Precipitation hardening steels
- Aging**  
See Aging (artificial)  
Strain aging
- Aging (artificial)**  
Mechanical Properties of Nitrogen—Ferrite. 45-50A  
Effect of Single Aging on Microstructure and Impact Property of INCONEL X-750. 821-829A  
Crystallography and Tempering Behavior of Iron—Nitrogen Martensite. 1371-1384A  
Cellular Decomposition in a Cu—25Ni—15Co Side-Band Alloy. 1751-1757A  
The Role of Aging Reactions in the Hydrogen Embrittlement Susceptibility of an HSLA Steel. 1879-1886A  
Observations of Adiabatic Shear Band Formation in 7039 Aluminum Alloy. 1900-1903A  
Discussion of "Effect of Retrogression and Reaging Treatments on the Microstructure of Al-7075-T651". 2068A
- Agitation**  
See Electromagnetic stirring
- Air, Environment**  
The Effect of Environment on the Sustained Load Crack Growth Rates of Forged Waspaloy. 1515-1521A
- Aircraft components**  
Thermally Induced Porosity in Ti—6Al—4V Prealloyed Powder Compacts. 1528-1531A
- Aircraft equipment**  
See Aircraft components
- Alkali metal compounds**  
See Lithium compounds  
Sodium chloride  
Sodium hydroxide
- Alkali metals**  
See Lithium
- Alkaline earth metal alloys**  
See Magnesium base alloys
- Alkaline earth metal compounds**  
See Calcium compounds  
Lime  
Magnesium oxide
- Alkaline earth metals**  
See Beryllium  
Calcium  
Magnesium
- Alkaline leaching**  
See Ammonia pressure leaching
- Allotropic transformation**  
A Shear-Type Allotropic Transformation in Alumina. 345-353B  
Discussion of "The Bainite Transformation in a Silicon Steel" and Authors' Reply. 457-468A
- Alloy powders, Fabrication**  
Laser-Melting/Spin-Atomization Method for the Production of Titanium Alloy Powders. 1897-1900A
- Alloy steels**  
See Austenitic stainless steels  
Chromium molybdenum steels  
Chromium steels  
Electrical steels  
Ferritic stainless steels  
High strength low alloy steels  
High strength steels  
Low alloy steels  
Manganese steels  
Molybdenum steels  
Nickel chromium molybdenum steels  
Nickel chromium steels  
Nickel molybdenum steels  
Nickel steels  
Precipitation hardening steels  
Silicon manganese steels  
Silicon steels  
Stainless steels
- Alloying**  
See Surface alloying
- Alloys**  
See Dispersion hardening alloys  
Ferrous alloys  
Master alloys  
Precipitation hardening alloys  
Superalloys
- Alpha annealing**  
See Annealing
- Alpha iron, Mechanical properties**  
Effect of Hydrogen on the Young's Modulus of Iron. 1655-1662A
- Alphatizing**  
See Annealing
- Alumina**  
See Aluminum oxide
- Aluminates**  
Applicability of Central Atoms Models to Binary Silicate and Aluminate Melts. 325-331B
- Aluminates, Environment**  
Stress Corrosion Cracking of Carbon Steel in Caustic Aluminate Solutions—Crack Propagation Studies. 979-986A
- Aluminates, Thermal properties**  
The Utilization of Galvanic Cells Using Ca Beta Double Prime—Alumina Solid Electrolytes in a Thermodynamic Investigation of the CaO—Al<sub>2</sub>O<sub>3</sub> System. 107-112B
- Aluminum, Alloying elements**  
Grain Boundary Fracture of L<sub>12</sub> Type Intermetallic Compound Ni<sub>3</sub>Al. 441-443A
- Aluminum, Bonding**  
Pressure Effects in Multiphase Binary Diffusion Couples. 605-611A
- Aluminum, Casting**  
Metal/Mold Interfacial Heat Transfer. 585-594B
- Aluminum, Coatings**  
Microstructural Investigation of Intermediate Phase Formation in Uranium—Aluminum Diffusion Couples. 589-595A
- Aluminum, Composite materials**  
The Effects of Hot Pressing Parameters on the Strength of Aluminum/Stainless Steel Composites. 623-628A
- Aluminum, Crystal growth**  
Heterogeneous Nucleation Model of Twinned Crystal Growth From the Melt. 680-692A

## Aluminum

- Aluminum, Crystal lattices**  
Impurity Effect on Cube Texture in Pure Aluminum Foils. 27-38A  
On the Relation Between Grain Size and Grain Topology. 2007-2011A
- Aluminum, Diffusion**  
Microstructural Investigation of Intermediate Phase Formation in Uranium—Aluminum Diffusion Couples. 589-595A
- Aluminum, Extraction**  
Determination of the Lithium Content of Molten Aluminum Using a Solid Electrolyte. 41-46B  
Interfacial Tension of Aluminum in Cryolite Melts. 333-338B  
Hydrolytic Stripping of Single and Mixed Metal—Versatic Solutions. 671-677B
- Aluminum, Mechanical properties**  
Tensile Stress—Strain Analysis of Cold Worked Metals and Steels and Dual-Phase Steels. 865-872A
- Aluminum, Phase transformations**  
Criterion for Predicting the Morphology of Crystalline Cubic Precipitates in a Cubic Matrix. 197-202A
- Aluminum, Structural hardening**  
Polycrystalline Strengthening. 2167-2190A
- Aluminum, Ternary systems**  
Role of Alloying Elements in Phase Decomposition in Alnico Magnet Alloys. 179-185 ;  
Phase Equilibria in the Ni—Al—Ti System at 1173K. 319-322A
- Aluminum, Welding**  
Fundamental Aspects of Formation and Stability of Explosive Welds. 841-852A
- Aluminum base alloys, Casting**  
Mathematical Modeling of Porosity Formation in Solidification. 359-366B  
Experimental Study of Continuous Electromagnetic Casting of Aluminum Alloys. 377-384B  
Inverse Segregation. 595-604B  
Grain Refinement of Aluminum by TiC. 2065-2068A
- Aluminum base alloys, Composite materials**  
Mechanical Properties and Failure Characteristics of FP/Aluminum and W/Aluminum Composites. 853-864A  
Analysis of Stress—Strain, Fracture, and Ductility Behavior of Aluminum Matrix Composites Containing Discontinuous Silicon Carbide Reinforcement. 1105-1115A
- Aluminum base alloys, Corrosion**  
Stress Corrosion Cracking of an Aluminum Alloy Under Compressive Stress. 1663-1670A
- Aluminum base alloys, Crystal growth**  
Coarsening Rate of Beta Precipitates in Al—11Mg Alloy. Cellular and Dendritic Growth. I.—Experiment. 709-713A  
Cellular and Dendritic Growth. II.—Theory. 1799-1805A  
1807-1814A
- Aluminum base alloys, Crystal lattices**  
On the Relation Between Grain Size and Grain Topology. 2007-2011A
- Aluminum base alloys, Diffusion**  
Inverse Segregation in Directionally Solidified Al—Cu—Ti Alloys With Equiaxed Grains. 579-587A
- Aluminum base alloys, Mechanical properties**  
Fatigue Crack Deflection and Fracture Surface Contact: Micromechanical Models. 249-260A  
Lithium-Containing Aluminum Alloys: Cyclic Fracture. 475-477A  
On the Development of Crack Closure and the Threshold Condition for Short and Long Fatigue Cracks in 7150 Aluminum Alloy. 1467-1477A  
The Embrittlement of Al—Zn—Mg and Al—Mg Alloys by Water Vapor. 1503-1514A  
Hill's Plastic Strain Ratio of Sheet Metals. 1531-1535A  
Observations of Adiabatic Shear Band Formation in 7039 Aluminum Alloy. 1900-1903A  
Superplastic Al—Cu—Li—Mg—Zr Alloys. 2319-2332A
- Aluminum base alloys, Melting**  
Examination of the Strength of Oxide Skins on Aluminum Alloy Melts. 47-51B  
Fluid Flow Phenomena in a Single Phase Coreless Induction Furnace. 227-235B
- Aluminum base alloys, Metal working**  
Effects of Plastic Anisotropy and Yield Surface Shape on Sheet Metal Stretchability. 629-639A
- Aluminum base alloys, Microstructure**  
Microstructure of Rapidly Solidified Laser Molten Al—4.5 wt.% Cu Surfaces. 149-161B  
Orientation Relationship Between Precipitated  $Al_3(Fe,Ni)_2$  Phase and Alpha-Aluminum. 683-686A  
The Microstructure of Rapidly Solidified  $Al_3Mn$ . 1005-1012A
- Aluminum base alloys, Phases (state of matter)**  
Microanalytical Study of the Heterogeneous Phases in Commercial Al—Zn—Mg—Cu Alloys. 1925-1936A  
Mössbauer Effect of Al—Fe—Si Intermetallic Compounds. 1937-1942A
- Aluminum base alloys, Powder technology**  
Effect of Cobalt Content on the Stress-Corrosion Cracking Behavior of 7091-Type Aluminum Powder Alloys. 945-951A  
The Development of Two Texture Variants and Their Effect on the Mechanical Behavior of a High Strength P/M Aluminum Alloy, X7091. 1089-1103A  
Explosive Consolidation of Rapidly Solidified Aluminum Alloy Powders. 1445-1455A
- Aluminum base alloys, Structural hardening**  
Work Hardening Correlations Based on State Variables in Some F.C.C. Metals in Monotonic Loading. 411-420A  
Experimental Observations on the Nucleation and Growth of  $\delta'$  ( $Al_3Li$ ) in Dilute Al—Li Alloys. 1203-1211A
- Discussion of "Effect of Retrogression and Reaging Treatments on the Microstructure of Al-7075-T651". 2068A  
Precipitation Hardening. 2131-216E ;
- Aluminum base alloys, Thermal properties**  
New Eutectic Alloys and Their Heats of Transformation. 323-328A
- Aluminum base alloys, Welding**  
Fluid Flow and Weld Penetration in Stationary Arc Welds. 203-213A  
Grain Structure and Solidification Cracking in Oscillated Arc Welds of 5052 Aluminum Alloy. 1345-1352A  
Alternating Grain Orientation and Weld Solidification Cracking. 1887-1896A
- Aluminum brasses, Microstructure**  
Lattice Image Studies on the Intervariant Boundary Structure and Substructure of Cu—Zn—Al 18R Martensite. 1551-1566A
- Aluminum bronzes, Casting**  
Metal/Mold Interfacial Heat Transfer. 585-594B
- Aluminum compounds**  
See also Aluminum oxide
- Aluminum compounds, Corrosion**  
Effect of Boron on the Corrosion Behavior of Polycrystalline  $Ni_3Al$ . 2072-2073A
- Aluminum compounds, Mechanical properties**  
Grain Boundary Fracture of  $L_{12}$  Type Intermetallic Compound  $Ni_3Al$ . 441-443A
- Aluminum oxide**  
See also Sapphire
- Aluminum oxide, Composite materials**  
Mechanical Properties and Failure Characteristics of FP/Aluminum and W/Aluminum Composites. 853-864A  
The Influence of Thermal Exposure on Interfacial Reactions and Strength in Aluminum Oxide Fiber Reinforced Magnesium Alloy Composites. 2069-2072A
- Aluminum oxide, Extraction**  
Sodium Aluminate Leaching and Desilication in Lime—Soda Sinter Process for Alumina From Coal Wastes. 707-713B
- Aluminum oxide, Phase transformations**  
A Shear-Type Allotropic Transformation in Alumina. 345-353B
- Aluminum oxide, Recovering**  
Sintering Kinetics and Alumina Yield in Lime—Soda Sinter Process for Alumina From Coal Wastes. 385-395B
- Aluminum oxide, Reduction (chemical)**  
Formation of Chlorinated Carbon Products During Carbochlorination Reactions. 847-849B
- Ammonia pressure leaching**  
Leaching of Chrysocolla With Ammonia—Ammonium Carbonate Solutions. 441-448B
- Amorphous materials**  
See also Metallic glasses
- Amorphous materials, Atomic properties**  
Dislocations in Amorphous Metals. 2227-2230A
- Amperage**  
See Electric current
- Amplifiers**  
See Lasers
- Analyzing**  
See Electron probe analysis  
Mathematical analysis  
Microanalysis  
Numerical analysis  
X ray diffraction  
X ray powder diffraction
- Andrade method**  
See Crystal growth
- Androforming**  
See Stretch forming
- Anelasticity**  
A Model for Anelastic Relaxation Controlled Cyclic Creep. 1117-1122A
- Annealing**  
See also Isothermal annealing  
Solution annealing  
Spheroidizing  
Austenitization During Intercritical Annealing of an Fe—C—Si—Mn Dual-Phase Steel. 1237-1245A  
Ferrite Recrystallization and Austenite Formation in Cold-Rolled Intercritically Annealed Steel. 1385-1392A  
Transmission Kossel Study of the Formation of  $\{110\}[001]$  Grains After an Intermediate Annealing in Grain Oriented Silicon Steel Containing a Small Amount of Molybdenum. 1613-1623A
- Anodic polarization**  
Dislocation Structures of Monocrystalline Copper During Corrosion Fatigue in 0.1 M Perchloric Acid. 1151-1157A
- Antimony, Impurities**  
Subcritical Intergranular Crack Growth Rates and Thresholds of Iron and Iron + Antimony. 123-131A  
Activities of Arsenic, Antimony, Bismuth and Lead in Copper Matrices. 129-141B
- Antimony base alloys, Casting**  
Inverse Segregation. 595-604B
- AOD vessels**  
Turbulent Fluid Flow Phenomena in a Water Model of an AOD System. 67-75B

- Arc welding**  
See Gas tungsten arc welding  
Shielded metal arc welding  
Submerged arc welding
- Arc welds**  
See Welded joints
- Argon, Environment**  
The Effect of Environment on the Sustained Load Crack Growth Rates of Forged WASPALOY. 1515-1521A
- Argon arc welding**  
See Gas tungsten arc welding
- Arrhenius activation energy**  
See Activation energy
- Arsenic, Impurities**  
Activities of Arsenic, Antimony, Bismuth and Lead in Copper Matrices. 129-141B  
The Solubility of Barium Arsenate: Sherritt's Barium Arsenate Process. 404-406B  
Correction to "The Solubility of Barium Arsenate: Sherritt's Barium Arsenate Process". 662B  
Stress Corrosion Cracking of  $\alpha$ -Brass in Waters With and Without Additions. 1671-1681A
- Arsenic compounds**  
See Gallium arsenide
- Arsenides**  
See Gallium arsenide
- Artificial aging**  
See Aging (artificial)
- Artillery shells**  
See Projectiles
- Astroceraam**  
See Ceramics
- Atomic diffusion**  
See Diffusion
- Atomic properties**  
See Atomic structure
- Atomic structure**  
Determination of the Coordination Number of Liquid Metals Near the Melting Point. 267-274A
- Atomization**  
See Atomizing
- Atomizing**  
Laser-Melting/Spin-Atomization Method for the Production of Titanium Alloy Powders. 1897-1900A
- Austempering**  
Embrittlement of Austempered Nodular Irons: Grain Boundary Phosphorus Enrichment Resulting From Precipitate Decomposition. 797-805A
- Austenite**  
See also Retained austenite  
A Mössbauer Spectrometry Study of the Mechanical Transformation of Precipitated Austenite in 8Ni Steel. 173-177A
- Austenite, Crystal growth**  
Estimation of Nucleation Rate and Growth Rate From Time Dependence of Global Microstructural Properties During Phase Transformations. 559-564A  
Ferrite Recrystallization and Austenite Formation in Cold-Rolled Intercritically Annealed Steel. 1385-1392A
- Austenite, Heating effects**  
The Stability of Precipitated Austenite and the Toughness of 9Ni Steel. 2237-2249A
- Austenitic stainless steels, Corrosion**  
Effect of Cold Work on Stress Corrosion Cracking Behavior of Types 304 and 316 Stainless Steels. 285-289A  
A Unified Mechanism of Stress Corrosion and Corrosion Fatigue Cracking. 1133-1141A  
Stress Corrosion Cracking of Stainless Steels. 1909-1923A
- Austenitic stainless steels, Diffusion**  
Grain Boundary Segregation of Phosphorus in 304L Stainless Steel. 2061-2062A
- Austenitic stainless steels, Mechanical properties**  
The Deformation-Path Dependence of Fracture Strain in 304L Stainless Steel. 145-148A  
Mathematical Modeling of Thermal Stresses in Basic Oxygen Furnace Hood Tubes. 247-261B  
Plastic and Viscous Deformation of Metals. 375-392A  
The Relationship Between Microstructure and Fracture Behavior of Fully Austenitic Type 316L Weldments at 4.2K. 1835-1848A  
Small-Angle Neutron Scattering Investigation of Creep Damage in Type 304 Stainless Steel and Alloy 800. 2283-2289A
- Austenitic stainless steels, Metallography**  
The Concept of an Effective Quench Temperature and its Use in Studying Elevated-Temperature Microstructures. 1521-1523A
- Austenitic stainless steels, Phase transformations**  
Microstructural and Microchemical Aspects of the Solid-State Decomposition of Delta Ferrite in Austenitic Stainless Steels. 1363-1369A  
Phase Transformations During Aging of a Nitrogen-Strengthened Austenitic Stainless Steels. 1759-1771A
- Austenitic stainless steels, Structural hardening**  
Work Hardening Correlations Based on State Variables in Some F.C.C. Metals in Monotonic Loading. 411-420A
- Some Trends Observed in the Elevated-Temperature Kinematic and Isotropic Hardening of Type 304 Stainless Steel. 1069-1076A  
Polycrystalline Strengthening. 2167-2190A
- Austenitizing**  
Estimation of Nucleation Rate and Growth Rate From Time Dependence of Global Microstructural Properties During Phase Transformations. 559-564A  
Austenitization During Intercritical Annealing of an Fe—C—Si—Mn Dual-Phase Steel. 1237-1245A  
Microstructural and Microchemical Aspects of the Solid-State Decomposition of Delta Ferrite in Austenitic Stainless Steels. 1363-1369A  
Correlation of Microstructure and Fracture Toughness in Two 4340 Steels. 1633-1648A  
The Mechanical Stability of Precipitated Austenite in 9Ni Steel. 2251-2256A
- Auto oxidation**  
See Oxidation
- Autodiffusion**  
See Diffusion
- Autogenous smelting**  
See Flash smelting
- Automobiles**  
See Automotive bodies
- Automotive bodies**  
Microstructure—Mechanical Property Relationships of Dual-Phase Steel Wire. 831-840A
- Automotive components**  
See Automotive bodies
- Bacterial leaching**  
Kinetics of Bio-Chemical Leaching of Sphalerite Concentrate. 667-670B
- Bainite, Crystal growth**  
Discussion of "The Bainite Transformation in a Silicon Steel" and Authors' Reply. 457-468A
- Ballistics**  
Adiabatic Shear Localization in Titanium and Ti—6Al—4V Alloy. 761-775A
- Banded structure**  
Adiabatic Shear Localization in Titanium and Ti—6Al—4V Alloy. 761-775A
- Basic converters, Service life**  
Mathematical Modeling of Thermal Stresses in Basic Oxygen Furnace Hood Tubes. 247-261B
- Basic oxygen furnaces**  
See Basic converters
- Basic oxygen processes**  
See Oxygen steel making
- Basic oxygen steel making**  
See Oxygen steel making
- Batch type furnaces**  
See Basic converters
- Batteries (electric)**  
See Electric batteries
- Bauschinger effect, Microstructural effects**  
Plastic Flow in Dispersion Hardened Materials. 2191-2200A
- Bayer process**  
Stress Corrosion Cracking of Carbon Steel in Caustic Aluminate Solutions—Crack Propagation Studies. 979-986A
- Bearing steels, Mechanical properties**  
Fracture Toughness and Its Development in High Purity Cast Carbon and Low Alloy Steels. 613-622A  
Fatigue Crack Propagation in Carburized High Alloy Bearing Steels. 1253-1265A
- Beehive kilns**  
See Kilns
- Bendability**  
See Formability
- Beryllium, Mechanical properties**  
Correlation of Microyield Behavior With Silicon in X-520 and HIP-50 Beryllium. 807-814A
- Beryllium bronzes, Structural hardening**  
Improvement of Strength and Electrical Conductivity of Copper Alloy by Means of Thermo-Mechanical Treatment. 2073-2077A
- Beryllium copper**  
See Beryllium bronzes
- Bibliographies**  
A Brief History of Dislocation Theory. 2085-2090A
- Binary systems**  
On the Arrangement of Monovariant Lines in Two-Dimensional Potential Phase Diagrams. 137-139A
- Binary systems, Phases (state of matter)**  
The Correlation of the Thermodynamic Properties and Phase Diagram of the System Tin—Lead Using a Gaussian Plus Krupkowski Formalism. 91-96B  
Phase Relationships and Thermodynamic Properties of the Pd—S System. 143-146B  
The Structure of  $R_{(1-x)}Ga_{2(1+x)}$  ( $0 < x < 0.33$ ) and its Relation to  $RGa_2$  ( $R$  = Rare Earth Element) and Gallium. 167-171A  
Thermodynamics and Phase Relationships of Transition Metal—Sulfur Systems. V.—A Reevaluation of the Fe—S

## Binary systems

- System Using an Associated Solution Model for the Liquid Phase.** 277-285B  
**New Eutectic Alloys and Their Heats of Transformation.** 323-328A  
**Thermodynamics of Formation of Y—Ni Alloys.** 577-584B  
**Effect of Magnetic Transition on Solubility of Carbon in B.C.C. Iron and F.C.C. Co—Ni Alloys.** 913-921A  
**Thermodynamics of Formation of Y—Co Alloys.** 1195-1201A  
**The Niobium (Columbium)—Platinum Constitution Diagram.** 1943-1949A  
**Discussion of "A Thermodynamic Analysis of the Fe—C and the Fe—N Phase Diagrams" and Author's Reply.** 2063-2065A
- Binding energy (nuclear)**  
**Trapping of Hydrogen and Helium at Grain Boundaries in Nickel: an Atomic Study.** 1625-1631A
- Bismuth, Diffusion**  
**Discussion of "An Analytical Electron Microscope Study of the Kinetics of the Equilibrium Segregation of Bismuth in Copper" and Authors Reply.** 686-690A
- Bismuth, impurities**  
**Activities of Arsenic, Antimony, Bismuth and Lead in Copper Matrices.** 129-141B
- Blades**  
**See Rotor blades**  
**Turbine blades**
- Blast furnace chemistry**  
**Kinetics of the Reaction of SiO(g) With Carbon Saturated Iron.** 121-127B  
**The Rate of Formation of SiO by the Reaction of CO or Hydrogen With Silica and Silicate Slags.** 801-806B  
**Correction to "Kinetics of the Reaction of SiO(g) With Carbon Saturated Iron".** 857B
- Blast furnace slags**  
**The Rate of Formation of SiO by the Reaction of CO or Hydrogen With Silica and Silicate Slags.** 801-806B
- Blowing**  
**Hydrodynamic Modeling of Some Gas Injection Procedures in Ladle Metallurgy Operations.** 83-90B  
**Characteristics of Round Vertical Gas Bubble Jets.** 263-275B  
**Mixing in Ladles by Vertical Injection of Gas and Gas-Particle Jets—a Water Model Study.** 850-853B
- Blunging**  
**See Mixing**
- BOF**  
**See Basic converters**
- Bohr model**  
**See Atomic structure**
- Boiler scale**  
**See Scale (corrosion)**
- Boiling water reactors**  
**Effect of Single Aging on Microstructure and Impact Property of INCONEL X-750.** 821-829A
- Bombs (pressure vessels)**  
**See Pressure vessels**
- Bornite, Reduction (chemical)**  
**Mineralogical Changes Occurring During the Ferric Ion Leaching of Bornite.** 679-693B
- Boron, Alloying additive**  
**Effect of Boron on the Corrosion Behavior of Polycrystalline Ni<sub>3</sub>Al.** 2072-2073A
- BOS process**  
**See Oxygen steel making**
- Boundaries**  
**See Grain boundaries**  
**Phase boundary**
- Brasses**  
**See also Aluminum brasses**
- Brasses, Corrosion**  
**Sulfidation Under Atmospheric Conditions of Cu—Ni, Cu—Sn and Cu—Zn Binary and Cu—Ni—Sn and Cu—Ni—Zn Ternary Systems.** 275-284A  
**Stress Corrosion Cracking of Alpha—Beta Brass in Distilled Water and Sodium Sulfate Solutions.** 971-978A  
**Stress Corrosion Cracking of  $\alpha$ -Brass in Waters With and Without Additions.** 1671-1681A
- Brasses, Mechanical properties**  
**Plastic and Viscous Deformation of Metals.** 375-392A  
**The Effect of Grain Size and Plastic Strain on Slip Length in 70-30 Brass.** 1025-1029A  
**Hill's Plastic Strain Ratio of Sheet Metals.** 1531-1535A
- Brasses, Structural hardening**  
**Polycrystalline Strengthening.** 2167-2190A  
**Hardening Behavior in Fatigue.** 2201-2214A
- Brick kilns**  
**See Kilns**
- Bridgman method**  
**See Crystal growth**
- Brittleness**  
**See Temper brittleness**
- Bronzes**  
**See Aluminum bronzes**  
**Beryllium bronzes**  
**Phosphor bronzes**
- Bubbles**  
**Hydrogen Attack Kinetics of 2.25 Cr—1 Mo Steel Weld Metals.** 1143-1149A
- Bullets**  
**See Projectiles**
- BV process**  
**See Degassing**
- Byproducts**  
**Formation of Chlorinated Carbon Products During Carbochlorination Reactions.** 847-849B
- Cadmium, Extraction**  
**Kinetics of Bio-Chemical Leaching of Sphalerite Concentrate.** 667-670B
- Calcium, Extraction**  
**Hydrolytic Stripping of Single and Mixed Metal—Versatic Solutions.** 671-677B
- Calcium, Ternary systems**  
**Thermodynamics of the Ca—S—O, Mg—S—O, and La—S—O Systems at High Temperatures.** 287-294B
- Calcium compounds**  
**See also Lime**
- Calcium compounds, Reactions (chemical)**  
**Cyclic Thermogravimetric Methods for the Study of the Decomposition of Carbonates—CaCO<sub>3</sub>.** 743-749B
- Calcium compounds, Thermal properties**  
**The Utilization of Galvanic Cells Using Ca Beta Double Prime—Alumina Solid Electrolytes in a Thermodynamic Investigation of the CaO—Al<sub>2</sub>O<sub>3</sub> System.** 107-112B
- Calcium oxide**  
**See Lime**
- Carbides**  
**See also Silicon carbide**  
**Tungsten carbide**  
**The Effect of Initial Carbide Morphology on Abnormal Grain Growth in Decarburized Low Carbon Steel.** 897-906A
- Carbides, Crystal growth**  
**Growth Kinetics and Morphology of Grain Boundary Ferrite Allotriomorphs in an Fe—C—V Alloy.** 521-527A  
**Low Temperature Carbide Precipitation in a Nickel Base Superalloy.** 1213-1223A  
**Superalloy Microstructural Variations Induced by Gravity Level During Directional Solidification.** 1683-1687A  
**Phase Transformations During Aging of a Nitrogen-Strengthened Austenitic Stainless Steels.** 1759-1771A
- Carbides, Heating effects**  
**Carbide Stability in Nimonic 80A Alloy.** 511-520A
- Carbon, Alloying elements**  
**Phase Constitution and Lattice Parameter Relationships in Rapidly Solidified (Fe<sub>0.85</sub>Mn<sub>0.35</sub>)<sub>0.83</sub>Al<sub>0.17</sub>—xC and Fe<sub>3</sub>Al—xC Pseudobinary Alloys.** 5-10A
- Carbon, Binary systems**  
**Discussion of "A Thermodynamic Analysis of the Fe—C and the Fe—N Phase Diagrams" and Author's Reply.** 2063-2065A
- Carbon, Diffusion**  
**Short-Range Reordering of Heavy Interstitials in Ta, Nb, and Fe During Relaxation and Static Strain Aging.** 361-368A  
**An Instability in Fe—C—M Alloys.** 1608-1611A
- Carbon, Reactions (chemical)**  
**Kinetics of the Reaction of SiO(g) With Carbon Saturated Iron.** 121-127B  
**Correction to "Kinetics of the Reaction of SiO(g) With Carbon Saturated Iron".** 857B
- Carbon, Solubility**  
**Discussion of "Effects of Tempering on the Carbon Activity and Hydrogen Attack Kinetics of 2.25Cr—1Mo Steel" and Authors' Reply.** 1355-1357A
- Carbon, Ternary systems**  
**Correction to "Phase Relationships in the Fe—Cr—C System at Solidification Temperatures".** 662B  
**Effect of Magnetic Transition on Solubility of Carbon in B.C.C. Iron and F.C.C. Co—Ni Alloys.** 913-921A  
**Thermodynamics of the Fe—Cr—C System at 985K.** 1479-1490A  
**The Fe-Rich Corner of the Metastable C—Cr—Fe Liquidus Surface.** 1541-1549A
- Carbon compounds**  
**See Carbides**  
**Carbon dioxide**  
**Halocarbons**  
**Tungsten carbide**
- Carbon dioxide, Solubility**  
**Solubilities of Carbon Dioxide in Sodium Silicate Melts.** 561-566B
- Carbon equivalent**  
**Metallurgical Thermodynamics and the Carbon Equivalent Expression.** 169-170B  
**Effect of Carbon Content and Ferrite Grain Size on the Tensile Flow Stress of Ferritic Spheroidal Graphite Cast Iron.** 667-673A
- Carbon steels, Cleaning**  
**Studies on the Analysis of Hydrogen in High Strength Steels.** 1694-1695A
- Carbon steels, Corrosion**  
**Stress Corrosion Cracking of Carbon Steel in Caustic Aluminate Solutions—Crack Propagation Studies.** 979-986A
- Carbon steels, Crystal growth**  
**The Effect of Initial Carbide Morphology on Abnormal Grain Growth in Decarburized Low Carbon Steel.** 897-906A



- Carbon steels, Heat treatment**  
 Ferrite Recrystallization and Austenite Formation in Cold-Rolled Intercritically Annealed Steel. 1385-1392A
- Carbon steels, Mechanical properties**  
 Thermal Gradients, Strain Rate and Ductility in Sheet Steel Tensile Specimens. 37-43A  
 Effects of Gaseous Hydrogen on Fatigue Crack Growth in Pipeline Steel. 115-122A  
 Fracture Toughness and Its Development in High Purity Cast Carbon and Low Alloy Steels. 613-622A  
 Adiabatic Shear Localization in Titanium and Ti—6Al—4V Alloy. 761-775A  
 Tensile Stress—Strain Analysis of Cold Worked Metals and Steels and Dual-Phase Steels. 865-872A  
 Hydrogen Degradation of Spheroidized AISI 1090 Steel. 1417-1425A  
 An Analysis of the Nonisothermal Tensile Test. 2299-2308A
- Carbon steels, Phase transformations**  
 Estimation of Nucleation Rate and Growth Rate From Time Dependence of Global Microstructural Properties During Phase Transformations. 559-564A  
 Kinetics of Austenite—Ferrite and Austenite—Pearlite Transformations in a 1025 Carbon Steel. 565-578A  
 The Effect of Alloying Elements on Pearlite Growth. 597-603A  
 Isothermal Martensite Transformation in a 1.80 Carbon Steel. 2257-2262A
- Carbon steels, Phases (state of matter)**  
 The Development of Some Dual-Phase Steel Structures From Different Starting Microstructures. 543-557A
- Carbon steels, Reactions (chemical)**  
 The Effect of Carbon Content on the Kinetics of Decarburization in Fe—C Alloys. 1160-1163A
- Carbon steels, Sorption**  
 The Use of Palladium to Obtain Reproducible Boundary Conditions for Permeability Measurements Using Galvanostatic Charging. 715-719A
- Carbon steels, Welding**  
 Chemical Reactions During Submerged Arc Welding With FeO—MnO—SiO<sub>2</sub> Fluxes. 237-245B
- Carbonates, Reactions (chemical)**  
 Cyclic Thermogravimetric Methods for the Study of the Decomposition of Carbonates—CaCO<sub>3</sub>. 743-749B
- Carbothermic reactions**  
 Formation of Chlorinated Carbon Products During Carbochlorination Reactions. 847-849B
- Carburization**  
 See Carburizing
- Carburizing**  
 Fatigue Crack Propagation in Carburized High Alloy Bearing Steels. 1253-1265A  
 Fatigue Crack Propagation in Carburized X-2M Steel. 1267-1271A
- Case carburizing**  
 See Carburizing
- Case hardening**  
 See Carburizing
- Cast iron**  
 See also Nodular iron
- Cast iron, Casting**  
 Metallurgical Thermodynamics and the Carbon Equivalent Expression. 169-170B  
 Modeling of Heat Flow in Sand Castings. II.—Applications of the Boundary Curvature Method. 203-209B
- Casting**  
 See Chill casting  
 Continuous casting  
 Ingot casting  
 Melt spinning  
 Rheocasting  
 Sand casting  
 Squeeze casting
- Casting defects**  
 Mathematical Modeling of Porosity Formation in Solidification. 359-366B  
 Effect of Oscillation-Mark Formation on the Surface Quality of Continuously Cast Steel Slabs. 605-624B  
 Centerline Porosity in Plate Castings. 823-829B  
 Correction to "Effect of Oscillation-Mark Formation on the Surface Quality of Continuously Cast Steel Slabs". 858B
- Castings**  
 See Centrifugal castings  
 Sand castings
- Cathodic coatings (oxide)**  
 See Oxide coatings
- Caustic soda**  
 See Sodium hydroxide
- Cemented carbides, Mechanical properties**  
 Binder Deformation in WC—(Co, Ni) Cemented Carbide Composites. 2309-2317A
- Centrifugal castings, Mechanical properties**  
 Mechanical Properties and Microstructure of Centrifugally Cast Alloy 718. 1295-1306A
- Ceramics, Reactions (chemical)**  
 Interfacial Phenomena Between Molten Metals and Sapphire Substrate. 567-575B
- Chalcocite, Reduction (chemical)**  
 Intrinsic Kinetics of the Hydrogen Reduction of Cu<sub>2</sub>S. 831-839B
- Chalcogenides**  
 See Sulfides
- Chalcopyrite, Reduction (chemical)**  
 Effect of Suspension Potential on the Oxidation Rate of Copper Concentrate in a Sulfuric Acid Solution. 695-705B
- Chemical analysis**  
 See Microanalysis
- Chemical attack**  
 See Intergranular corrosion
- Chemical cleaning**  
 See Acid cleaning
- Chemical composition, Microstructural effects**  
 Equilibrium Solute Concentration Surrounding Elastically Interacting Precipitates. 337-347A
- Chemical equilibrium**  
 Computation of Gas Phase Equilibria—a General Algorithm Using the Newton—Raphson Method. 793-799B
- Chemical kinetics**  
 See Reaction kinetics
- Chemical properties**  
 See Heat of formation
- Chemical tests**  
 See Huey test  
 Microanalysis
- Chemistry**  
 See Thermochemistry
- Chill casting**  
 Inverse Segregation. 595-604B
- Chlorides**  
 See also Sodium chloride  
 Reaction Mechanism for the Ferric Chloride Leaching of Sphalerite. 715-724B
- Chlorides, Environment**  
 Stress Corrosion Cracking of Stainless Steels. 1909-1923A
- Chlorination**  
 Separation of Niobium From Ferroniobium by Chlorination. 639-644B  
 Formation of Chlorinated Carbon Products During Carbochlorination Reactions. 847-849B
- Chlorine, Environment**  
 The Effect of Chlorine on the Kinetics of Oxidation of Cobalt in Environments Containing 0.5 Atmosphere of Oxygen Between 900K and 1200K. 751-761B
- Chlorine, Reactions (chemical)**  
 Separation of Niobium From Ferroniobium by Chlorination. 639-644B
- Chlorocarbons**  
 See Halocarbons
- Chromium, Alloying elements**  
 The Influence of Grain Boundary Precipitation on the Measurement of Chromium Redistribution and Phosphorus Segregation in Ni—18Cr—9Fe. 349-359A  
 Isopiestic Solubility of Hydrogen in Vanadium Alloys at Low Temperatures. 367-374A  
 The Effect of Alloying Elements on Pearlite Growth. 597-603A  
 Fracture Toughness and Its Development in High Purity Cast Carbon and Low Alloy Steels. 613-622A  
 On the Improvement of Creep Strength and Ductility of Ni—20% Cr by Small Zirconium Additions. 651-660A
- Chromium, Diffusion**  
 Grain Boundary Segregation of Phosphorus in 304L Stainless Steel. 2061-2062A
- Chromium, Reactions (chemical)**  
 Displacement Reactions Between Chromium and MoO<sub>3</sub> in a Nickel-Base Alloy Matrix. 1815-1830A
- Chromium, Ternary systems**  
 The Co—Cr—S Ternary System at 1223K and Applications to Corrosion. 503-510A  
 Correction to "Phase Relationships in the Fe—Cr—C System at Solidification Temperatures". 662B  
 Thermodynamics of the Fe—Cr—C System at 985K. 1479-1490A  
 The Fe-Rich Corner of the Metastable C—Cr—Fe Liquidus Surface. 1541-1549A
- Chromium molybdenum nickel steels**  
 See Nickel chromium molybdenum steels
- Chromium molybdenum steels**  
 See also Nickel chromium molybdenum steels
- Chromium molybdenum steels, Corrosion**  
 Sulfide Stress Cracking of High Strength Modified Cr—Mo Steels. 935-944A  
 Crack Size Effects on the Chemical Driving Force for Aqueous Corrosion Fatigue. 953-969A  
 Hydrogen Attack Kinetics of 2.25 Cr—1 Mo Steel Weld Metals. 1143-1149A
- Chromium molybdenum steels, Heat treatment**  
 Modified Heat Treatment for Lower Temperature Improvement of the Mechanical Properties of Two Ultra-High-Strength Low-Alloy Steels. 83-91A
- Chromium molybdenum steels, Mechanical properties**  
 Mechanical Properties of a Low Alloy Steel in a Molten Nitrate Salt Environment. 1031-1041A  
 Variation of the Fracture Mode in Temper Embrittled 2.25 Cr—1 Mo Steel. 1325-1331A  
 A Study of Fatigue Crack Propagation in Prior Hydrogen Attacked Pressure Vessel Steels. 1491-1501A

## Chromium molybdenum steels

- A "Hydrogen Partitioning" Model for Hydrogen Assisted Crack Growth. 2039-2050A
- Chromium molybdenum steels, Microstructure**  
Microstructural Changes in 1Cr—0.5Mo Steel After 20 Years of Service. 109-114A
- Chromium molybdenum steels, Solubility**  
Discussion of "Effects of Tempering on the Carbon Activity and Hydrogen Attack Kinetics of 2.25Cr—1Mo Steel" and Authors' Reply. 1355-1357A
- Chromium nickel molybdenum steels**  
See Nickel chromium molybdenum steels
- Chromium nickel steels**  
See Nickel chromium steels
- Chromium steels**  
See also Austenitic stainless steels  
Chromium molybdenum steels  
Ferritic stainless steels  
Nickel chromium molybdenum steels  
Nickel chromium steels  
Stainless steels
- Chromium steels, Mechanical properties**  
Fracture Toughness and Its Development in High Purity Cast Carbon and Low Alloy Steels. 613-622A
- Chromium steels, Phase transformations**  
The Effect of Alloying Elements on Pearlite Growth. 597-603A
- Cleaning**  
See Acid cleaning
- Coal**  
Sintering Kinetics and Alumina Yield in Lime—Soda Sinter Process for Alumina From Coal Wastes. 385-395B
- Coal gasification**  
A Study of Fatigue Crack Propagation in Prior Hydrogen Attacked Pressure Vessel Steels. 1491-1501A
- Coatings**  
See Electrocoatings  
Oxide coatings  
Protective coatings
- Cobalt, Alloying elements**  
Effect of Cobalt Content on the Stress-Corrosion Cracking Behavior of 7091-Type Aluminum Powder Alloys. 945-951A  
The Influence of Cobalt, Tantalum, and Tungsten on the Microstructure of Single Crystal Nickel-Base Superalloys. 1849-1862A  
The Influence of Cobalt, Tantalum, and Tungsten on the Elevated Temperature Mechanical Properties of Single Crystal Nickel-Base Superalloys. 1863-1870A
- Cobalt, Binary systems**  
Thermodynamics of Formation of Y—Co Alloys. 1195-1201A
- Cobalt, Composite materials**  
Binder Deformation in WC—(Co, Ni) Cemented Carbide Composites. 2309-2317A
- Cobalt, Materials substitution**  
The Substitution of Nickel for Cobalt in Hot Isostatically Pressed Powder Metallurgy UDIMET 700 Alloys. 993-1003A
- Cobalt, Oxidation**  
The Effect of Chlorine on the Kinetics of Oxidation of Cobalt in Environments Containing 0.5 Atmosphere of Oxygen Between 900K and 1200K. 751-761B
- Cobalt, Ternary systems**  
The Co—Cr—S Ternary System at 1223K and Applications to Corrosion. 503-510A  
Effect of Magnetic Transition on Solubility of Carbon in B.C.C. Iron and F.C.C. Co—Ni Alloys. 913-921A  
Phases in Ni—Co—Ga Alloys Close to (Ni, Co)<sub>0.5</sub>Ga<sub>0.5</sub>. 1159-1160A
- Cobalt, Thermal properties**  
Magnetic Contributions to the Thermodynamic Functions of Pure Nickel, Cobalt and Iron. 153-165A
- Cobalt base alloys, Composite materials**  
Binder Deformation in WC—(Co, Ni) Cemented Carbide Composites. 2309-2317A
- Cobalt base alloys, Corrosion**  
The Co—Cr—S Ternary System at 1223K and Applications to Corrosion. 503-510A
- Cobalt base alloys, Powder technology**  
Effect of Dihedral Angle on the Morphology of Grains in a Matrix Phase. 923-928A
- Cobalt base alloys, Refining**  
Thermodynamic Properties of S—Fe—Co—Ni and Fe—Co—Ni Systems. 907-911A
- COD**  
See Crack opening displacement
- Cold cracking (welds)**  
See Weld defects
- Cold deformation**  
See Deformation
- Cold ductility**  
See Ductility
- Cold formability**  
See Formability
- Cold forming**  
See Cold working
- Cold reduction**  
See Cold working
- Cold rolling**  
The Effect of Cold Rolling on the Fatigue Properties of Ti—6Al—4V. 144-145A  
Ferrite Recrystallization and Austenite Formation in Cold-Rolled Intercritically Annealed Steel. 1385-1392A
- Cold swaging**  
See Swaging
- Cold working**  
See also Cold rolling  
Stretch forming  
Effect of Cold Work on Stress Corrosion Cracking Behavior of Types 304 and 316 Stainless Steels. 285-289A
- Columbium**  
See Niobium
- Columbium base alloys**  
See Niobium base alloys
- Compacting**  
See Explosive compacting  
Hot isostatic pressing
- Compacts**  
See Powder compacts  
Sintered compacts
- Compliance (elasticity)**  
See Modulus of elasticity
- Composite materials**  
See also Fiber composites
- Composite materials, Mechanical properties**  
Analysis of Stress—Strain, Fracture, and Ductility Behavior of Aluminum Matrix Composites Containing Discontinuous Silicon Carbide Reinforcement. 1105-1115A
- Compositions**  
See Chemical composition
- Compressibility**  
A Model for Deformation and Segregation of Solid—Liquid Mixtures. 1393-1403A
- Compression strength**  
See Compressive strength
- Compressive modulus**  
See Modulus of elasticity
- Compressive strength**  
Mechanical Properties and Failure Characteristics of FP/Aluminum and W/Aluminum Composites. 853-864A
- Compressive yield strength**  
See Compressive strength
- Computer programs**  
Fluid Flow and Weld Penetration in Stationary Arc Welds. 203-213A  
Computation of Gas Phase Equilibria—A General Algorithm Using the Newton—Raphson Method. 793-799B
- Computer simulation**  
Modeling of Heat Flow in Sand Castings. II.—Applications of the Boundary Curvature Method. 203-209B  
Mechanism for the Formation of High Cycle Fatigue Cracks at FCC Annealing Twin Boundaries. 873-880A  
Trapping of Hydrogen and Helium at Grain Boundaries in Nickel: an Atomistic Study. 1625-1631A
- Concast**  
See Continuous casting
- Concentration (stress)**  
See Stress concentration
- Concentration cell corrosion**  
See Pitting (corrosion)
- Conducting sheet analog**  
See Heat transmission
- Constitutional diagrams**  
See Phase diagrams
- Continuous casting**  
Experimental Study of Continuous Electromagnetic Casting of Aluminum Alloys. 377-384B  
Numerical Calculation of Fluid Flow in a Continuous Casting Tundish. 497-504B  
Effect of Oscillation-Mark Formation on the Surface Quality of Continuously Cast Steel Slabs. 605-624B  
Correction to "Effect of Oscillation-Mark Formation on the Surface Quality of Continuously Cast Steel Slabs". 858B
- Contours**  
See Shape
- Controlled rolling**  
Measurement and Evaluation of the Anisothermal Softening of Austenite After Hot Deformation. 67-72A  
Effect of Finish Rolling Temperature on the Structure and Properties of Directly Quenched Nb Containing Low Steel. 471-474A  
Thermomechanical Processing of Microalloyed Powder Forged Steels and a Cast Vanadium Steel. 1599-1605A  
Low Temperature Mechanical Behavior of Microalloyed and Controlled-Rolled Fe—Mn—Al—C—X Alloys. 1689-1693A
- Converters**  
See Basic converters
- Cooling rate**  
Kinetics of Austenite—Ferrite and Austenite—Pearlite Transformations in a 1025 Carbon Steel. 565-578A



- Microstructural and Microchemical Aspects of the Solid-State Decomposition of Delta Ferrite in Austenitic Stainless Steels. 1363-1369A
- The Concept of an Effective Quench Temperature and Its Use in Studying Elevated-Temperature Microstructures. 1521-1523A
- Copes (molds)**  
See Sand molds
- Copper, Bonding**  
Pressure Effects in Multiphase Binary Diffusion Couples. 605-611A
- Copper, Casting**  
Grain Refinement of Copper by the Addition of Iron and by Electromagnetic Stirring. 505-511B
- Copper, Chemical analysis**  
A New Type of Oxygen Analyzer Utilizing a Potentiostatic Coulometric Titration Technique. 113-119B
- Copper, Composite materials**  
Discussion of "Enhanced Tensile Strength for Electrodeposited Nickel—Copper Multilayer Composites". 1693A
- Copper, Diffusion**  
Inverse Segregation in Directionally Solidified Al—Cu—Ti Alloys With Equiaxed Grains. 579-587A  
Discussion of "An Analytical Electron Microscope Study of the Kinetics of the Equilibrium Segregation of Bismuth in Copper" and Authors Reply. 686-690A  
Quaternary Diffusion in the Cu—Ni—Zn—Mn System at 775°C. 1123-1132A
- Copper, Extraction**  
Direct Copper Precipitation From a Loaded Chelating Extractant by Pressure Hydrogen Stripping. 13-22B  
Distribution of Gold and Silver Between Copper and Matte. 53-59B  
Intrinsic Kinetics of the Hydrogen Reduction of Copper Sulfate: Determination by a Nonisothermal Technique. 397-401B  
Determination of Cu(II) and Fe(III) in Chloride Solutions Concentrated in Both Copper and Iron. 403-404B  
Kinetics of Bio-Chemical Leaching of Sphalerite Concentrate. 667-670B  
Mineralogical Changes Occurring During the Ferric Ion Leaching of Bornite. 679-693B  
Effect of Suspension Potential on the Oxidation Rate of Copper Concentrate in a Sulfuric Acid Solution. 695-705B
- Copper, Mechanical properties**  
A Note on Grain Boundary Diffusion Controlled Cavity Growth During Elevated-Temperature Fatigue. 300-302A  
Plastic and Viscous Deformation of Metals. 375-392A  
Tensile Stress—Strain Analysis of Cold Worked Metals and Steels and Dual-Phase Steels. 865-872A  
Hill's Plastic Strain Ratio of Sheet Metals. 1531-1535A
- Copper, Microstructure**  
Dislocation Structures of Monocrystalline Copper During Corrosion Fatigue in 0.1 M Perchloric Acid. 1151-1157A
- Copper, Phase transformations**  
Criterion for Predicting the Morphology of Crystalline Cubic Precipitates in a Cubic Matrix. 197-202A
- Copper, Reactions (chemical)**  
Effect of Arsenic on the Activity of Oxygen Dissolved in Dilute Liquid Copper Solutions. 339-344B  
Interfacial Phenomena Between Molten Metals and Sapphire Substrate. 567-575B
- Copper, Refining**  
Thermodynamics of Removing Selenium and Tellurium From Liquid Copper by Sodium Carbonate Slags. 171-172B  
Solute Interactions in Multicomponent Solutions. 807-813B
- Copper, Structural hardening**  
Work Hardening Correlations Based on State Variables in Some F.C.C. Metals in Monotonic Loading. 411-420A  
Hardening Behavior in Fatigue. 2201-2214A
- Copper, Welding**  
Fundamental Aspects of Formation and Stability of Explosive Welds. 841-852A
- Copper base alloys**  
See also Aluminum brasses  
Aluminum bronzes  
Beryllium bronzes  
Brasses  
Cupronickel  
Phosphor bronzes
- Copper base alloys, Corrosion**  
Sulfidation Under Atmospheric Conditions of Cu—Ni, Cu—Sn and Cu—Zn Binary and Cu—Ni—Sn and Cu—Ni—Zn Ternary Systems. 275-284A
- Copper base alloys, Metallography**  
The Early Stages of the Decomposition of Alloys. 1173-1184A
- Copper base alloys, Phase transformations**  
Decomposition of Rapidly Solidified Cu—Ti Solid Solutions. 1353-1354A  
Mobility of the  $\beta_1/\gamma_1$  Martensitic Interface in Cu—Al—Ni. I.—Experimental Measurements. 1723-1734A  
Mobility of the  $\beta_1/\gamma_1$  Martensitic Interface in Cu—Al—Ni. II.—Model Calculations. 1735-1744A  
Cellular Decomposition in a Cu—25Ni—15Co Side-Band Alloy. 1751-1757A
- Copper base alloys, Structural hardening**  
Precipitation Hardening. 2131-2165A  
Hardening Behavior in Fatigue. 2201-2214A
- Copper base alloys, Thermal properties**  
New Eutectic Alloys and Their Heats of Transformation. 323-328A
- Copper compounds, Reduction (chemical)**  
Intrinsic Kinetics of the Hydrogen Reduction of Copper Sulfate: Determination by a Nonisothermal Technique. 397-401B  
Successive Gas—Solid Reaction Model for the Hydrogen Reduction of Cuprous Sulfide in the Presence of Lime. 645-662B  
Intrinsic Kinetics of the Hydrogen Reduction of  $\text{Cu}_2\text{S}$ . 831-839B
- Copper mattes**  
Distribution of Gold and Silver Between Copper and Matte. 53-59B  
Activities of Arsenic, Antimony, Bismuth and Lead in Copper Mattes. 129-141B
- Copper ores**  
See also Bornite  
Chalcocite  
Chalcopyrite
- Copper ores, Reduction (chemical)**  
Leaching of Chrysocolla With Ammonia—Ammonium Carbonate Solutions. 441-448B
- Core hardness**  
See Hardness
- Coreless induction furnaces**  
Fluid Flow Phenomena in a Single Phase Coreless Induction Furnace. 227-235B
- Corrodents**  
See Corrosion environments
- Corrosion**  
See Corrosion fatigue  
Corrosion mechanisms  
Hot gas corrosion  
Intergranular corrosion  
Pitting (corrosion)  
Scale (corrosion)  
Sulfurization
- Corrosion cracking**  
See Stress corrosion cracking
- Corrosion effects**  
See Dezincification  
Pitting (corrosion)  
Scale (corrosion)
- Corrosion environments**  
Crack Size Effects on the Chemical Driving Force for Aqueous Corrosion Fatigue. 953-969A  
Stress Corrosion Cracking of Alpha—Beta Brass in Distilled Water and Sodium Sulfate Solutions. 971-978A  
Stress Corrosion Cracking of Carbon Steel in Caustic Aluminate Solutions—Crack Propagation Studies. 979-986A
- Corrosion fatigue**  
Crack Size Effects on the Chemical Driving Force for Aqueous Corrosion Fatigue. 953-969A  
Dislocation Structures of Monocrystalline Copper During Corrosion Fatigue in 0.1 M Perchloric Acid. 1151-1157A
- Corrosion mechanisms**  
See also Intergranular corrosion  
Scale (corrosion)  
A Unified Mechanism of Stress Corrosion and Corrosion Fatigue Cracking. 1133-1141A
- Corrosion prevention**  
Sulfation of  $\text{Y}_2\text{O}_3$  and  $\text{HfO}_2$  in Relation to MCrAl Coatings. 303-306A
- Corrosion products**  
See Scale (corrosion)
- Corrosion rate, Alloying effects**  
Sulfide Stress Cracking of High Strength Modified Cr—Mo Steels. 935-944A
- Corrosion rate, Composition effects**  
Effect of Cobalt Content on the Stress-Corrosion Cracking Behavior of 7091-Type Aluminum Powder Alloys. 945-951A
- Corrosion rate, Diffusion effects**  
Grain Boundary Segregation of Phosphorus in 304L Stainless Steel. 2061-2062A
- Corrosion resistance**  
Investigation of Stress Corrosion Crack Growth in Magnesium Alloys Using J-Integral Estimations. 101-108A
- Corrosion resistance, Alloying effects**  
Sulfidation Under Atmospheric Conditions of Cu—Ni, Cu—Sn and Cu—Zn Binary and Cu—Ni—Sn and Cu—Ni—Zn Ternary Systems. 275-284A  
The Embrittlement of Al—Zn—Mg and Al—Mg Alloys by Water Vapor. 1503-1514A  
Effect of Boron on the Corrosion Behavior of Polycrystalline Ni<sub>3</sub>Al. 2072-2073A
- Corrosion resistance, Deformation effects**  
Effect of Cold Work on Stress Corrosion Cracking Behavior of Types 304 and 316 Stainless Steels. 285-289A
- Corrosion resistance, Heating effects**  
Effect of Single Aging on Microstructure and Impact Property of INCONEL X-750. 821-829A  
The Microstructural Response of Mill—Annealed and Solution—Annealed INCONEL 600 to Heat Treatment. 1225-1236A  
The Role of Aging Reactions in the Hydrogen Embrittlement Susceptibility of an HSLA Steel. 1879-1886A
- Corrosion resistance, Welding effects**  
Hydrogen Attack Kinetics of 2.25 Cr—1 Mo Steel Weld Metals. 1143-1149A
- Corrosion tests**  
See Huey test  
Stress corrosion tests

## Cost savings

### Cost savings

See Economics

### Crack closure, Heating effects

On the Development of Crack Closure and the Threshold Condition for Short and Long Fatigue Cracks in 7150 Aluminum Alloy.

1467-1477A

### Crack growth

See Crack propagation

### Crack opening displacement

Crack Size Effects on the Chemical Driving Force for Aqueous Corrosion Fatigue.

953-969A

### Crack propagation

Investigation of Stress Corrosion Crack Growth in Magnesium Alloys Using J-Integral Estimations.

101-108A

On Macroscopic and Microscopic Analyses for Crack Initiation and Crack Growth Toughness in Ductile Alloys.

233-248A

Fatigue Crack Deflection and Fracture Surface Contact: Micromechanical Models.

249-260A

A Note on Grain Boundary Diffusion Controlled Cavity Growth During Elevated-Temperature Fatigue.

300-302A

A Unified Mechanism of Stress Corrosion and Corrosion Fatigue Cracking.

1133-1141A

Correction to "On Macroscopic and Microscopic Analyses for Crack Initiation and Crack Growth Toughness in Ductile Alloys".

1358A

Stress Corrosion Cracking of  $\alpha$ -Brass in Waters With and Without Additions.

1671-1681A

A "Hydrogen Partitioning" Model for Hydrogen Assisted Crack Growth.

2039-2050A

### Crack propagation, Alloying effects

Lithium-Containing Aluminum Alloys: Cyclic Fracture.

475-477A

### Crack propagation, Corrosion effects

Fatigue Microcrack Initiation in Polycrystalline Alpha-Iron With Polished and Oxidized Surfaces.

641-649A

### Crack propagation, Diffusion effects

Hydrogen Degradation of Spherulitized AISI 1090 Steel. A Study of Fatigue Crack Propagation in Prior Hydrogen Attacked Pressure Vessel Steels.

1417-1425A

1491-1501A

### Crack propagation, Environmental effects

Effects of Gaseous Hydrogen on Fatigue Crack Growth in Pipeline Steel.

115-122A

Stress Corrosion Cracking of Carbon Steel in Caustic Aluminate Solutions—Crack Propagation Studies.

979-986A

The Effect of Environment on the Sustained Load Crack Growth Rates of Forged Waspaloy.

1515-1521A

### Crack propagation, Heating effects

The Development of Two Texture Variants and Their Effect on the Mechanical Behavior of a High Strength P/M Aluminum Alloy, X7091.

1069-1103A

On the Development of Crack Closure and the Threshold Condition for Short and Long Fatigue Cracks in 7150 Aluminum Alloy.

1467-1477A

### Crack propagation, Impurity effects

Subcritical Intergranular Crack Growth Rates and Thresholds of Iron and Iron + Antimony.

123-131A

### Crack propagation, Microstructural effects

A Mössbauer Spectrometry Study of the Mechanical Transformation of Precipitated Austenite in 6Ni Steel.

173-177A

High-Cycle Fatigue Properties of the ODS-Alloy MA 6000 at 850°C.

393-399A

Microstructural Influences on Fatigue Crack Propagation in Ti-10V-2Fe-3Al.

739-751A

Influence of Microstructure on Fatigue Crack Initiation in Fully Pearlitic Steels.

753-760A

Effects of Temperature and Environment on Fatigue Crack Growth in Ordered (Fe, Ni)<sub>3</sub>V-Type Alloys.

815-820A

Mechanism for the Formation of High Cycle Fatigue Cracks at FCC Annealing Twin Boundaries.

873-880A

The Effect of Microstructural Changes on the Caustic Stress Corrosion Cracking Resistance of a NiCrMoV Rotor Steel.

1333-1344A

The Dependence of Some Tensile and Fatigue Properties of a Dual-Phase Steel on Its Microstructure.

1405-1415A

High Cycle Fatigue and Fatigue Crack Growth of the Oxide Dispersion Strengthened Alloy MA 754.

1437-1444A

Alternating Grain Orientation and Weld Solidification Cracking.

1887-1896A

### Crack propagation, Size effects

Crack Size Effects on the Chemical Driving Force for Aqueous Corrosion Fatigue.

953-969A

### Crack propagation, Stress effects

Fatigue Crack Propagation in Carburized High Alloy Bearing Steels.

1253-1265A

Fatigue Crack Propagation in Carburized X-2M Steel.

1267-1271A

### Crack resistance

See Crack propagation

### Cracking (fracturing)

See Stress corrosion cracking

### Cratering (welding)

See Weld defects

### Creep (materials)

See also Creep life

Creep rate

Creep rupture strength

Creep strength

Plastic and Viscous Deformation of Metals.

375-392A

Elevated Temperature Creep-Rupture Behavior of the Single Crystal Nickel-Base Superalloy NASAIR 100.

427-439A

Some Trends Observed in the Elevated-Temperature Kinematic and Isotropic Hardening of Type 304 Stainless Steel. Small-Angle Neutron Scattering Investigation of Creep Damage in Type 304 Stainless Steel and Alloy 800.

1069-1076A

2283-2289A

### Creep (materials), Alloying effects

The Substitution of Nickel for Cobalt in Hot Isostatically Pressed Powder Metallurgy UDIMET 700 Alloys.

993-1003A

### Creep life, Microstructural effects

Low Temperature Carbide Precipitation in a Nickel Base Superalloy.

1213-1223A

### Creep limit

See Creep (materials)

### Creep properties

See Creep (materials)

### Creep rate

Elevated Temperature Creep-Rupture Behavior of the Single Crystal Nickel-Base Superalloy NASAIR 100.

427-439A

A Model for Anelastic Relaxation Controlled Cyclic Creep.

1117-1122A

### Creep rate, Stress effects

Plastic and Viscous Deformation of Metals.

375-392A

### Creep resistance

See Creep strength

### Creep rupture strength

Elevated Temperature Creep-Rupture Behavior of the Single Crystal Nickel-Base Superalloy NASAIR 100.

427-439A

### Creep rupture strength, Alloying effects

On the Improvement of Creep Strength and Ductility of Ni-20% Cr by Small Zirconium Additions.

651-660A

### Creep rupture strength, Cooling effects

Mechanical Properties and Microstructure of Centrifugally Cast Alloy 718.

1295-1306A

### Creep strength

Elevated Temperature Creep-Rupture Behavior of the Single Crystal Nickel-Base Superalloy NASAIR 100.

427-439A

The Development of  $\gamma$ - $\gamma'$  Lamellar Structures in a Nickel-Base Superalloy During Elevated Temperature Mechanical Testing.

1969-1982A

### Creep strength, Alloying effects

Dynamic Recrystallization During Creep in a 45% Ni-35% Fe-20% Cr Alloy System.

51-57A

On the Improvement of Creep Strength and Ductility of Ni-20% Cr by Small Zirconium Additions.

651-660A

### Creep strength, Composition effects

The Influence of Cobalt, Tantalum, and Tungsten on the Elevated Temperature Mechanical Properties of Single Crystal Nickel-Base Superalloys.

1863-1870A

### Creep strength, Microstructural effects

The Effect of Grain Morphology on Longitudinal Creep Properties of INCONEL MA 754 at Elevated Temperatures.

1307-1324A

The Effects of Orientation and Thickness on the Notch-Tensile Creep Strength of Single Crystals of a Nickel-Base Superalloy.

1457-1466A

### Creep tests

Microstructure and Crystallography of Unidirectionally Solidified Ni-W Eutectic Alloy.

1185-1193A

### Creeping

See Creep (materials)

### Critical materials

See Strategic materials

### Cross tension test

See Tension tests

### Crushing strength

See Compressive strength

### Cryogenic properties

Low Temperature Mechanical Behavior of Microalloyed and Controlled-Rolled Fe-Mn-Al-C-X Alloys.

1689-1693A

### Cryogenic properties, Microstructural effects

A Mössbauer Spectrometry Study of the Mechanical Transformation of Precipitated Austenite in 6Ni Steel.

173-177A

The Stability of Precipitated Austenite and the Toughness of 9Ni Steel.

2237-2249A

### Cryolite

Interfacial Tension of Aluminum in Cryolite Melts.

333-338B

### Crystal defects

See also Dislocation loops

Dislocations

Displacements (lattice)

Interstitial impurities

Point defects

Stacking faults

### Crystal defects, Crystal growth

Influence of Dendrite Network Defects on Channel Segregate Growth.

1687-1689A

### Crystal defects, Deformation effects

High Strain Rate Deformation of Molybdenum and Mo-33Re by Shock Loading. II.—Rates of Defect Generation and Accumulation of Plastic Strain.

891-895A

### Crystal growth

See also Epitaxial growth

Entropy Criteria Applied to Pattern Selection in Systems With Free Boundaries.

1781-1797A

Cellular and Dendritic Growth. II.—Theory.

1807-1814A

- Crystal lattices**  
See also Superlattices
- Crystal lattices, Deformation effects**  
An X-Ray Diffraction Line Profile of Cold-Worked Hexagonal Alloys Zn—Ag:  $\gamma$  and  $\epsilon$  Phase. 1427-1435A
- Crystal orientation**  
See Crystal structure
- Crystal structure**  
The Structure of  $R_{1-x}Ga_{2(1-x)}$  ( $0 < x < 0.33$ ) and Its Relation to  $RGa_2$  ( $R$  = Rare Earth Element) and Gallium. The Effects of Orientation and Thickness on the Notch-Tensile Creep Strength of Single Crystals of a Nickel-Base Superalloy. 167-171A  
Electron Microscopic Study of  $\theta$ -Phase Martensite in Ni—Mn Alloys. 1457-1468A  
Low Temperature Aging of the Freshly Formed Martensite in an Fe—Ni—C Alloy. 1581-1597A  
1745-1750A
- Crystal structure, Cooling effects**  
The Concept of an Effective Quench Temperature and Its Use in Studying Elevated-Temperature Microstructures. 1521-1523A
- Crystal structure, Stress effects**  
Criterion for Predicting the Morphology of Crystalline Cubic Precipitates in a Cubic Matrix. 197-202A
- Crystallinity**  
See Crystal structure
- Crystallization**  
See Recrystallization  
Secondary recrystallization
- Crystallography**  
A New Method for Determining the Defocusing Correction for Crystallographic Texture Measurement. 299-300A
- Crystals**  
See Single crystals
- Cube texture, impurity effects**  
Impurity Effect on Cube Texture in Pure Aluminum Foils. 27-36A
- Cupping**  
See Deep drawing
- Cupronickel, Corrosion**  
Sulfidation Under Atmospheric Conditions of Cu—Ni, Cu—Sn and Cu—Zn Binary and Cu—Ni—Sn and Cu—Ni—Zn Ternary Systems. 275-284A
- Currents**  
See Electric current  
Plasma arcs
- Curves**  
See Stress strain curves
- Cyanides**  
Heterogeneous Equilibria in the Au—CN—H<sub>2</sub>O and Ag—CN—H<sub>2</sub>O Systems. 455-463B
- Cyclic loads**  
A Model for Anelastic Relaxation Controlled Cyclic Creep. 1117-1122A
- Czochralski process**  
See Crystal growth
- Decarburizing**  
The Effect of Carbon Content on the Kinetics of Decarburization in Fe—C Alloys. 1160-1163A
- Decomposition**  
See Decomposition reactions  
Phase decomposition  
Spinodal decomposition
- Decomposition reactions**  
Cyclic Thermogravimetric Methods for the Study of the Decomposition of Carbonates—CaCO<sub>3</sub>. 743-749B
- Deep carburizing**  
See Carburizing
- Deep drawing**  
An Analysis of the Nonisothermal Tensile Test. 2299-2308A
- Defects**  
See Casting defects  
Crystal defects  
Dislocation loops  
Dislocations  
Displacements (lattice)  
Interstitial impurities  
Point defects  
Stacking faults  
Weld defects
- Deformability**  
See Formability
- Deformation**  
See also Plastic deformation  
Discussion of "Deformation Kinetics of Commercial Ti-50A (0.5 at.% Oeq) at Low Temperatures ( $T < 0.3 T_m$ )" and Authors Reply. 694-697A
- Deformation, Microstructural effects**  
High Temperature Deformation of Ultra-Fine-Grained Oxide Dispersion Strengthened Alloys. 777-787A  
Deformation Characteristics in Beta Phase Ti—Nb Alloys. 789-795A
- Deformation resistance, Heating effects**  
Observations of Adiabatic Shear Band Formation in 7039 Aluminum Alloy. 1900-1903A
- Deformation resistance, Microstructural effects**  
A Theoretical Model for the Flow Behavior of Commercial Dual-Phase Steels Containing Metastable Retained Austenite. I.—Derivation of Flow Curve Equations. 2013-2021A  
A Theoretical Model for the Flow Behavior of Commercial Dual-Phase Steels Containing Metastable Retained Austenite. II.—Calculation of Flow Curves. 2023-2029A  
Time-Dependent Deformation of Metals. 2215-2228A
- Deforming**  
See Deformation
- Degasification**  
See Degassing
- Degassing**  
Thermally Induced Porosity in Ti—6Al—4V Prealloyed Powder Compacts. 1526-1531A
- Dehydrogenation**  
Studies on the Analysis of Hydrogen in High Strength Steels. 1694-1695A
- Demetalization**  
See Dezincification
- Dendrite**  
See Dendritic structure
- Dendritic structure**  
Rapid Solidification Characteristics in Melt Spinning a Nickel-Base Superalloy. 1773-1779A  
Entropy Criteria Applied to Pattern Selection in Systems With Free Boundaries. 1781-1797A  
Cellular and Dendritic Growth. I.—Experiment. 1799-1805A  
Cellular and Dendritic Growth. II.—Theory. 1807-1814A  
Flow of Interdendritic Liquid and Permeability in Pb—20Sn Alloys. 2263-2271A
- Dendritic structure, Crystal growth**  
Influence of Dendrite Network Defects on Channel Segregate Growth. 1687-1689A
- Dendritic structure, Field effects**  
Superalloy Microstructural Variations Induced by Gravity Level During Directional Solidification. 1683-1687A
- Densification**  
Explosive Consolidation of Rapidly Solidified Aluminum Alloy Powders. 1445-1455A  
Discussion of "Practical Applications of Hot-Isostatic Pressing Diagrams: From Case Studies". 1903-1904A
- Dephosphorizing**  
Simultaneous Desulfurization and Dephosphorization Reactions of Molten Iron by Soda Ash Treatment. 303-312B
- Deposition**  
See Vapor deposition
- Desilicizing**  
A Unified Approach to Bubbling—Jetting Phenomena in Powder Injection Into Iron and Steel. 203-209B  
Sodium Aluminate Leaching and Desilication in Lime—Soda Sinter Process for Alumina From Coal Wastes. 707-713B
- Desulfurizing**  
A Unified Approach to Bubbling—Jetting Phenomena in Powder Injection Into Iron and Steel. 203-209B  
Simultaneous Desulfurization and Dephosphorization Reactions of Molten Iron by Soda Ash Treatment. 303-312B  
Equilibria Between Rare Earth Elements and Sulfur in Molten Iron. 785-792B
- Development**  
See Technology transfer
- Dezincification**  
Stress Corrosion Cracking of  $\alpha$ -Brass in Waters With and Without Additions. 1671-1681A
- Diagrams**  
See Phase diagrams  
S N diagrams
- Die steels, Mechanical properties**  
Fatigue Crack Propagation in Carburized X-2M Steel. 1267-1271A
- Diffraction**  
See X ray diffraction
- Diffusion**  
Quaternary Diffusion in the Cu—Ni—Zn—Mn System at 775°C. 1123-1132A
- Diffusion, Pressure effects**  
Pressure Effects in Multiphase Binary Diffusion Couples. 605-611A
- Diffusion bonding**  
See Diffusion welding
- Diffusion coefficient**  
See Diffusion
- Diffusion couples**  
See Diffusion
- Diffusion rate**  
The Effect of Pressure Modulation on the Flow of Gas Through a Solid Membrane: Surface Inhibition and Internal Traps. 1013-1024A
- Diffusion welding**  
Pressure Effects in Multiphase Binary Diffusion Couples. 605-611A
- Diffusivity**  
Measurement and Analysis of Distribution Coefficients in Fe—Ni Alloys Containing Sulfur and/or Phosphorus. II.— $K_b$ ,  $K_{Ge}$ , and  $K_{Co}$ . 1871-1878A

## Diffusivity

### Diffusivity, Heating effects

The Role of Aging Reactions in the Hydrogen Embrittlement Susceptibility of an HSLA Steel.

1879-1886A

### Diffusivity, Impurity effects

Trapping of Hydrogen by Sulfur-Associated Defects in Steel.

401-409A

### Digesters, Materials selection

Stress Corrosion Cracking of Carbon Steel in Caustic Aluminate Solutions—Crack Propagation Studies.

979-986A

### Dioxides

See Carbon dioxide  
Silicon dioxide  
Sulfur dioxide

### Direct reduction

See also Hydrogen reduction

Intrinsic Kinetics of the Hydrogen Reduction of Copper Sulfate: Determination by a Nonisothermal Technique.

397-401B

Direct Reduction of Lead Sulfide With Carbon and Lime; Effect of Catalysts: I.—Experimental.

465-475B

Direct Reduction of Lead Sulfide With Carbon and Lime; Effect of Catalysts: II.—Analytical Model.

477-488B

Oxidation of Pyrrhotite Particles Falling Through a Vertical Tube.

627-638B

Successive Gas—Solid Reaction Model for the Hydrogen Reduction of Cuprous Sulfide in the Presence of Lime.

645-662B

Correction to "The Breakdown of Dense Iron Layers on Wustite in CO/CO<sub>2</sub> and H<sub>2</sub>/H<sub>2</sub>O Systems".

857B

Correction to "Establishment of Product Morphology During the Initial Stages of Wustite Reduction".

857B

### Directional solidification

Discussion of "Mathematical Model for the Unidirectional Solidification of Metals. I.—Cooled Molds".

406-407B

Heterogeneous Nucleation Model of Twinned Crystal Growth From the Melt.

690-692A

Superalloy Microstructural Variations Induced by Gravity Level During Directional Solidification.

1683-1687A

Cellular and Dendritic Growth. I.—Experiment.

1799-1805A

Cellular and Dendritic Growth. II.—Theory.

1807-1814A

### Directionally solidified eutectics, Diffusion

Inverse Segregation in Directionally Solidified Al—Cu—Ti Alloys With Equiaxed Grains.

579-587A

### Directionally solidified eutectics, Microstructure

Microstructure and Crystallography of Unidirectionally Solidified Ni—W Eutectic Alloy.

1185-1193A

### Dislocation climb

See Dislocation mobility

### Dislocation density

The Effect of Initial Carbide Morphology on Abnormal Grain Growth in Decarburized Low Carbon Steel.

897-906A

Some Trends Observed in the Elevated-Temperature Kinematic and Isotropic Hardening of Type 304 Stainless Steel.

1069-1076A

The Dependence of Some Tensile and Fatigue Properties of a Dual-Phase Steel on Its Microstructure.

1405-1415A

### Dislocation density, Deformation effects

High Strain Rate Deformation of Molybdenum and Mo—33Re by Shock Loading. I.—Substructure Development.

881-890A

An X-Ray Diffraction Line Profile of Cold-Worked Hexagonal Alloys Zn—Ag:  $\eta$  and  $\epsilon$  Phase.

1427-1435A

### Dislocation loops, Deformation effects

High Strain Rate Deformation of Molybdenum and Mo—33Re by Shock Loading. I.—Substructure Development.

881-890A

### Dislocation loops, Field effects

Dislocation Structures of Monocrystalline Copper During Corrosion Fatigue in 0.1 M Perchloric Acid.

1151-1157A

### Dislocation mobility, Deformation effects

High Strain Rate Deformation of Molybdenum and Mo—33Re by Shock Loading. II.—Rates of Defect Generation and Accumulation of Plastic Strain.

891-895A

### Dislocations

See also Dislocation loops

On the Hierarchy of Interfacial Dislocation Structure.

529-541A

Electron Microscopic Study of  $\beta$ -Phase Martensite in Ni—Mn Alloys.

1581-1597A

A Brief History of Dislocation Theory.

2085-2090A

Time-Dependent Deformation of Metals.

2215-2226A

Dislocations in Amorphous Metals.

2227-2230A

Whither Dislocations? en 2231-2236A

### Dislocations, Heating effects

The Mechanical Stability of Precipitated Austenite in 9Ni Steel.

2251-2256A

### Dispersion hardening

Oxide Dispersion Strengthened Nickel-Base Heat Resistant Alloys by Means of the Spray-Dispersion Method.

1043-1048A

The Formation of Austenite at Low Intercritical Annealing Temperatures in a Normalized 0.08C—1.45Mn—0.21Si Steel.

1523-1526A

Plastic Flow in Dispersion Hardened Materials.

2191-2200A

### Dispersion hardening alloys, Alloy development

Microstructural Development in High Volume Fraction Gamma Prime Ni-Base Oxide-Dispersion-Strengthened Superalloys.

1285-1294A

### Dispersion hardening alloys, Mechanical properties

High Temperature Deformation of Ultra-Fine-Grained Oxide Dispersion Strengthened Alloys.

777-787A

The Effect of Grain Morphology on Longitudinal Creep Properties of INCONEL MA 754 at Elevated Temperatures.

1307-1324A

High Cycle Fatigue and Fatigue Crack Growth of the Oxide Dispersion Strengthened Alloy MA 754.

1437-1444A

Plastic Flow in Dispersion Hardened Materials.

2191-2200A

### Displacement spikes

See Displacements (lattice)

### Displacements (lattice)

See also Interstitial impurities

Mobility of the  $\beta_1/\gamma_1$  Martensitic Interface in Cu—Al—Ni. II.—Model Calculations.

1735-1744A

### Dissimilar metals, Welding

Fundamental Aspects of Formation and Stability of Explosive Welds.

841-852A

### Drags (molds)

See Sand molds

### Drawing

See Deep drawing

Wire drawing

### Drawing (heat treatment)

See Tempering

### Dual phase steels, Heat treatment

Austenitization During Inter-critical Annealing of an Fe—C—Si—Mn Dual-Phase Steel.

1237-1245A

Ferrite Recrystallization and Austenite Formation in Cold-Rolled Inter-critically Annealed Steel.

1385-1392A

The Formation of Austenite at Low Inter-critical Annealing Temperatures in a Normalized 0.08C—1.45Mn—0.21Si Steel.

1523-1526A

### Dual phase steels, Mechanical properties

Mechanical Properties of 0.40% C—Ni—Cr—Mo High-Strength Steel Having a Mixed Structure of Martensite and Bainite.

73-82A

Microstructure—Mechanical Property Relationships of Dual-Phase Steel Wire.

831-840A

Tensile Stress—Strain Analysis of Cold Worked Metals and Steels and Dual-Phase Steels.

865-872A

The Dependence of Some Tensile and Fatigue Properties of a Dual-Phase Steel on Its Microstructure.

1405-1415A

A Theoretical Model for the Flow Behavior of Commercial Dual-Phase Steels Containing Metastable Retained Austenite. I.—Derivation of Flow Curve Equations.

2013-2021A

A Theoretical Model for the Flow Behavior of Commercial Dual-Phase Steels Containing Metastable Retained Austenite. II.—Calculation of Flow Curves.

2023-2029A

### Dual phase steels, Metal working

Plastic Behavior of Dual Phase Steel Following Plane-Strain Deformation.

421-425A

### Dual phase steels, Phase transformations

The Development of Some Dual-Phase Steel Structures From Different Starting Microstructures.

543-557A

An Instability in Fe—C—M Alloys.

1609-1611A

### Ductile brittle transition, Impurity effects

Subcritical Intergranular Crack Growth Rates and Thresholds of Iron and Iron + Antimony.

123-131A

### Ductile brittle transition, Microstructural effects

A Mössbauer Spectrometry Study of the Mechanical Transformation of Precipitated Austenite in 6Ni Steel.

173-177A

### Ductile fracture, Microstructural effects

The Relationship Between Microstructure and Fracture Behavior of Fully Austenitic Type 316L Weldments at 4.2K.

1835-1848A

### Ductile iron

See Nodular iron

### Ductility

Analysis of Stress—Strain, Fracture, and Ductility Behavior of Aluminum Matrix Composites Containing Discontinuous Silicon Carbide Reinforcement.

1105-1115A

An Analysis of the Nonisothermal Tensile Test.

2299-2308A

### Ductility, Alloying effects

Dynamic Recrystallization During Creep in a 45% Ni—35% Fe—20% Cr Alloy System.

51-57A

Effect of Silicide Precipitation on Tensile Properties and Fracture of Alloy Ti—6Al—5Zr—0.5Mo—0.25Si.

227-231A

### Ductility, Composition effects

The Influence of Cobalt, Tantalum, and Tungsten on the Elevated Temperature Mechanical Properties of Single Crystal Nickel-Base Superalloys.

1863-1870A

### Ductility, Deformation effects

Thermal Gradients, Strain Rate and Ductility in Sheet Steel Tensile Specimens.

37-43A

The Deformation-Path Dependence of Fracture Strain in 304L Stainless Steel.

145-148A

### Ductility, Diffusion effects

The Influence of Multiaxial States of Stress on the Hydrogen Embrittlement of Zirconium Alloy Sheet.

675-681A

### Ductility, Environmental effects

Stress Corrosion Cracking of Alpha—Beta Brass in Distilled Water and Sodium Sulfate Solutions.

971-978A

Mechanical Properties of a Low Alloy Steel in a Molten Nitrate Salt Environment.

1031-1041A

### Ductility, Heating effects

Carbide Precipitation, Grain Boundary Segregation, and Temper Embrittlement in NiCrMoV Rotor Steels.

721-737A

### Ductility, Microstructural effects

Microstructure and Mechanical Properties of Fe—Ni—Cr—Al Steel Wires Produced by In-Rotating-Water Spinning Method.

215-226A

Plastic Behavior of Dual Phase Steel Following Plane-Strain Deformation.

421-425A



- High Temperature Deformation of Ultra-Fine-Grained Oxide Dispersion Strengthened Alloys. 777-787A  
The Influence of Strain Rate and Porosity on the Deformation and Fracture of Titanium and Nickel. 2273-2281A
- Ductility, Stress effects**  
Influence of Strain Rate and Temperature on the Deformation Behavior of a Metastable High Carbon Iron—Nickel Austenite. 445-452A
- Dynamics**  
See Hydrodynamics  
Kinetics
- Economics**  
Of Perspectives, Issues, and Politics in Materials Technology. 5-11B  
Of Perspectives, Issues, and Politics in Materials Technology. 311-317A
- Elastic constants**  
See also Modulus of elasticity  
Elastic Constants of a Monocrystalline Nickel-Base Superalloy. 661-665A
- Elastic modulus**  
See Modulus of elasticity
- Elastic properties**  
See Elastic constants
- Electric arcs**  
See Plasma arcs
- Electric batteries**  
Thermodynamic Stabilities of Some Beta and Beta Double Prime Aluminas. 295-301B  
Product Microstructures and Properties Induced by Hot Working at Pb—1.85% Sb Alloy. 1273-1285A
- Electric conductors (materials)**  
See Electrolytes
- Electric current**  
See also Plasma arcs  
A Novel Solidification Technique of Metals and Alloys: Under the Influence of Applied Potential. 1354-1355A
- Electric discharges**  
See Plasma arcs
- Electric furnaces**  
See Coreless induction furnaces
- Electric induction furnaces**  
See Coreless induction furnaces
- Electric welding**  
See Gas tungsten arc welding  
Shielded metal arc welding  
Submerged arc welding
- Electrical phenomena**  
See Electric current  
Plasma arcs
- Electrical steels, Microstructure**  
Transmission Kossel Study of the Formation of (110)[001] Grains After an Intermediate Annealing in Grain Oriented Silicon Steel Containing a Small Amount of Molybdenum. 1613-1623A
- Electroceraamics**  
See Ceramics
- Electrocoatings, Composite materials**  
Discussion of "Enhanced Tensile Strength for Electrodeposited Nickel—Copper Multilayer Composites". 1693A
- Electrolysis**  
See Electrowinning  
Fused salt electrolysis
- Electrolytes**  
Determination of the Lithium Content of Molten Aluminum Using a Solid Electrolyte. 41-46B  
The Utilization of Galvanic Cells Using Ca Beta Double Prime—Alumina Solid Electrolytes in a Thermodynamic Investigation of the CaO—Al<sub>2</sub>O<sub>3</sub> System. 107-112B  
Thermodynamic Stabilities of Some Beta and Beta Double Prime Aluminas. 295-301B  
Interfacial Tension of Aluminum in Cryolite Melts. 333-338B
- Electromagnetic fields**  
Experimental Study of Continuous Electromagnetic Casting of Aluminum Alloys. 377-384B
- Electromagnetic stirring**  
Fluid Flow Phenomena in a Single Phase Coreless Induction Furnace. 227-235B  
Grain Refinement of Copper by the Addition of Iron and by Electromagnetic Stirring. 505-511B
- Electron beam melting**  
Microstructure of Rapidly Solidified Laser Molten Al—4.5 wt.% Cu Surfaces. 149-161B
- Electron beam vacuum melting**  
See Electron beam melting
- Electron microbeam analysis**  
See Electron probe analysis
- Electron microscopy**  
See Transmission electron microscopy
- Electron probe analysis**  
Measurement and Analysis of Distribution Coefficients in Fe—Ni Alloys Containing Sulfur and/or Phosphorus. II.—K<sub>Fe</sub>, K<sub>Co</sub>, and K<sub>Cu</sub>. 1871-1878A
- Electroreduction**  
See Electrowinning
- Electrowinning**  
Electrodeposition of Lead From Aqueous Acetate and Chloride Solutions. 489-496B
- Elongation**  
A Simplified Numerical Analysis of the Sheet Tensile Test. 2291-2298A
- Elongation, Microstructural effects**  
Effects of Temperature and Environment on Fatigue Crack Growth in Ordered (Fe, Ni)<sub>3</sub> V-Type Alloys. 815-820A  
The Effect of Hydrogen as a Temporary Alloying Element on the Microstructure and Tensile Properties of Ti—6Al—4V. 1077-1087A
- Elongation, Stress effects**  
Tensile Stress—Strain Analysis of Cold Worked Metals and Steels and Dual-Phase Steels. 865-872A
- Embrittlement**  
See also Hydrogen embrittlement
- Embrittlement, Environmental effects**  
The Effect of Environment on the Sustained Load Crack Growth Rates of Forged Waspaloy. 1515-1521A
- Endurance limit**  
See Fatigue limit
- Energy**  
See Activation energy  
Binding energy (nuclear)  
Free energy  
Heat of formation  
Heat of fusion  
Heat of mixing  
Specific heat  
Stacking fault energy  
Surface energy
- Energy of activation**  
See Activation energy
- Engineering**  
See also Technology transfer  
Of Perspectives, Issues, and Politics in Materials Technology. 5-11B  
Of Perspectives, Issues, and Politics in Materials Technology. 311-317A
- Entropy**  
See also Entropy of transformation  
Entropy Criteria Applied to Pattern Selection in Systems With Free Boundaries. 1781-1797A
- Entropy of transformation**  
Mobility of Martensitic Interfaces. 1713-1722A
- Environment**  
See Corrosion environments
- Epitaxial growth**  
The Ga—As—H—Cl Vapor Phase Epitaxial Growth System. 97-105B
- Equilibrium**  
See Chemical equilibrium
- Equilibrium constants**  
See Chemical equilibrium
- Equilibrium diagrams**  
See Phase diagrams
- Eutectic composition**  
The Morphology of Eutectic Carbides in M2-Grade High Speed Steel. 2341-2342A
- Eutectics**  
See also Directionally solidified eutectics
- Eutectics, Thermal properties**  
New Eutectic Alloys and Their Heats of Transformation. 323-328A
- Explosive compacting**  
Explosive Consolidation of Rapidly Solidified Aluminum Alloy Powders. 1445-1455A
- Explosive welding**  
Fundamental Aspects of Formation and Stability of Explosive Welds. 841-852A
- Extraction**  
See Solvent extraction
- Extractive metallurgy**  
See Hydrometallurgy
- Extrusion**  
See Hot extrusion
- Face centered cubic metals**  
See FCC metals
- Fatigue (materials)**  
See also Corrosion fatigue  
Fatigue life  
Fatigue limit  
Fatigue strength  
Low cycle fatigue  
Fatigue Crack Deflection and Fracture Surface Contact: Micromechanical Models. 249-260A  
A Note on Grain Boundary Diffusion Controlled Cavity Growth During Elevated-Temperature Fatigue. 300-302A  
Discussion of "Deformation Kinetics of Commercial Ti-50A (0.5 at.% Oeq) at Low Temperatures (T < 0.3 T<sub>m</sub>)" and Authors Reply. 694-697A  
Influence of Microstructure on Fatigue Crack Initiation in Fully Pearlitic Steels. 753-760A

## Fatigue (materials)

- Hardenability Behavior in Fatigue.** 2201-2214A
- Fatigue (materials), Alloying effects**  
Lithium-Containing Aluminum Alloys: Cyclic Fracture. 475-477A
- Fatigue (materials), Deformation effects**  
The Effect of Cold Rolling on the Fatigue Properties of Ti-6Al-4V. 144-145A
- Fatigue (materials), Diffusion effects**  
A Study of Fatigue Crack Propagation in Prior Hydrogen Attacked Pressure Vessel Steels. 1491-1501A
- Fatigue (materials), Heating effects**  
On the Development of Crack Closure and the Threshold Condition for Short and Long Fatigue Cracks in 7150 Aluminum Alloy. 1467-1477A
- Fatigue (materials), Microstructural effects**  
Effects of Temperature and Environment on Fatigue Crack Growth in Ordered (Fe, Ni)<sub>3</sub> V-Type Alloys.  
The Dependence of Some Tensile and Fatigue Properties of a Dual-Phase Steel on Its Microstructure. 815-820A  
1405-1415A
- Fatigue cracking**  
See Fatigue failure
- Fatigue failure**  
Fatigue Crack Deflection and Fracture Surface Contact: Micromechanical Models. 249-260A
- Fatigue failure, Corrosion effects**  
Fatigue Microcrack Initiation in Polycrystalline Alpha-Iron With Polished and Oxidized Surfaces. 641-649A
- Fatigue failure, Microstructural effects**  
High-Cycle Fatigue Properties of the ODS-Alloy MA 6000 at 850°C.  
Mechanism for the Formation of High Cycle Fatigue Cracks at FCC Annealing Twin Boundaries. 393-399A  
873-880A
- Fatigue fracture**  
See Fatigue failure
- Fatigue life, Environmental effects**  
Effects of Gaseous Hydrogen on Fatigue Crack Growth in Pipeline Steel. 115-122A
- Fatigue life, Microstructural effects**  
Effect of Inclusions on LCF Life of HIP Plus Heat Treated Powder Metal René 95.  
High Cycle Fatigue and Fatigue Crack Growth of the Oxide Dispersion Strengthened Alloy MA 754. 775-784B  
1437-1444A
- Fatigue limit, Microstructural effects**  
High-Cycle Fatigue Properties of the ODS-Alloy MA 6000 at 850°C. 393-399A
- Fatigue properties**  
See Fatigue (materials)
- Fatigue strength, Cooling effects**  
Mechanical Properties and Microstructure of Centrifugally Cast Alloy 718. 1295-1306A
- Fatigue strength, Microstructural effects**  
High-Cycle Fatigue Properties of the ODS-Alloy MA 6000 at 850°C.  
Microstructural Influences on Fatigue Crack Propagation in Ti-10V-2Fe-3Al. 393-399A  
739-751A
- FCC metals, Mechanical properties**  
Mechanism for the Formation of High Cycle Fatigue Cracks at FCC Annealing Twin Boundaries. 873-880A
- FCC metals, Structural hardening**  
Kinetics of Solution Hardening. 2109-2129A
- Ferrite, Structural hardening**  
Mechanical Properties of Nitrogen-Ferrite. 45-50A
- Ferritic stainless steels, Corrosion**  
Stress Corrosion Cracking of Stainless Steels. 1909-1923A
- Ferritic stainless steels, Mechanical properties**  
Mathematical Modeling of Thermal Stresses in Basic Oxygen Furnace Hood Tubes. 247-261B
- Ferritic stainless steels, Sorption**  
The Use of Palladium to Obtain Reproducible Boundary Conditions for Permeability Measurements Using Galvanostatic Charging. 715-719A
- Ferroalloys**  
See Ferroniobium
- Ferrocolumbium**  
See Ferroniobium
- Ferromagnetic films**  
See Ferromagnetic materials
- Ferromagnetic materials**  
Effect of Magnetic Transition on Solubility of Carbon in B.C.C. Iron and F.C.C. Co-Ni Alloys. 913-921A
- Ferroniobium, Reduction (chemical)**  
Separation of Niobium From Ferroniobium by Chlorination. 639-644B
- Ferrous alloys**  
See also Cast Iron Steels
- Ferrous alloys, Chemical analysis**  
Measurement and Analysis of Distribution Coefficients in Fe-Ni Alloys Containing Sulfur and/or Phosphorus. II.—K<sub>S</sub>, K<sub>Ge</sub>, and K<sub>Cu</sub>. 1871-1878A
- Ferrous alloys, Composite materials**  
Interdiffusional Effects Between Tungsten Fibers and an Iron-Nickel-Base Alloy. 1961-1968A
- Ferrous alloys, Corrosion**  
Formation of Aluminum Oxide Scales in Sulfur-Containing High Temperature Environments. 2051-2059A
- Ferrous alloys, Crystal lattices**  
On the Hierarchy of Interfacial Dislocation Structure. 529-541A
- Ferrous alloys, Mechanical properties**  
Low Temperature Mechanical Behavior of Microalloyed and Controlled-Rolled Fe-Mn-Al-C-X Alloys.  
Small-Angle Neutron Scattering Investigation of Creep Damage in Type 304 Stainless Steel and Alloy 800. 1669-1693A  
2283-2289A
- Ferrous alloys, Metallography**  
The Early Stages of the Decomposition of Alloys. 1173-1184A
- Ferrous alloys, Oxidation**  
An Effect of Chemisorbing Surface Reaction Poisons on the Transition From Internal to External Oxidation. 133-136A
- Ferrous alloys, Phase transformations**  
The Mean Size of Plate Martensite: Influence of Austenite Grain Size, Partitioning, and Transformation Heterogeneity.  
Crystallography and Tempering Behavior of Iron-Nitrogen Martensite.  
Mobility of Martensitic Interfaces. 329-336A  
1371-1384A  
1713-1722A
- Ferrous alloys, Phases (state of matter)**  
Phase Constitution and Lattice Parameter Relationships in Rapidly Solidified (Fe<sub>0.85</sub>Mn<sub>0.35</sub>Co<sub>0.85</sub>Al<sub>0.17</sub>-X C and Fe-Al-X C Pseudobinary Alloys.  
Equilibrium Solute Concentration Surrounding Elastically Interacting Precipitates.  
The Fe-Rich Corner of the Metastable C-Cr-Fe Liquidus Surface. 5-10A  
337-347A  
1541-1549A
- Ferrous alloys, Powder technology**  
Effect of Dihedral Angle on the Morphology of Grains in a Matrix Phase. 923-928A
- Ferrous alloys, Refining**  
Thermodynamic Properties of S-Fe-Co-Ni and Fe-Co-Ni Systems. 907-911A
- Ferrous alloys, Solubility**  
Nitrogen Solubility and Nitride Formation in Austenitic Fe-Ti Alloys. 815-822B
- Ferrous alloys, Sorption**  
The Use of Palladium to Obtain Reproducible Boundary Conditions for Permeability Measurements Using Galvanostatic Charging. 715-719A
- Ferrous alloys, Structural hardening**  
Precipitation Hardening. 2131-2165A
- Ferrous metals**  
See Ferrous alloys
- Fiber composites, Directional solidification**  
Microstructure and Crystallography of Unidirectionally Solidified Ni-W Eutectic Alloy. 1185-1193A
- Fiber composites, Mechanical properties**  
Mechanical Properties and Failure Characteristics of FP/Aluminum and W/Aluminum Composites.  
The Influence of Thermal Exposure on Interfacial Reactions and Strength in Aluminum Oxide Fiber Reinforced Magnesium Alloy Composites. 853-864A  
2069-2072A
- Fiber composites, Powder technology**  
The Effects of Hot Pressing Parameters on the Strength of Aluminum/Stainless Steel Composites. 623-628A
- Fiber composites, Reactions (chemical)**  
Interdiffusional Effects Between Tungsten Fibers and an Iron-Nickel-Base Alloy. 1961-1968A
- Fiber metallurgy**  
See Fiber composites
- Field ion microscopy**  
The Early Stages of the Decomposition of Alloys. 1173-1184A
- Fields (physics)**  
See Electromagnetic fields  
Magnetic fields
- Filler metal, Mechanical properties**  
The Relationship Between Microstructure and Fracture Behavior of Fully Austenitic Type 316L Weldments at 4.2K. 1835-1848A
- Films**  
See Thin films
- Filtering**  
See Filtration
- Filters (fluid)**  
Physical Refining of Steel Melts by Filtration. 725-742B
- Filtration**  
Physical Refining of Steel Melts by Filtration. 725-742B
- Finite element method**  
Stress Corrosion Cracking of an Aluminum Alloy Under Compressive Stress. 1663-1670A
- Finsider process**  
See Direct reduction
- Flame reduction process**  
See Direct reduction
- Flash smelting**  
Oxidation of Pyrrhotite Particles Falling Through a Vertical Tube. 627-638B



- Flexural vibration**  
See Fatigue (materials)
- Flow**  
See Fluid flow  
Plastic flow  
Turbulent flow
- Flow stress**  
See Yield strength
- Fluid bed reduction**  
See Fluidized bed reduction
- Fluid dynamics**  
See Hydrodynamics
- Fluid flow**  
See also Turbulent flow  
Turbulent Fluid Flow Phenomena in a Water Model of an AOD System. 67-75B  
Fluid Flow and Weld Penetration in Stationary Arc Welds. 203-213A  
Numerical Calculation of Fluid Flow in a Continuous Casting Tundish. 497-504B  
Influence of Dendrite Network Defects on Channel Segregate Growth. 1687-1689A  
Flow of Interdendritic Liquid and Permeability in Pb—20Sn Alloys. 2263-2271A
- Fluid flow, Field effects**  
Fluid Flow Phenomena in a Single Phase Coreless Induction Furnace. 227-235B
- Fluid flow, Pressure effects**  
A Model for Deformation and Segregation of Solid—Liquid Mixtures. 1393-1403A
- Fluid form deep drawing**  
See Deep drawing
- Fluid mechanics**  
See Hydrodynamics
- Fluidized bed reduction**  
The Reduction of Hematite to Wustite in a Laboratory Fluidized Bed. 425-432B
- Fluidized beds, Corrosion**  
Hot Corrosion of B-1900 in  $\text{CaSO}_4/\text{Na}_2\text{SO}_4$  Salt Mixtures in Reducing Atmospheres. 291-297A
- Fluids**  
See Gases
- Fluorocarbons**  
See Halocarbons
- Flux**  
Distribution of the Heat and Current Fluxes in Gas Tungsten Arcs. 841-846B
- Flux density**  
See Flux
- Fluxes**  
See Welding fluxes
- Fluxing**  
Thermodynamics of Removing Selenium and Tellurium From Liquid Copper by Sodium Carbonate Slags. 171-172B
- Focussing**  
See Displacements (lattice)
- Foil (metal), Crystal lattices**  
Impurity Effect on Cube Texture in Pure Aluminum Foils. 27-36A
- Foil (metal), Diffusion**  
The Effect of Pressure Modulation on the Flow of Gas Through a Solid Membrane: Surface Inhibition and Internal Traps. 1013-1024A
- Force**  
See Cyclic loads  
Shock loading
- Forging**  
See Hot forging  
Liquid metal forging
- Formability**  
Hill's Plastic Strain Ratio of Sheet Metals. 1531-1535A  
A Simplified Numerical Analysis of the Sheet Tensile Test. 2291-2298A  
An Analysis of the Nonisothermal Tensile Test. 2299-2308A
- Formability, Microstructural effects**  
Plastic Behavior of Dual Phase Steel Following Plane-Strain Deformation. 421-425A  
Microstructure—Mechanical Property Relationships of Dual-Phase Steel Wire. 831-840A
- Forming**  
See Cold rolling  
Controlled rolling  
Deep drawing  
Hot extrusion  
Hot isostatic pressing  
Hot pressing  
Liquid metal forging  
Stamping  
Stretch forming  
Swaging  
Thermomechanical treatment  
Wire drawing
- Fossil fuels**  
See Coal  
Sour gas
- Fracture mechanics**  
See also Crack opening displacement  
Investigation of Stress Corrosion Crack Growth in Magnesium Alloys Using J-Integral Estimations. 101-108A  
On Macroscopic and Microscopic Analyses for Crack Initiation and Crack Growth Toughness in Ductile Alloys. 233-248A  
Fatigue Crack Deflection and Fracture Surface Contact: Micromechanical Models. 249-260A  
Lithium-Containing Aluminum Alloys: Cyclic Fracture. 475-477A  
Fracture Toughness and Its Development in High Purity Cast Carbon and Low Alloy Steels. 613-622A  
Correction to "On Macroscopic and Microscopic Analyses for Crack Initiation and Crack Growth Toughness in Ductile Alloys". 1358A  
A Plastic Flow Induced Fracture Theory for  $K_{ISCC}$ . 2333-2340A
- Fracture mechanics, Microstructural effects**  
The Influence of Thermal Exposure on Interfacial Reactions and Strength in Aluminum Oxide Fiber Reinforced Magnesium Alloy Composites. 2069-2072A
- Fracture toughness**  
On Macroscopic and Microscopic Analyses for Crack Initiation and Crack Growth Toughness in Ductile Alloys. 233-248A  
Analysis of Stress—Strain, Fracture, and Ductility Behavior of Aluminum Matrix Composites Containing Discontinuous Silicon Carbide Reinforcement. 1105-1115A  
Correction to "On Macroscopic and Microscopic Analyses for Crack Initiation and Crack Growth Toughness in Ductile Alloys". 1358A  
Binder Deformation in WC—(Co, Ni) Cemented Carbide Composites. 2309-2317A
- Fracture toughness, Composition effects**  
Fracture Toughness and Its Development in High Purity Cast Carbon and Low Alloy Steels. 613-622A
- Fracture toughness, Diffusion effects**  
Hydrogen Degradation of Spheroidized AISI 1090 Steel. 1417-1425A
- Fracture toughness, Environmental effects**  
Effects of Gaseous Hydrogen on Fatigue Crack Growth in Pipeline Steel. 115-122A
- Fracture toughness, Heating effects**  
Effect of Single Aging on Microstructure and Impact Property of INCONEL X-750. 821-829A
- Fracture toughness, Microstructural effects**  
A Mössbauer Spectrometry Study of the Mechanical Transformation of Precipitated Austenite in 6Ni Steel. 173-177A  
Correlation of Microstructure and Fracture Toughness in Two 4340 Steels. 1633-1648A  
The Relationship Between Microstructure and Fracture Behavior of Fully Austenitic Type 316L Weldments at 4.2K. 1835-1848A
- Fracturing**  
See Ductile fracture  
Intergranular fracture
- Free energy**  
See also Activation energy  
Stacking fault energy  
Thermodynamics of Formation of Y—Co Alloys. 1195-1201A
- Free energy, Field effects**  
Magnetic Contributions to the Thermodynamic Functions of Pure Nickel, Cobalt and Iron. 153-165A
- Free energy of activation**  
See Activation energy
- Fuel elements**  
See Nuclear fuel elements
- Fuels**  
See Coal  
Sour gas
- Fuming (slag)**  
See Slag fuming
- Furnaces**  
See AOD vessels  
Basic converters  
Coreless induction furnaces  
Kilns
- Fused salt electrolysis**  
Determination of the Lithium Content of Molten Aluminum Using a Solid Electrolyte. 41-46B
- Fused salts, Thermal properties**  
A Two-Sublattice Model for Molten Solutions With Different Tendency for Ionization. 261-266A
- Fusion welding**  
See Gas tungsten arc welding  
Laser beam welding  
Shielded metal arc welding  
Submerged arc welding
- Galena, Reduction (chemical)**  
Representation of the Kinetics of Leaching of Galena by Ferric Chloride in Concentrated Sodium Chloride Solutions by a Modified Mixed Kinetics Model. 31-39B
- Gallium, Binary systems**  
The Structure of  $\text{R}_{1-x}\text{Ga}_x$  ( $0 < x < 0.33$ ) and Its Relation to  $\text{RGa}$  (R = Rare Earth Element) and Gallium. 167-171A
- Gallium, Ternary systems**  
Phases in Ni—Co—Ga Alloys Close to (Ni,  $\text{Co}_{0.5}\text{Ga}_{0.5}$ ). 1159-1160A
- Gallium arsenide, Crystal growth**  
The Ga—As—H—Cl Vapor Phase Epitaxial Growth System. 97-105B

## Gallium compounds

**Gallium compounds**  
See Gallium arsenide

**Galvannealing**  
See Annealing

**Gas**  
See Gases

**Gas permeability**  
See Permeability

**Gas phases**  
Computation of Gas Phase Equilibria—a General Algorithm Using the Newton—Raphson Method. 793-799B

**Gas tungsten arc welding**  
Fluid Flow and Weld Penetration in Stationary Arc Welds. 203-213A  
Distribution of the Heat and Current Fluxes in Gas Tungsten Arcs. 841-846B  
Discussion of "Microstructural and Mechanical Properties of a Welded Titanium Alloy" and Authors' Reply. 987A  
Grain Structure and Solidification Cracking in Oscillated Arc Welds of 5052 Aluminum Alloy. 1345-1352A  
Alternating Grain Orientation and Weld Solidification Cracking. 1887-1896A

**Gas turbines**  
Microstructural Development in High Volume Fraction Gamma Prime Ni-Base Oxide-Dispersion-Strengthened Superalloys. 1285-1294A  
High Cycle Fatigue and Fatigue Crack Growth of the Oxide Dispersion Strengthened Alloy MA 754. 1437-1444A  
The Effect of Environment on the Sustained Load Crack Growth Rates of Forged Waspaloy. 1515-1521A

**Gases, Diffusion**  
The Effect of Pressure Modulation on the Flow of Gas Through a Solid Membrane: Surface Inhibition and Internal Traps. 1013-1024A

**Gasification**  
See Coal gasification

**Gating and risering**  
Modeling of Heat Flow in Sand Castings. I.—The Boundary Curvature Method. 195-202B

**Gearing**  
See Gears

**Gears**  
Fatigue Crack Propagation in Carburized X-2M Steel. 1267-1271A

**Gibbs free energy**  
See Free energy

**Glass**  
See Metallic glasses

**Gold, Crystal lattices**  
On the Hierarchy of Interfacial Dislocation Structure. 529-541A

**Gold, Extraction**  
Heterogeneous Equilibria in the Au—CN—H<sub>2</sub>O and Ag—CN—H<sub>2</sub>O Systems. 455-463B

**Gold, Recovering**  
Distribution of Gold and Silver Between Copper and Matte. 53-59B

**Gold base alloys, Thermal properties**  
Thermochemistry of Binary Liquid Gold Alloys: the Systems (Gold + Chromium), (Gold + Vanadium), (Gold + Titanium) and (Gold + Scandium) at 1379K. 93-99A

**Grain boundaries**  
Driving Force for Discontinuous Coarsening in a Ni—Al—Mo Base Superalloy. 11-16A  
Serrated Grain Boundary Formation Potential of Nickel-Based Superalloys and Its Implications. 17-26A  
Subcritical Intergranular Crack Growth Rates and Thresholds of Iron and Iron + Antimony. 123-131A  
The Influence of Grain Boundary Precipitation on the Measurement of Chromium Redistribution and Phosphorus Segregation in Ni—18Cr—9Fe. 349-359A  
On the Hierarchy of Interfacial Dislocation Structure. Discussion of "An Analytical Electron Microscope Study of the Kinetics of the Equilibrium Segregation of Bismuth in Copper" and Authors Reply. 529-541A  
Lattice Image Studies on the Intervariant Boundary Structure and Substructure of Cu—Zn—Al 18R Martensite. 688-690A  
Grain Boundary Segregation of Phosphorus in 304L Stainless Steel. 1551-1566A  
2061-2062A

**Grain boundaries, Diffusion**  
Trapping of Hydrogen and Helium at Grain Boundaries in Nickel: an Atomistic Study. 1625-1631A

**Grain boundaries, Mechanical properties**  
The Embrittlement of Al—Zn—Mg and Al—Mg Alloys by Water Vapor. 1503-1514A

**Grain growth**  
Austenitization During Intercritical Annealing of an Fe—C—Si—Mn Dual-Phase Steel. 1237-1245A  
Correlation of Microstructure and Fracture Toughness in Two 4340 Steels. 1633-1648A

**Grain growth, Microstructural effects**  
The Effect of Initial Carbide Morphology on Abnormal Grain Growth in Decarburized Low Carbon Steel. 897-906A

**Grain growth, Temperature effects**  
Experimental Observations on the Nucleation and Growth of  $\delta'$  (Al<sub>3</sub>Li) in Dilute Al—Li Alloys. 1203-1211A

**Grain orientation**  
Deformation Characteristics in Beta Phase Ti—Nb Alloys. 789-795A

Mechanism for the Formation of High Cycle Fatigue Cracks at FCC Annealing Twin Boundaries. 873-880A  
Effect of Dihedral Angle on the Morphology of Grains in a Matrix Phase. 923-928A  
Crystallography and Tempering Behavior of Iron—Nitrogen Martensite. 1371-1384A  
Transmission Kossel Study of the Formation of (110)[001] Grains After an Intermediate Annealing in Grain Oriented Silicon Steel Containing a Small Amount of Molybdenum. 1613-1623A

**Grain orientation, Vibration effects**  
Alternating Grain Orientation and Weld Solidification Cracking. 1887-1896A

**Grain refinement**  
Grain Refinement of Copper by the Addition of Iron and by Electromagnetic Stirring. 505-511B  
Coarsening Rate of Beta Precipitates in Al—11Mg Alloy. 709-713A  
Thermomechanical Processing of Microalloyed Powder Forged Steels and a Cast Vanadium Steel. 1599-1608A  
Transmission Kossel Study of the Formation of (110)[001] Grains After an Intermediate Annealing in Grain Oriented Silicon Steel Containing a Small Amount of Molybdenum. 1613-1623A  
Grain Refinement of Aluminum by TiC. 2065-2068A

**Grain refinement, Field effects**  
A Novel Solidification Technique of Metals and Alloys: Under the Influence of Applied Potential. 1354-1355A

**Grain refinement, Vibration effects**  
Grain Structure and Solidification Cracking in Oscillated Arc Welds of 5052 Aluminum Alloy. 1345-1352A

**Grain size**  
Effect of Carbon Content and Ferrite Grain Size on the Tensile Flow Stress of Ferritic Spheroidal Graphite Cast Iron. 667-673A  
High Temperature Deformation of Ultra-Fine-Grained Oxide Dispersion Strengthened Alloys. 777-787A  
The Effect of Grain Size and Plastic Strain on Slip Length in 70-30 Brass. 1025-1029A  
The Effect of Grain Morphology on Longitudinal Creep Properties of INCONEL MA 754 at Elevated Temperatures. 1307-1324A

**Grain size, Alloying effects**  
Grain Refinement of Copper by the Addition of Iron and by Electromagnetic Stirring. 505-511B

**Grain size, Deformation effects**  
Effect of Cold Work on Recrystallization Behavior and Grain Size Distribution in Titanium. 703-708A

**Grain size, Heating effects**  
Coarsening Rate of Beta Precipitates in Al—11Mg Alloy. 709-713A  
The Effect of Microstructural Changes on the Caustic Stress Corrosion Cracking Resistance of a NiCrMoV Rotor Steel. 1333-1344A

**Grain structure**  
Effect of Dihedral Angle on the Morphology of Grains in a Matrix Phase. 923-928A  
Microstructural Development in High Volume Fraction Gamma Prime Ni-Base Oxide-Dispersion-Strengthened Superalloys. 1285-1294A  
On the Relation Between Grain Size and Grain Topology. 2007-2011A

**Grain structure, Alloying effects**  
The Effect of Hydrogen as a Temporary Alloying Element on the Microstructure and Tensile Properties of Ti—6Al—4V. 1077-1087A

**Grain structure, Cooling effects**  
The Microstructure of Rapidly Solidified Al<sub>6</sub>Mn. 1005-1012A  
Rapid Solidification Characteristics in Melt Spinning a Nickel-Base Superalloy. 1773-1779A

**Grain structure, Heating effects**  
The Formation of Austenite at Low Intercritical Annealing Temperatures in a Normalized 0.08C—1.45Mn—0.21Si Steel. 1523-1526A

**Grain structure, Vibration effects**  
Grain Structure and Solidification Cracking in Oscillated Arc Welds of 5052 Aluminum Alloy. 1345-1352A

**Gravitation**  
Superalloy Microstructural Variations Induced by Gravity Level During Directional Solidification. 1683-1687A

**Gravity**  
See Gravitation

**Gray iron**  
See Nodular iron

**Growth**  
See Crystal growth  
Epitaxial growth  
Grain growth  
Growth rate

**Growth rate**  
Use of Stereological Measurements for the Study of Grain Boundary Diffusion Controlled Precipitate Growth Kinetics. Estimation of Nucleation Rate and Growth Rate From Time Dependence of Global Microstructural Properties During Phase Transformations. 559-564A  
Cellular and Dendritic Growth. I.—Experiment. 1799-1805A  
Cellular and Dendritic Growth. II.—Theory. 1807-1814A

**Growth rate, Cooling effects**  
Rapid Solidification Characteristics in Melt Spinning a Nickel-Base Superalloy. 1773-1779A

**Hafnium, Alloying elements**  
Sulfation of Y<sub>2</sub>O<sub>3</sub> and HfO<sub>2</sub> in Relation to MCrAl Coatings. 303-306A

**Halides**  
See Chlorides  
Sodium chloride

- Halocarbons**  
Formation of Chlorinated Carbon Products During Carbochlorination Reactions. 847-849B
- Halogenation**  
See Chlorination
- Halogens**  
See Chlorine
- Hard metals**  
See Cemented carbides
- Hardenability**  
See Strain hardenability
- Hardening**  
See Aging (artificial)  
Carburizing  
Dispersion hardening  
Precipitation hardening  
Solution strengthening  
Strain aging  
Strain hardening
- Hardmetals**  
See Cemented carbides
- Hardness, Deformation effects**  
Effect of Cold Work on Recrystallization Behavior and Grain Size Distribution in Titanium. 703-708A  
Adiabatic Shear Localization in Titanium and Ti—6Al—4V Alloy. 761-775A
- Hardness, Heating effects**  
Coarsening Rate of Beta Precipitates in Al—11Mg Alloy. 709-713A  
Effect of Single Aging on Microstructure and Impact Property of INCONEL X-750. 821-829A  
Crystallography and Tempering Behavior of Iron—Nitrogen Martensite. 1371-1384A
- Hardness, Microstructural effects**  
Microstructure—Mechanical Property Relationships of Dual-Phase Steel Wire. 831-840A
- Hazelett process**  
See Continuous casting
- HCP metals, Crystal lattices**  
An X-Ray Diffraction Line Profile of Cold-Worked Hexagonal Alloys Zn—Ag:  $\eta$  and  $\epsilon$  Phase. 1427-1435A
- Heat affected zone, Microstructure**  
Discussion of "Microstructural and Mechanical Properties of a Welded Titanium Alloy" and Authors' Reply. 987A
- Heat capacity**  
See Specific heat
- Heat flow**  
See Heat transmission
- Heat flux**  
See Heat transmission
- Heat of decomposition**  
See Heat of formation
- Heat of dissociation**  
See Heat of formation
- Heat of formation**  
The Utilization of Galvanic Cells Using Ca Beta Double Prime—Alumina Solid Electrolytes in a Thermodynamic Investigation of the CaO—Al<sub>2</sub>O<sub>3</sub> System. 107-112B  
Thermodynamics of Formation of Y—Ni Alloys. 577-584B
- Heat of fusion, Thermal properties**  
New Eutectic Alloys and Their Heats of Transformation. 323-328A
- Heat of mixing**  
Thermochemistry of Binary Liquid Gold Alloys: the Systems (Gold + Chromium), (Gold + Vanadium), (Gold + Titanium) and (Gold + Scandium) at 1379K. 93-99A
- Heat of mixing, Composition effects**  
A Two-Sublattice Model for Molten Solutions With Different Tendency for Ionization. 261-266A
- Heat of solidification**  
See Heat of fusion
- Heat resistant alloys**  
See Superalloys
- Heat storage, Alloy development**  
New Eutectic Alloys and Their Heats of Transformation. 323-328A
- Heat transfer**  
Turbulent Fluid Flow Phenomena in a Water Model of an AOD System. 67-75B  
Fluid Flow and Weld Penetration in Stationary Arc Welds. 203-213A  
The Influence of Convection on Heat Transfer in Liquid Tin. Metal/Mold Interfacial Heat Transfer. 355-357B  
585-594B
- Heat transmission**  
Modeling of Heat Flow in Sand Castings. I.—The Boundary Curvature Method. 195-202B  
Modeling of Heat Flow in Sand Castings. II.—Applications of the Boundary Curvature Method. 203-209B
- Heat treatment**  
See Aging (artificial)  
Annealing  
Austempering  
Austenitizing  
Carburizing  
Grain refinement
- Isothermal annealing  
Precipitation hardening  
Precipitation heat treatment  
Solution annealing  
Solution heat treatment  
Spheroidizing  
Tempering
- Heating**  
See Laser beam heating  
Solar heating
- Heats (energies)**  
See Heat of formation  
Heat of fusion  
Heat of mixing  
Specific heat
- Heavy metals**  
See Antimony  
Bismuth  
Cadmium  
Lead (metal)  
Tin
- Heliarc welding**  
See Gas tungsten arc welding
- Helium, Diffusion**  
Trapping of Hydrogen and Helium at Grain Boundaries in Nickel: an Atomistic Study. 1625-1631A
- Helmholtz free energy**  
See Free energy
- Hematite, Reduction (chemical)**  
The Leaching of Hematite in Acid Solutions. 23-30B  
The Reduction of Hematite to Wustite in a Laboratory Fluidized Bed. 425-432B
- Hexagonal close packed metals**  
See HCP metals
- High alloy steels**  
See Austenitic stainless steels  
Ferritic stainless steels  
Stainless steels
- High speed tool steels, Phases (state of matter)**  
The Morphology of Eutectic Carbides in M2-Grade High Speed Steel. 2341-2342A
- High strength low alloy steels, Corrosion**  
The Role of Aging Reactions in the Hydrogen Embrittlement Susceptibility of an HSLA Steel. 1879-1886A
- High strength low alloy steels, Diffusion**  
Trapping of Hydrogen by Sulfur-Associated Defects in Steel. 401-409A
- High strength low alloy steels, Mechanical properties**  
Effect of Finish Rolling Temperature on the Structure and Properties of Directly Quenched Nb Containing Low Steel. 471-474A
- High strength low alloy steels, Metal working**  
Effects of Plastic Anisotropy and Yield Surface Shape on Sheet Metal Stretchability. 629-639A
- High strength low alloy steels, Phase transformations**  
Growth Kinetics and Morphology of Grain Boundary Ferrite Allotriomorphs in an Fe—C—V Alloy. 521-527A
- High strength low alloy steels, Powder technology**  
Thermomechanical Processing of Microalloyed Powder Forged Steels and a Cast Vanadium Steel. 1599-1608A
- High strength low alloy steels, Refining**  
Equilibria Between Rare Earth Elements and Sulfur in Molten Iron. 785-792B
- High strength steels, Diffusion**  
Tetragonal Distortion Field of Hydrogen Atoms in Iron. 1649-1653A
- High strength steels, Heat treatment**  
Modified Heat Treatment for Lower Temperature Improvement of the Mechanical Properties of Two Ultra-High-Strength Low-Alloy Steels. 83-91A
- High strength steels, Mechanical properties**  
Mechanical Properties of 0.40% C—Ni—Cr—Mo High-Strength Steel Having a Mixed Structure of Martensite and Bainite. 73-82A  
A "Hydrogen Partitioning" Model for Hydrogen Assisted Crack Growth. 2039-2050A
- High strength steels, Metal working**  
Plastic Behavior of Dual Phase Steel Following Plane-Strain Deformation. 421-425A
- HIP**  
See Hot isostatic pressing
- Historical metallurgy**  
Of Perspectives, Issues, and Politics in Materials Technology. 5-11B  
Of Perspectives, Issues, and Politics in Materials Technology. 311-317A
- Hot compression**  
See Hot pressing
- Hot cracking (welds)**  
See Weld defects
- Hot deformation**  
See Deformation
- Hot ductility**  
See Ductility

## Hot extrusion

- Hot extrusion**  
Product Microstructures and Properties Induced by Hot Working at Pb—1.85% Sb Alloy. 1273-1285A
- Hot forging**  
Thermomechanical Processing of Microalloyed Powder Forged Steels and a Cast Vanadium Steel. 1599-1606A
- Hot gas corrosion**  
Hot Corrosion of B-1900 in  $\text{CaSO}_4/\text{Na}_2\text{SO}_4$  Salt Mixtures in Reducing Atmospheres. 291-297A
- Hot hardness**  
See Hardness
- Hot isostatic pressing**  
Thermally Induced Porosity in Ti—6Al—4V Prealloyed Powder Compacts. 1526-1531A  
Microporosity in Hot Isostatically Pressed Ti—6Al—4V Powder Compacts. 1831-1834A  
Discussion of "Practical Applications of Hot-Isostatic Pressing Diagrams: From Case Studies". 1903-1904A
- Hot pressing**  
See also Hot isostatic pressing  
The Effects of Hot Pressing Parameters on the Strength of Aluminum/Stainless Steel Composites. 623-628A
- Hot strength**  
See Tensile strength
- Hot stretch forming**  
See Stretch forming
- Hot swaging**  
See Swaging
- Hot tensile strength**  
See Tensile strength
- Hot work tool steels, Mechanical properties**  
Fatigue Crack Propagation in Carburized X-2M Steel. 1267-1271A
- Hot working**  
See Hot extrusion  
Hot forging
- Huey test**  
Grain Boundary Segregation of Phosphorus in 304L Stainless Steel. 2061-2062A
- Hydrodynamics**  
Fluid Flow Phenomena in a Single Phase Coreless Induction Furnace. 227-235B
- Hydrogen, Alloying additive**  
The Effect of Hydrogen as a Temporary Alloying Element on the Microstructure and Tensile Properties of Ti—6Al—4V. 1077-1087A
- Hydrogen, Diffusion**  
X-Ray Diffraction and Resistivity Studies of Titanium—Molybdenum Alloys. 187-195A  
Trapping of Hydrogen by Sulfur-Associated Defects in Steel. Identification of Defects Generated During Cathodic Charging in Pure Iron by Thermal Analysis Technique. 468-471A  
The Effect of Pressure Modulation on the Flow of Gas Through a Solid Membrane: Surface Inhibition and Internal Traps. 1013-1024A  
Hydrogen Degradation of Spheroidized AISI 1090 Steel. 1417-1425A  
A Study of Fatigue Crack Propagation in Prior Hydrogen Attacked Pressure Vessel Steels. 1491-1501A  
Trapping of Hydrogen and Helium at Grain Boundaries in Nickel: an Atomistic Study. 1625-1631A  
Tetragonal Distortion Field of Hydrogen Atoms in Iron. 1649-1653A  
Effect of Hydrogen on the Young's Modulus of Iron. 1655-1662A  
The Role of Aging Reactions in the Hydrogen Embrittlement Susceptibility of an HSLA Steel. 1879-1886A
- Hydrogen, Environment**  
Effects of Gaseous Hydrogen on Fatigue Crack Growth in Pipeline Steel. 115-122A
- Hydrogen, Impurities**  
Studies on the Analysis of Hydrogen in High Strength Steels. 1694-1695A
- Hydrogen, Solubility**  
Isopiestic Solubility of Hydrogen in Vanadium Alloys at Low Temperatures. 367-374A
- Hydrogen, Sorption**  
The Use of Palladium to Obtain Reproducible Boundary Conditions for Permeability Measurements Using Galvanostatic Charging. 715-719A
- Hydrogen compounds**  
See Inorganic acids
- Hydrogen embrittlement**  
Effects of Hydrogen on Some Mechanical Properties of Vanadium—Titanium Alloys. 59-66A  
Identification of Defects Generated During Cathodic Charging in Pure Iron by Thermal Analysis Technique. 468-471A  
Sulfide Stress Cracking of High Strength Modified Cr—Mo Steels. 935-944A  
Effect of Cobalt Content on the Stress-Corrosion Cracking Behavior of 7091-Type Aluminum Powder Alloys. 945-951A  
Crack Size Effects on the Chemical Driving Force for Aqueous Corrosion Fatigue. 953-969A  
Stress Corrosion Cracking of Alpha—Beta Brass in Distilled Water and Sodium Sulfate Solutions. 971-978A  
Discussion of "Effects of Tempering on the Carbon Activity and Hydrogen Attack Kinetics of 2.25Cr—1Mo Steel" and Authors' Reply. 1355-1357A  
Hydrogen Degradation of Spheroidized AISI 1090 Steel. 1417-1425A  
A Study of Fatigue Crack Propagation in Prior Hydrogen Attacked Pressure Vessel Steels. 1491-1501A
- The Embrittlement of Al—Zn—Mg and Al—Mg Alloys by Water Vapor. 1503-1514A  
Tetragonal Distortion Field of Hydrogen Atoms in Iron. 1649-1653A  
A "Hydrogen Partitioning" Model for Hydrogen Assisted Crack Growth. 2039-2050A  
A Plastic Flow Induced Fracture Theory for  $K_{ISCC}$ . 2333-2340A
- Hydrogen embrittlement, Heating effects**  
The Role of Aging Reactions in the Hydrogen Embrittlement Susceptibility of an HSLA Steel. 1879-1886A
- Hydrogen embrittlement, Pressure effects**  
Hydrogen Attack Kinetics of 2.25 Cr—1 Mo Steel Weld Metals. 1143-1149A
- Hydrogen embrittlement, Stress effects**  
The Influence of Multiaxial States of Stress on the Hydrogen Embrittlement of Zirconium Alloy Sheet. 675-681A
- Hydrogen reduction**  
Intrinsic Kinetics of the Hydrogen Reduction of Copper Sulfate: Determination by a Nonisothermal Technique. 397-401B  
Successive Gas—Solid Reaction Model for the Hydrogen Reduction of Cuprous Sulfide in the Presence of Lime. 645-662B  
Intrinsic Kinetics of the Hydrogen Reduction of  $\text{Cu}_2\text{S}$ . 831-839B
- Hydromechanics**  
See Hydrodynamics
- Hydrometallurgy**  
Heterogeneous Equilibria in the Au—CN— $\text{H}_2\text{O}$  and Ag—CN— $\text{H}_2\text{O}$  Systems. 455-463B
- Hydroxides**  
See Sodium hydroxide
- Hysteresis**  
Hardening Behavior in Fatigue. 2201-2214A
- Impact strength, Deformation effects**  
Adiabatic Shear Localization in Titanium and Ti—6Al—4V Alloy. 761-775A
- Impact strength, Heating effects**  
Observations of Adiabatic Shear Band Formation in 7039 Aluminum Alloy. 1900-1903A
- Impact strength, Low temperature effects**  
Low Temperature Mechanical Behavior of Microalloyed and Controlled-Rolled Fe—Mn—Al—C—X Alloys. 1689-1693A
- Impact strength, Microstructural effects**  
The Stability of Precipitated Austenite and the Toughness of 9Ni Steel. 2237-2249A
- Impact toughness**  
See Impact strength
- Impermeability**  
See Permeability
- Impurities**  
See also Interstitial impurities
- Impurities, Diffusion**  
Grain Boundary Fracture of  $\text{L}_{12}$  Type Intermetallic Compound  $\text{Ni}_3\text{Al}$ . 441-443A
- In situ leaching**  
Catalytic Decomposition of Hydrogen Peroxide by Ferric Ion in Dilute Sulfuric Acid Solutions. 181-186B
- Inclusions**  
See also Nonmetallic inclusions  
Examination of the Strength of Oxide Skins on Aluminum Alloy Melts. 47-51B  
Effect of Inclusions on LCF Life of HIP Plus Heat Treated Powder Metal René 95. 775-784B
- Inconel, Mechanical properties**  
High Cycle Fatigue and Fatigue Crack Growth of the Oxide Dispersion Strengthened Alloy MA 754. 1437-1444A
- Indium, Chemical analysis**  
A New Type of Oxygen Analyzer Utilizing a Potentiostatic Coulometric Titration Technique. 113-119B
- Inert gas welding**  
See Gas tungsten arc welding
- Ingot casting**  
Experimental Study of Continuous Electromagnetic Casting of Aluminum Alloys. 377-384B
- Injection**  
A Unified Approach to Bubbling—Jetting Phenomena in Powder Injection Into Iron and Steel. 203-209B
- Inorganic acids, Environment**  
Dislocation Structures of Monocrystalline Copper During Corrosion Fatigue in 0.1 M Perchloric Acid. 1151-1157A
- Inorganic salts, Environment**  
Mechanical Properties of a Low Alloy Steel in a Molten Nitrate Salt Environment. 1031-1041A
- Inter crystalline structure**  
See Intergranular structure
- Interface reactions**  
Interfacial Phenomena Between Molten Metals and Sapphire Substrate. 567-575B  
Microstructural Investigation of Intermediate Phase Formation in Uranium—Aluminum Diffusion Couples. 589-595A  
Fundamental Aspects of Formation and Stability of Explosive Welds. 841-852A  
Displacement Reactions Between Chromium and  $\text{MoO}_2$  in a Nickel-Base Alloy Matrix. 1815-1830A



- Interdiffusional Effects Between Tungsten Fibers and an Iron-Nickel-Base Alloy.**  
The Influence of Thermal Exposure on Interfacial Reactions and Strength in Aluminum Oxide Fiber Reinforced Magnesium Alloy Composites. 1961-1968A 2069-2072A
- Interface reactions, Pressure effects**  
Pressure Effects in Multiphase Binary Diffusion Couples. 605-611A
- Interfaces**  
Metal/Mold Interfacial Heat Transfer. 585-594B  
Atom-Probe Microanalysis of a Nickel-Base Superalloy. 1703-1711A  
The Influence of Thermal Exposure on Interfacial Reactions and Strength in Aluminum Oxide Fiber Reinforced Magnesium Alloy Composites. 2069-2072A
- Interfacial energy**  
See Surface energy
- Interfacial surface tension**  
See Surface tension
- Intergranular corrosion, Alloying effects**  
The Embrittlement of Al-Zn-Mg and Al-Mg Alloys by Water Vapor. 1503-1514A
- Intergranular fracture, Microstructural effects**  
Grain Boundary Fracture of L<sub>1</sub>2 Type Intermetallic Compound Ni<sub>3</sub>Al. 441-443A
- Intergranular fracture, Temperature effects**  
Variation of the Fracture Mode in Temper Embrittled 2.25 Cr-1 Mo Steel. 1325-1331A
- Intergranular structure, Cooling effects**  
Low Temperature Carbide Precipitation in a Nickel Base Superalloy. 1213-1223A
- Intergranular structure, Heating effects**  
Austenitization During Intercritical Annealing of an Fe-C-Si-Mn Dual-Phase Steel. 1237-1245A
- Intermetallic phases**  
Thermodynamics of Formation of Y-Ni Alloys. 577-584B  
The Microstructure of Rapidly Solidified Al<sub>6</sub>Mn. 1005-1012A
- Intermetallic phases, Alloying effects**  
Ordering Reactions in Ni-Al-Mo-Ta and Ni-Al-Mo-W Superalloys. 1983-1995A  
Rhenium Additions to a Nickel-Base Superalloy: Effects on Microstructure. 1997-2005A
- Intermetallic phases, Chemical analysis**  
Atom-Probe Microanalysis of a Nickel-Base Superalloy. 1703-1711A  
Microanalytical Study of the Heterogeneous Phases in Commercial Al-Zn-Mg-Cu Alloys. 1925-1936A  
Mössbauer Effect of Al-Fe-Si Intermetallic Compounds. 1937-1942A
- Intermetallic phases, Crystal growth**  
Pressure Effects in Multiphase Binary Diffusion Couples. 605-611A
- Intermetallic phases, Crystal lattices**  
The Structure of R<sub>1</sub>(1-x)Ga<sub>2</sub>(1-x) (0 < x < 0.33) and Its Relation to RGe<sub>2</sub> (R = Rare Earth Element) and Gallium. 167-171A
- Intermetallic phases, Heating effects**  
Carbide Stability in Nimonic 80A Alloy. 511-520A
- Internal oxidation**  
Displacement Reactions Between Chromium and MoO<sub>2</sub> in a Nickel-Base Alloy Matrix. 1815-1830A
- Internal oxidation, Environmental effects**  
An Effect of Chemisorbing Surface Reaction Poisons on the Transition From Internal to External Oxidation. 133-136A
- Internal stress**  
See Residual stress
- Interstitial defects**  
See Interstitial impurities
- Interstitial impurities, Diffusion**  
Short-Range Reordering of Heavy Interstitials in Ta, Nb, and Fe During Relaxation and Static Strain Aging. 361-366A
- Intragranular structure**  
Serrated Grain Boundary Formation Potential of Nickel-Based Superalloys and Its Implications. 17-26A
- Iron**  
See also Alpha iron  
Cast iron  
Nodular iron
- Iron, Alloying additive**  
Grain Refinement of Copper by the Addition of Iron and by Electromagnetic Stirring. 505-511B
- Iron, Alloying elements**  
The Embrittlement of Al-Zn-Mg and Al-Mg Alloys by Water Vapor. 1503-1514A  
Mössbauer Effect of Al-Fe-Si Intermetallic Compounds. 1937-1942A
- Iron, Binary systems**  
Thermodynamics and Phase Relationships of Transition Metal-Sulfur Systems. V.—A Reevaluation of the Fe-S System Using an Associated Solution Model for the Liquid Phase. 277-285B  
Effect of Magnetic Transition on Solubility of Carbon in B.C.C. Iron and F.C.C. Co-Ni Alloys. 913-921A  
Discussion of "A Thermodynamic Analysis of the Fe-C and the Fe-N Phase Diagrams" and Author's Reply. 2063-2065A
- Iron, Crystal lattices**  
On the Relation Between Grain Size and Grain Topology. 2007-2011A
- Iron, Diffusion**  
Tetragonal Distortion Field of Hydrogen Atoms in Iron. 1649-1653A
- Iron, Extraction**  
The Leaching of Hematite in Acid Solutions. 23-30B  
Reductive Stripping of Fe(III)-Loaded D2EHPA With the Aqueous Solutions Containing Sulfur Dioxide. 187-194B  
Determination of Cu(II) and Fe(III) in Chloride Solutions Concentrated in Both Copper and Iron. 403-404B  
Oxidation of Pyrrhotite Particles Falling Through a Vertical Tube. 627-639B
- Iron, Impurities**  
Impurity Effect on Cube Texture in Pure Aluminum Foils. 27-36A  
Interaction of Iron Particles With a Solid/Liquid Interface in Lead and Lead Alloys. 367-375B
- Iron, Mechanical properties**  
Subcritical Intergranular Crack Growth Rates and Thresholds of Iron and Iron + Antimony. 123-131A  
Identification of Defects Generated During Cathodic Charging in Pure Iron by Thermal Analysis Technique. 468-471A  
Fatigue Microcrack Initiation in Polycrystalline Alpha-Iron With Polished and Oxidized Surfaces. 641-649A
- Iron, Reactions (chemical)**  
Interfacial Phenomena Between Molten Metals and Sapphire Substrate. 567-575B
- Iron, Refining**  
Solute Interactions in Multicomponent Solutions. 807-813B
- Iron, Solubility**  
Nitrogen Solubility and Nitride Formation in Austenitic Fe-Ti Alloys. 815-822B
- Iron, Sorption**  
The Kinetics of the Nitrogen Reaction With Liquid Iron-Sulfur Alloys. 551-559B
- Iron, Structural hardening**  
Mechanical Properties of Nitrogen-Ferrite. 45-50A  
Short-Range Reordering of Heavy Interstitials in Ta, Nb, and Fe During Relaxation and Static Strain Aging. 361-366A
- Iron, Ternary systems**  
Role of Alloying Elements in Phase Decomposition in Alnico Magnet Alloys. 179-185A  
Correction to "Phase Relationships in the Fe-Cr-C System at Solidification Temperatures". 862B  
Thermodynamics of the Fe-Cr-C System at 985K. 1479-1490A  
The Fe-Rich Corner of the Metastable C-Cr-Fe Liquidus Surface. 1541-1549A
- Iron, Thermal properties**  
Magnetic Contributions to the Thermodynamic Functions of Pure Nickel, Cobalt and Iron. 153-165A
- Iron, Welding**  
Fundamental Aspects of Formation and Stability of Explosive Welds. 841-852A
- Iron and steel making**  
See also Oxygen steel making  
Steel making  
Solubilities of Carbon Dioxide in Sodium Silicate Melts. 561-568B
- Iron base alloys**  
See Ferrous alloys
- Iron compounds**  
See Hematite  
Pyrrhotite  
Wustite
- Iron constituents**  
See Alpha iron
- Iron ores**  
See Hematite  
Pyrrhotite
- Iron oxides**  
See Hematite  
Wustite
- Iron powder**  
See Iron
- Isomer shift**  
See Mossbauer spectroscopy
- Isostatic pressing**  
See Hot isostatic pressing
- Isothermal annealing**  
The Microstructural Response of Mill-Annealed and Solution-Annealed INCONEL 600 to Heat Treatment. 1225-1236A
- Isothermal treatment**  
See Austempering  
Isothermal annealing
- Joints**  
See Welded joints
- Junghans Rosal casting**  
See Continuous casting
- Kaldo process**  
See Oxygen steel making
- Kilns**  
An Experimental Study of Segregation in Rotary Kilns. 763-774B
- Kinetics**  
See also Reaction kinetics  
Mixing in Ladles by Vertical Injection of Gas and Gas-Particle Jets—a Water Model Study. 850-853B  
Kinetics of Solution Hardening. 2109-2129A

## Ladle additions

### Ladle additions

Mixing in Ladles by Vertical Injection of Gas and Gas-Particle Jets—a Water Model Study.

850-853B

### Ladle metallurgy

Determination and Prediction of Water Vapor Solubilities in CaO—MgO—SiO<sub>2</sub> Slags.

61-66B

Turbulent Fluid Flow Phenomena in a Water Model of an AOD System.

67-75B

Hydrodynamic Modeling of Some Gas Injection Procedures in Ladle Metallurgy Operations.

83-90B

A Unified Approach to Bubbling—Jetting Phenomena in Powder Injection Into Iron and Steel.

203-209B

Characteristics of Round Vertical Gas Bubble Jets.

263-275B

The Kinetics of the Nitrogen Reaction With Liquid Iron—Sulfur Alloys.

551-559B

### Lamellar structure

Influence of Microstructure on Fatigue Crack Initiation in Fully Pearlitic Steels.

753-760A

Entropy Criteria Applied to Pattern Selection in Systems With Free Boundaries.

1781-1797A

### Lamina

See Laminates

### Laminates, Mechanical properties

Discussion of "Enhanced Tensile Strength for Electrodeposited Nickel—Copper Multilayer Composites".

1693A

### Lances

Mixing in Ladles by Vertical Injection of Gas and Gas-Particle Jets—a Water Model Study.

850-853B

### Lanthanide metals

See Lanthanum

### Lanthanum, Ternary systems

Thermodynamics of the Ca—S—O, Mg—S—O, and La—S—O Systems at High Temperatures.

287-294B

### Laser beam heating

Microstructure of Rapidly Solidified Laser Molten Al—4.5 wt.% Cu Surfaces.

149-161B

### Laser beam welding

Absorption of CO<sub>2</sub> Laser Beam by AISI 4340 Steel. The Concept of an Effective Quench Temperature and Its Use in Studying Elevated-Temperature Microstructures.

853-856B

1521-1523A

### Laser welding

See Laser beam welding

### Lasers

Laser-Melting/Spin-Atomization Method for the Production of Titanium Alloy Powders.

1897-1900A

### Latent heat

See Heat of fusion

### Latent heat of fusion

See Heat of fusion

### Lattice constant

See Lattice parameters

### Lattice defects

See Crystal defects

### Lattice displacements

See Displacements (lattice)

### Lattice parameters

Transformation Behavior of Nearly Stoichiometric Ni—Mn Alloys.

1567-1579A

### Lattice parameters, Composition effects

Phase Constitution and Lattice Parameter Relationships in Rapidly Solidified (Fe<sub>0.85</sub>Mn<sub>0.35</sub>)<sub>0.83</sub>Al<sub>0.17</sub>—xC and Fe<sub>2</sub>Al—xC Pseudobinary Alloys.

5-10A

### Lattices

See Crystal lattices

Superlattices

### Leaching

See also Acid leaching

Ammonia pressure leaching

Bacterial leaching

In situ leaching

Sulfuric acid leaching

Representation of the Kinetics of Leaching of Galena by Ferric Chloride in Concentrated Sodium Chloride Solutions by a Modified Mixed Kinetics Model.

31-39B

Determination of Cu(II) and Fe(III) in Chloride Solutions Concentrated in Both Copper and Iron.

403-404B

Kinetic Model for the Chemical Dissolution of Multiparticle Systems.

449-454B

Mineralogical Changes Occurring During the Ferric Ion Leaching of Bornite.

679-693B

Sodium Aluminate Leaching and Desilication in Lime—Soda Sinter Process for Alumina From Coal Wastes.

707-713B

Reaction Mechanism for the Ferric Chloride Leaching of Sphalerite.

715-724B

### Lead (metal), Binary systems

The Correlation of the Thermodynamic Properties and Phase Diagram of the System Tin—Lead Using a Gaussian Plus Krupkowski Formalism.

91-96B

### Lead (metal), Extraction

Representation of the Kinetics of Leaching of Galena by Ferric Chloride in Concentrated Sodium Chloride Solutions by a Modified Mixed Kinetics Model.

31-39B

Direct Reduction of Lead Sulfide With Carbon and Lime; Effect of Catalysts: I.—Experimental.

465-475B

Direct Reduction of Lead Sulfide With Carbon and Lime; Effect of Catalysts: II.—Analytical Model.

477-488B

Electrodeposition of Lead From Aqueous Acetate and Chloride Solutions.

489-496B

### Lead (metal), Impurities

Activities of Arsenic, Antimony, Bismuth and Lead in Copper Mattes.

129-141B

### Lead (metal), Melting

Electronic and Ionic Transport in Liquid PbO—SiO<sub>2</sub> Systems.

77-82B

### Lead (metal), Refining

Solute Interactions in Multicomponent Solutions.

807-813B

### Lead base alloys, Crystal growth

Interaction of Iron Particles With a Solid/Liquid Interface in Lead and Lead Alloys.

367-375B

Flow of Interdendritic Liquid and Permeability in Pb—20Sn Alloys.

2263-2271A

### Lead base alloys, Extrusion

Product Microstructures and Properties Induced by Hot Working at Pb—1.85%Sn Alloy.

1273-1285A

### Lead base alloys, Microstructure

A Novel Solidification Technique of Metals and Alloys: Under the Influence of Applied Potential.

1354-1355A

### Lead compounds, Reduction (chemical)

Direct Reduction of Lead Sulfide With Carbon and Lime; Effect of Catalysts: I.—Experimental.

465-475B

Direct Reduction of Lead Sulfide With Carbon and Lime; Effect of Catalysts: II.—Analytical Model.

477-488B

### Lead ores

See Galena

### Life

See Fatigue life

### Light metals

See Aluminum

Aluminum base alloys

Beryllium

Magnesium

Magnesium base alloys

Titanium

Titanium base alloys

### Light water reactors

See Boiling water reactors

### Lime, Reactions (chemical)

Kinetics of the Reaction Between Hydrogen Sulfide and Lime Particles.

163-168B

### Line defects

See Dislocations

### Liquid metal forging

A Model for Deformation and Segregation of Solid—Liquid Mixtures.

1393-1403A

### Liquid metals, Atomic properties

Determination of the Coordination Number of Liquid Metals Near the Melting Point.

267-274A

### Liquid metals, Chemical analysis

A New Type of Oxygen Analyzer Utilizing a Potentiostatic Coulometric Titration Technique.

113-119B

### Liquid metals, Crystal growth

Discussion of "Mathematical Model for the Unidirectional Solidification of Metals. I.—Cooled Molds".

406-407B

### Liquid metals, Physical properties

A Model for Deformation and Segregation of Solid—Liquid Mixtures.

1393-1403A

### Liquid metals, Reactions (chemical)

Effect of Arsenic on the Activity of Oxygen Dissolved in Dilute Liquid Copper Solutions.

339-344B

Interfacial Phenomena Between Molten Metals and Sapphire Substrate.

567-575B

### Liquid metals, Sorption

The Kinetics of the Nitrogen Reaction With Liquid Iron—Sulfur Alloys.

551-559B

### Liquid metals, Thermal properties

The Influence of Convection on Heat Transfer in Liquid Tin. Thermodynamic Properties of S—Fe—Co—Ni and Fe—Co—Ni Systems.

355-357B

907-911A

### Liquid phase diffusion

See Diffusion

### Liquid phase sintering

Effect of Dihedral Angle on the Morphology of Grains in a Matrix Phase.

923-928A

The Contiguity of Liquid Phase Sintered Microstructures.

1247-1252A

### Lithium, Alloying elements

Lithium-Containing Aluminum Alloys: Cyclic Fracture. Experimental Observations on the Nucleation and Growth of δ' (Al<sub>3</sub>Li) in Dilute Al—Li Alloys.

475-477A

Explosive Consolidation of Rapidly Solidified Aluminum Alloy Powders.

1203-1211A

Superplastic Al—Cu—Li—Mg—Zr Alloys.

1445-1455A

2319-2332A

### Lithium compounds, Reactions (chemical)

Determination of the Lithium Content of Molten Aluminum Using a Solid Electrolyte.

41-46B

### Live loads

See Cyclic loads



- Lixivation**  
See Leaching
- Loads (forces)**  
See Cyclic loads  
Shock loading
- Long range order**  
Effects of Temperature and Environment on Fatigue Crack Growth in Ordered (Fe, Ni)<sub>3</sub> V-Type Alloys. 815-820A
- Loops (dislocation)**  
See Dislocation loops
- Low alloy steels**  
See also Electrical steels  
Silicon manganese steels  
Silicon steels
- Low alloy steels, Heat treatment**  
The Formation of Austenite at Low Intercritical Annealing Temperatures in a Normalized 0.08C—1.45Mn—0.21Si Steel. 1523-1526A
- Low alloy steels, Mechanical properties**  
The Dependence of Some Tensile and Fatigue Properties of a Dual-Phase Steel on Its Microstructure. 1405-1415A
- Low cycle fatigue, Microstructural effects**  
Effect of Inclusions on LCF Life of HIP Plus Heat Treated Powder Metal René 95. 775-784B
- Magnesia**  
See Magnesium oxide
- Magnesium, Composite materials**  
The Influence of Thermal Exposure on Interfacial Reactions and Strength in Aluminum Oxide Fiber Reinforced Magnesium Alloy Composites. 2069-2072A
- Magnesium, Ternary systems**  
Thermodynamics of the Ca—S—O, Mg—S—O, and La—S—O Systems at High Temperatures. 287-294B
- Magnesium base alloys, Composite materials**  
The Influence of Thermal Exposure on Interfacial Reactions and Strength in Aluminum Oxide Fiber Reinforced Magnesium Alloy Composites. 2069-2072A
- Magnesium base alloys, Corrosion**  
Investigation of Stress Corrosion Crack Growth in Magnesium Alloys Using J-Integral Estimations. 101-108A
- Magnesium base alloys, Thermal properties**  
New Eutectic Alloys and Their Heats of Transformation. 323-328A
- Magnesium compounds**  
See Magnesium oxide
- Magnesium oxide**  
Determination and Prediction of Water Vapor Solubilities in CaO—MgO—SiO<sub>2</sub> Slags. 61-66B
- Magnetic fields**  
Magnetic Contributions to the Thermodynamic Functions of Pure Nickel, Cobalt and Iron. 153-165A
- Magnetic force**  
See Magnetic fields
- Magnetic hysteresis**  
See Hysteresis
- Magnetic materials**  
See also Ferromagnetic materials
- Magnetic materials, Phase transformations**  
Role of Alloying Elements in Phase Decomposition in Alnico Magnet Alloys. 179-185A
- Magnetic transitions**  
Effect of Magnetic Transition on Solubility of Carbon in B.C.C. Iron and F.C.C. Co—Ni Alloys. 913-921A
- Magnets**  
See Permanent magnets
- Manganese, Alloying elements**  
The Effect of Alloying Elements on Pearlite Growth. 597-603A  
The Dependence of Some Tensile and Fatigue Properties of a Dual-Phase Steel on Its Microstructure. 1405-1415A  
The Formation of Austenite at Low Intercritical Annealing Temperatures in a Normalized 0.08C—1.45Mn—0.21Si Steel. 1523-1526A
- Manganese, Diffusion**  
Quaternary Diffusion in the Cu—Ni—Zn—Mn System at 775°C. 1123-1132A
- Manganese base alloys, Microstructure**  
Electron Microscopic Study of  $\delta$ -Phase Martensite in Ni—Mn Alloys. 1581-1597A
- Manganese base alloys, Phase transformations**  
Transformation Behavior of Nearly Stoichiometric Ni—Mn Alloys. 1567-1579A
- Manganese steels**  
See also Silicon manganese steels
- Manganese steels, Mechanical properties**  
Microstructure—Mechanical Property Relationships of Dual-Phase Steel Wire. 831-840A
- Manganese steels, Phase transformations**  
Discussion of "The Bainite Transformation in a Silicon Steel" and Authors' Reply. 457-468A
- Manual metal arc welding**  
See Shielded metal arc welding
- Martensite, Crystal lattices**  
Low Temperature Aging of the Freshly Formed Martensite in an Fe—Ni—C Alloy. 1745-1750A
- Martensite, Microstructure**  
Lattice Image Studies on the Intervariant Boundary Structure and Substructure of Cu—Zn—Al 18R Martensite. 1551-1566A  
Electron Microscopic Study of  $\delta$ -Phase Martensite in Ni—Mn Alloys. 1581-1597A
- Martensitic transformations**  
A Mössbauer Spectrometry Study of the Mechanical Transformation of Precipitated Austenite in 6Ni Steel. 173-177A  
The Mean Size of Plate Martensite: Influence of Austenite Grain Size, Partitioning, and Transformation Heterogeneity. 329-336A  
Transformation Behavior of Nearly Stoichiometric Ni—Mn Alloys. 1567-1579A  
Mobility of Martensitic Interfaces. 1713-1722A  
Mobility of the  $\beta_1/\gamma_1$  Martensitic Interface in Cu—Al—Ni. I.—Experimental Measurements. 1723-1734A  
Mobility of the  $\beta_1/\gamma_1$  Martensitic Interface in Cu—Al—Ni. II.—Model Calculations. 1735-1744A  
Low Temperature Aging of the Freshly Formed Martensite in an Fe—Ni—C Alloy. 1745-1750A  
The Mechanical Stability of Precipitated Austenite in 9Ni Steel. 2251-2256A  
Isothermal Martensite Transformation in a 1.80 Carbon Steel. 2257-2262A
- Martensitic transformations, Alloying effects**  
Crystallography and Tempering Behavior of Iron—Nitrogen Martensite. 1371-1384A
- Martensitic transformations, Heating effects**  
The Formation of Austenite at Low Intercritical Annealing Temperatures in a Normalized 0.08C—1.45Mn—0.21Si Steel. 1523-1526A  
The Stability of Precipitated Austenite and the Toughness of 9Ni Steel. 2237-2249A
- Mass spectroscopy**  
The Early Stages of the Decomposition of Alloys. 1173-1184A
- Massive type transformation**  
Microstructural and Microchemical Aspects of the Solid-State Decomposition of Delta Ferrite in Austenitic Stainless Steels. 1363-1369A
- Master alloys**  
Grain Refinement of Aluminum by TiC. 2065-2068A
- Materials testing**  
See Huey test  
Microanalysis
- Mathematical analysis**  
See also Numerical analysis  
Isotope Separation During Thin Film Compound Growth. 142-144A  
Metallurgical Thermodynamics and the Carbon Equivalent Expression. 169-170B  
Modeling of Heat Flow in Sand Castings. I.—The Boundary Curvature Method. 195-202B  
Criterion for Predicting the Morphology of Crystalline Cubic Precipitates in a Cubic Matrix. 197-202A  
Work Hardening Correlations Based on State Variables in Some F.C.C. Metals in Monotonic Loading. 411-420A  
Centerline Porosity in Plate Castings. 823-829B  
Effect of Dihedral Angle on the Morphology of Grains in a Matrix Phase. 923-928A  
Hill's Plastic Strain Ratio of Sheet Metals. 1531-1535A  
Mobility of the  $\beta_1/\gamma_1$  Martensitic Interface in Cu—Al—Ni. I.—Experimental Measurements. 1723-1734A  
Mobility of the  $\beta_1/\gamma_1$  Martensitic Interface in Cu—Al—Ni. II.—Model Calculations. 1735-1744A  
Discussion of "Practical Applications of Hot-Isostatic Pressing Diagrams: From Case Studies". 1903-1904A
- Mathematical models**  
An Effect of Chemisorbing Surface Reaction Poisons on the Transition From Internal to External Oxidation. 133-136A  
Fluid Flow and Weld Penetration in Stationary Arc Welds. 203-213A  
Discussion of "Mathematical Model for the Unidirectional Solidification of Metals. I.—Cooled Molds". 406-407B  
Kinetics of the Zinc Slag-Fuming Process. I.—Industrial Measurements. 513-527B  
Kinetics of the Zinc Slag-Fuming Process. II.—Mathematical Model. 529-540B  
Kinetics of the Zinc Slag-Fuming Process. III.—Model Predictions and Analysis of Process Kinetics. 541-549B  
Successive Gas—Solid Reaction Model for the Hydrogen Reduction of Cuprous Sulfide in the Presence of Lime. 645-662B  
High Strain Rate Deformation of Molybdenum and Mo—33Re by Shock Loading. II.—Rates of Defect Generation and Accumulation of Plastic Strain. 891-895A  
Orthogonal Coordinates for Systems of Many Components. 929-933A  
The Effect of Pressure Modulation on the Flow of Gas Through a Solid Membrane: Surface Inhibition and Internal Traps. 1013-1024A  
The Effect of Grain Size and Plastic Strain on Slip Length in 70-30 Brass. 1025-1029A  
Temperature and Strain Rate Dependence of Stress—Strain Behavior in a Nickel-Base Superalloy. 1049-1067A  
Some Trends Observed in the Elevated-Temperature Kinematic and Isotropic Hardening of Type 304 Stainless Steel. 1069-1076A  
A Model for Anelastic Relaxation Controlled Cyclic Creep. 1117-1122A  
The Effect of Carbon Content on the Kinetics of Decarburization in Fe—C Alloys. 1160-1163A  
A Model for Deformation and Segregation of Solid—Liquid Mixtures. 1393-1403A  
Mobility of Martensitic Interfaces. 1713-1722A  
Cellular and Dendritic Growth. II.—Theory. 1807-1814A

## Mathematical models

Discussion of "A Thermodynamic Analysis of the Fe—C and the Fe—N Phase Diagrams" and Author's Reply. 2063-2065A

## Mathematics

See Finite element method  
Mathematical analysis  
Mathematical models  
Numerical analysis

## Mattes

See Copper mattes

## Measuring instruments

See Oxygen probes

## Mechanical hysteresis

See Hysteresis

## Mechanical properties

See also Anelasticity  
Compressive strength  
Creep (materials)  
Creep life  
Creep rate  
Creep rupture strength  
Creep strength  
Deformation resistance  
Ductile brittle transition  
Ductility  
Elastic constants  
Elongation  
Fatigue (materials)  
Fatigue life  
Fatigue limit  
Fatigue strength  
Fracture toughness  
Hardness  
Hydrogen embrittlement  
Impact strength  
Modulus of elasticity  
Notch strength  
Notch toughness  
Plastic flow  
Residual stress  
Shear properties  
Shear strength  
Stress relaxation  
Superplasticity  
Temper brittleness  
Tensile properties  
Tensile strength  
Yield strength

## Mechanical properties, Microstructural effects

Microstructural Development in High Volume Fraction Gamma Prime Ni-Base Oxide-Dispersion-Strengthened Superalloys. 1285-1294A

## Mechanical tests

See Creep tests  
Tension tests

## Mechanics

See Fracture mechanics  
Hydrodynamics  
Kinetics

## Melt spinning

Microstructure and Mechanical Properties of Fe—Ni—Cr—Al Steel Wires Produced by In-Rotating-Water Spinning Method. 215-226A  
Rapid Solidification Characteristics in Melt Spinning a Nickel-Base Superalloy. 1773-1779A

## Melting

See Electron beam melting

## Melting furnaces

See Basic converters  
Coreless induction furnaces

## Melts

Examination of the Strength of Oxide Skins on Aluminum Alloy Melts. 47-51B

## Melts, Oxidation

Electronic and Ionic Transport in Liquid PbO—SiO<sub>2</sub> Systems. 77-82B

## Metal carbides

See Tungsten carbide

## Metal powders

See also Alloy powders  
Direct Copper Precipitation From a Loaded Chelating Extractant by Pressure Hydrogen Stripping. 13-22B

## Metal working

See Cold rolling  
Cold working  
Controlled rolling  
Deep drawing  
Liquid metal forging  
Stretch forming  
Swaging  
Thermomechanical treatment  
Wire drawing

## Metallic glasses, Atomic properties

Dislocations in Amorphous Metals. 2227-2230A

## Metallic glasses, Phases (state of matter)

Phase Constitution and Lattice Parameter Relationships in Rapidly Solidified (Fe<sub>0.85</sub>Mn<sub>0.35</sub>)<sub>0.83</sub>Al<sub>0.17</sub>—xC and Fe<sub>3</sub>Al—xC Pseudobinary Alloys. 5-10A

## Metallographic structures

See Microstructure

## Metallography

See Quantitative metallography

## Metalloid alloys

See Silicon base alloys

## Metalloid compounds

See Silicon carbide  
Silicon dioxide

## Metalloids

See Arsenic  
Boron  
Silicon  
Tellurium

## Metallurgical constituents

See Sigma phase

## Metathesis

See Decomposition reactions

## Meteorites

Measurement and Analysis of Distribution Coefficients in Fe—Ni Alloys Containing Sulfur and/or Phosphorus. II.—K<sub>S</sub>, K<sub>Se</sub>, and K<sub>Cu</sub>. 1871-1878A

## Microalloyed steels

See High strength low alloy steels

## Microanalysis

Microanalytical Study of the Heterogeneous Phases in Commercial Al—Zn—Mg—Cu Alloys. 1925-1936A

## Microbial leaching

See Bacterial leaching

## Microscopy

See Field ion microscopy  
Stereomicroscopy  
Transmission electron microscopy

## Microshrinkage

See Shrinkage

## Microstructure

See also Lamellar structure  
Transformation Behavior of Nearly Stoichiometric Ni—Mn Alloys. 1567-1579A  
Thermomechanical Processing of Microalloyed Powder Forged Steels and a Cast Vanadium Steel. 1599-1608A

## Microstructure, Cooling effects

Mechanical Properties and Microstructure of Centrifugally Cast Alloy 718. 1295-1306A  
The Effect of Cooling Conditions on the Microstructure of Rapidly Solidified Ti—6Al—4V. 1951-1959A

## Microstructure, Deformation effects

Effect of Finish Rolling Temperature on the Structure and Properties of Directly Quenched Nb Containing Low Steel. 471-474A  
Microstructure and Crystallography of Unidirectionally Solidified Ni—W Eutectic Alloy. 1185-1193A  
Product Microstructures and Properties Induced by Hot Working at Pb—1.85%Sn Alloy. 1273-1285A

## Microstructure, Diffusion effects

Driving Force for Discontinuous Coarsening in a Ni—Al—Mo Base Superalloy. 11-16A

## Microstructure, Environmental effects

Microstructural Changes in 1Cr—0.5Mo Steel After 20 Years of Service. 109-114A

## Microstructure, Heating effects

Microstructure of Rapidly Solidified Laser Molten Al—4.5 wt.% Cu Surfaces. 149-161B  
The Microstructural Response of Mill—Annealed and Solution—Annealed INCONEL 600 to Heat Treatment. 1225-1236A

## Mill scale

See Scale (corrosion)

## Mineral acids

See Inorganic acids

## Mixing

Mixing in Ladles by Vertical Injection of Gas and Gas-Particle Jets—a Water Model Study. 850-853B

## Mobility

See Dislocation mobility

## Modulus of elasticity, Impurity effects

Effect of Hydrogen on the Young's Modulus of Iron. 1655-1662A

## Modulus of elasticity, Microstructural effects

Microstructural Influences on Fatigue Crack Propagation in Ti—10V—2Fe—3Al. 739-751A

## Moisture

See Water

## Molds

See Sand molds

## Molten metals

See Liquid metals

## Molten salts

See Fused salts

## Molybdenum, Alloying additive

Transmission Kossel Study of the Formation of {110}[001] Grains After an Intermediate Annealing in Grain Oriented Silicon Steel Containing a Small Amount of Molybdenum. 1613-1623A

- Molybdenum, Alloying elements**  
X-Ray Diffraction and Resistivity Studies of Titanium—Molybdenum Alloys. 187-195A
- Molybdenum, Mechanical properties**  
Hill's Plastic Strain Ratio of Sheet Metals. 1531-1535A
- Molybdenum, Microstructure**  
High Strain Rate Deformation of Molybdenum and Mo—33Re by Shock Loading. I.—Substructure Development. 881-890A  
High Strain Rate Deformation of Molybdenum and Mo—33Re by Shock Loading. II.—Rates of Defect Generation and Accumulation of Plastic Strain. 891-895A
- Molybdenum base alloys, Microstructure**  
High Strain Rate Deformation of Molybdenum and Mo—33Re by Shock Loading. I.—Substructure Development. 881-890A  
High Strain Rate Deformation of Molybdenum and Mo—33Re by Shock Loading. II.—Rates of Defect Generation and Accumulation of Plastic Strain. 891-895A
- Molybdenum chromium nickel steels**  
See Nickel chromium molybdenum steels
- Molybdenum chromium steels**  
See Chromium molybdenum steels
- Molybdenum compounds, Reactions (chemical)**  
Displacement Reactions Between Chromium and MoO<sub>2</sub> in a Nickel-Base Alloy Matrix. 1815-1830A
- Molybdenum nickel chromium steels**  
See Nickel chromium molybdenum steels
- Molybdenum nickel steels**  
See Nickel molybdenum steels
- Molybdenum steels**  
See also Chromium molybdenum steels  
Nickel chromium molybdenum steels  
Nickel molybdenum steels
- Molybdenum steels, Cleaning**  
Studies on the Analysis of Hydrogen in High Strength Steels. 1694-1695A
- Monocrystals**  
See Single crystals
- Mossbauer spectroscopy**  
Mössbauer Effect of Al—Fe—Si Intermetallic Compounds. 1937-1942A
- Natural gas**  
See Sour gas
- Nickel, Alloying elements**  
Sulfidation Under Atmospheric Conditions of Cu—Ni, Cu—Sn and Cu—Zn Binary and Cu—Ni—Sn and Cu—Ni—Zn Ternary Systems. 275-284A  
The Effect of Alloying Elements on Pearlite Growth. 597-603A  
Fracture Toughness and Its Development in High Purity Cast Carbon and Low Alloy Steels. 613-622A  
The Embrittlement of Al—Zn—Mg and Al—Mg Alloys by Water Vapor. 1503-1514A  
Binder Deformation in WC—(Co, Ni) Cemented Carbide Composites. 2309-2317A
- Nickel, Binary systems**  
Thermodynamics of Formation of Y—Ni Alloys. 577-584B
- Nickel, Bonding**  
Pressure Effects in Multiphase Binary Diffusion Couples. 605-611A
- Nickel, Diffusion**  
Driving Force for Discontinuous Coarsening in a Ni—Al—Mo Base Superalloy. 11-16A  
Quaternary Diffusion in the Cu—Ni—Zn—Mn System at 775°C. 1123-1132A  
Trapping of Hydrogen and Helium at Grain Boundaries in Nickel: an Atomistic Study. 1625-1631A
- Nickel, Powder technology**  
The Influence of Strain Rate and Porosity on the Deformation and Fracture of Titanium and Nickel. 2273-2281A
- Nickel, Reactions (chemical)**  
Interfacial Phenomena Between Molten Metals and Sapphire Substrate. 567-575B
- Nickel, Structural hardening**  
Time-Dependent Deformation of Metals. 2215-2226A
- Nickel, Ternary systems**  
Role of Alloying Elements in Phase Decomposition in Alnico Magnet Alloys. 179-185A  
Phase Equilibria in the Ni—Al—Ti System at 1173K. 319-322A  
Effect of Magnetic Transition on Solubility of Carbon in B.C.C. Iron and F.C.C. Co—Ni Alloys. 913-921A  
Phases in Ni—Co—Ga Alloys Close to (Ni, Co)<sub>0.5</sub>Ga<sub>0.5</sub>. 1159-1160A
- Nickel, Thermal properties**  
Magnetic Contributions to the Thermodynamic Functions of Pure Nickel, Cobalt and Iron. 153-165A
- Nickel base alloys**  
See also Inconel
- Nickel base alloys, Alloy development**  
Microstructural Development in High Volume Fraction Gamma Prime Ni-Base Oxide-Dispersion-Strengthened Superalloys. 1285-1294A
- Nickel base alloys, Composite materials**  
Discussion of "Enhanced Tensile Strength for Electrodeposited Nickel—Copper Multilayer Composites". 1693A
- Nickel base alloys, Corrosion**  
Hot Corrosion of B-1900 in CaSO<sub>4</sub>/Na<sub>2</sub>SO<sub>4</sub> Salt Mixtures in Reducing Atmospheres. 291-297A
- Sulfation of Y<sub>2</sub>O<sub>3</sub> and HfO<sub>2</sub> in Relation to MCrAl Coatings. 303-306A
- Nickel base alloys, Crystal growth**  
Driving Force for Discontinuous Coarsening in a Ni—Al—Mo Base Superalloy. 11-16A  
Superalloy Microstructural Variations Induced by Gravity Level During Directional Solidification. 1683-1687A  
Rapid Solidification Characteristics in Melt Spinning a Nickel-Base Superalloy. 1773-1779A
- Nickel base alloys, Diffusion**  
The Influence of Grain Boundary Precipitation on the Measurement of Chromium Redistribution and Phosphorus Segregation in Ni—16Cr—9Fe. 349-359A
- Nickel base alloys, Directional solidification**  
Mechanical Properties and Microstructure of Centrifugally Cast Alloy 718. 1295-1306A
- Nickel base alloys, Heat treatment**  
Carbide Stability in Nimonic 80A Alloy. 511-520A  
Effect of Single Aging on Microstructure and Impact Property of INCONEL X-750. 821-829A  
The Microstructural Response of Mill—Annealed and Solution—Annealed INCONEL 600 to Heat Treatment. 1225-1236A
- Nickel base alloys, Mechanical properties**  
Dynamic Recrystallization During Creep in a 45% Ni—35% Fe—20% Cr Alloy System. 51-57A  
High-Cycle Fatigue Properties of the ODS-Alloy MA 6000 at 850°C. 393-399A  
Elevated Temperature Creep-Rupture Behavior of the Single Crystal Nickel-Base Superalloy NASAIR 100. 427-439A  
Grain Boundary Fracture of L<sub>12</sub> Type Intermetallic Compound Ni<sub>3</sub>Al. 441-443A  
On the Improvement of Creep Strength and Ductility of Ni—20% Cr by Small Zirconium Additions. 651-660A  
Elastic Constants of a Monocrystalline Nickel-Base Superalloy. 661-665A  
Effect of Inclusions on LCF Life of HIP Plus Heat Treated Powder Metal René 95. 775-784B  
High Temperature Deformation of Ultra-Fine-Grained Oxide Dispersion Strengthened Alloys. 777-787A  
Effects of Temperature and Environment on Fatigue Crack Growth in Ordered (Fe, Ni)<sub>3</sub>V-Type Alloys. 815-820A  
Temperature and Strain Rate Dependence of Stress—Strain Behavior in a Nickel-Base Superalloy. 1049-1067A  
A Model for Anelastic Relaxation Controlled Cyclic Creep. 1117-1122A  
The Effect of Grain Morphology on Longitudinal Creep Properties of INCONEL MA 754 at Elevated Temperatures. 1307-1324A  
High Cycle Fatigue and Fatigue Crack Growth of the Oxide Dispersion Strengthened Alloy MA 754. 1437-1444A  
The Effects of Orientation and Thickness on the Notch—Tensile Creep Strength of Single Crystals of a Nickel-Base Superalloy. 1457-1466A  
The Effect of Environment on the Sustained Load Crack Growth Rates of Forged WASPALOY. 1515-1521A  
The Influence of Cobalt, Tantalum, and Tungsten on the Elevated Temperature Mechanical Properties of Single Crystal Nickel-Base Superalloys. 1863-1870A
- Nickel base alloys, Metallography**  
The Early Stages of the Decomposition of Alloys. 1173-1184A
- Nickel base alloys, Microstructure**  
Microstructure and Crystallography of Unidirectionally Solidified Ni—W Eutectic Alloy. 1185-1193A  
Electron Microscopic Study of  $\beta$ -Phase Martensite in Ni—Mn Alloys. 1581-1597A  
The Influence of Cobalt, Tantalum, and Tungsten on the Microstructure of Single Crystal Nickel-Base Superalloys. 1849-1862A
- Nickel base alloys, Oxidation**  
An Effect of Chemisorbing Surface Reaction Poisons on the Transition From Internal to External Oxidation. 133-136A  
Reactive Element—Sulfur Interaction and Oxide Scale Adherence. 1164-1166A
- Nickel base alloys, Phase transformations**  
Transformation Behavior of Nearly Stoichiometric Ni—Mn Alloys. 1567-1579A
- Nickel base alloys, Phases (state of matter)**  
Atom-Probe Microanalysis of a Nickel-Base Superalloy. 1703-1711A
- Nickel base alloys, Powder technology**  
The Substitution of Nickel for Cobalt in Hot Isostatically Pressed Powder Metallurgy UDIMET 700 Alloys. 993-1003A
- Nickel base alloys, Reactions (chemical)**  
Displacement Reactions Between Chromium and MoO<sub>2</sub> in a Nickel-Base Alloy Matrix. 1815-1830A
- Nickel base alloys, Refining**  
Thermodynamic Properties of S—Fe—Co—Ni and Fe—Co—Ni Systems. 907-911A
- Nickel base alloys, Structural hardening**  
Serrated Grain Boundary Formation Potential of Nickel-Base Superalloys and Its Implications. 17-26A  
Oxide Dispersion Strengthened Nickel-Base Heat Resistant Alloys by Means of the Spray-Dispersion Method. 1043-1048A  
Low Temperature Carbide Precipitation in a Nickel Base Superalloy. 1213-1223A  
The Development of  $\gamma$ — $\gamma'$  Lamellar Structures in a Nickel-Base Superalloy During Elevated Temperature Mechanical Testing. 1969-1982A  
Ordering Reactions in Ni—Al—Mo—Ta and Ni—Al—Mo—W Superalloys. 1983-1995A  
Rhenium Additions to a Nickel-Base Superalloy: Effects on Microstructure. 1997-2005A  
Precipitation Hardening. 2131-2165A  
Time-Dependent Deformation of Metals. 2215-2226A

## Nickel chromium molybdenum steels

- Nickel chromium molybdenum steels, Corrosion**  
The Effect of Microstructural Changes on the Caustic Stress Corrosion Cracking Resistance of a NiCrMoV Rotor Steel. 1333-1344A
- Nickel chromium molybdenum steels, Heat treatment**  
Modified Heat Treatment for Lower Temperature Improvement of the Mechanical Properties of Two Ultra-High-Strength Low-Alloy Steels. 83-91A  
Carbide Precipitation, Grain Boundary Segregation, and Temper Embrittlement in NiCrMoV Rotor Steels. 721-737A
- Nickel chromium molybdenum steels, Mechanical properties**  
Mechanical Properties of 0.40% C—Ni—Cr—Mo High-Strength Steel Having a Mixed Structure of Martensite and Bainite. 73-82A  
Correlation of Microstructure and Fracture Toughness in Two 4340 Steels. 1633-1648A  
A "Hydrogen Partitioning" Model for Hydrogen Assisted Crack Growth. 2039-2050A  
A Plastic Flow Induced Fracture Theory for  $K_{ISCC}$ . 2333-2340A
- Nickel chromium molybdenum steels, Welding**  
Absorption of CO<sub>2</sub> Laser Beam by AISI 4340 Steel. 853-856B
- Nickel chromium steels**  
See also Nickel chromium molybdenum steels
- Nickel chromium steels, Heat treatment**  
Carbide Precipitation, Grain Boundary Segregation, and Temper Embrittlement in NiCrMoV Rotor Steels. 721-737A
- Nickel compounds, Corrosion**  
Effect of Boron on the Corrosion Behavior of Polycrystalline Ni<sub>3</sub>Al. 2072-2073A
- Nickel compounds, Mechanical properties**  
Grain Boundary Fracture of L<sub>12</sub> Type Intermetallic Compound Ni<sub>3</sub>Al. 441-443A
- Nickel molybdenum chromium steels**  
See Nickel chromium molybdenum steels
- Nickel molybdenum steels**  
See also Nickel chromium molybdenum steels
- Nickel molybdenum steels, Mechanical properties**  
A Study of Fatigue Crack Propagation in Prior Hydrogen Attacked Pressure Vessel Steels. 1491-1501A
- Nickel steels**  
See also Nickel chromium molybdenum steels  
Nickel chromium steels  
Nickel molybdenum steels
- Nickel steels, Mechanical properties**  
A Mössbauer Spectrometry Study of the Mechanical Transformation of Precipitated Austenite in 6Ni Steel. 173-177A  
Influence of Strain Rate and Temperature on the Deformation Behavior of a Metastable High Carbon Iron—Nickel Austenite. 445-452A  
Fracture Toughness and Its Development in High Purity Cast Carbon and Low Alloy Steels. 613-622A  
The Stability of Precipitated Austenite and the Toughness of 9Ni Steel. 2237-2249A
- Nickel steels, Phase transformations**  
The Effect of Alloying Elements on Pearlite Growth. 597-603A  
Low Temperature Aging of the Freshly Formed Martensite in an Fe—Ni—C Alloy. 1745-1750A  
The Mechanical Stability of Precipitated Austenite in 9Ni Steel. 2251-2256A
- Niobium, Alloying additive**  
Oxide Dispersion Strengthened Nickel-Base Heat Resistant Alloys by Means of the Spray-Dispersion Method. 1043-1048A
- Niobium, Alloying elements**  
Isopiestic Solubility of Hydrogen in Vanadium Alloys at Low Temperatures. 367-374A  
Low Temperature Mechanical Behavior of Microalloyed and Controlled-Rolled Fe—Mn—Al—C—X Alloys. 1689-1693A
- Niobium, Binary systems**  
The Niobium (Columbium)—Platinum Constitution Diagram. 1943-1949A
- Niobium, Extraction**  
Separation of Niobium From Ferroniobium by Chlorination. 639-644B
- Niobium, Structural hardening**  
Short-Range Reordering of Heavy Interstitials in Ta, Nb, and Fe During Relaxation and Static Strain Aging. 361-366A
- Niobium base alloys, Mechanical properties**  
Deformation Characteristics in Beta Phase Ti—Nb Alloys. 789-795A
- Nitrides, Crystal growth**  
Nitrogen Solubility and Nitride Formation in Austenitic Fe—Ti Alloys. 815-822B
- Nitrides, Heating effects**  
Carbide Stability in Nimonic 80A Alloy. 511-520A
- Nitrogen, Alloying elements**  
Crystallography and Tempering Behavior of Iron—Nitrogen Martensite. 1371-1384A
- Nitrogen, Diffusion**  
Mechanical Properties of Nitrogen—Ferrite. 45-50A  
Short-Range Reordering of Heavy Interstitials in Ta, Nb, and Fe During Relaxation and Static Strain Aging. 361-366A
- Nitrogen, Solubility**  
Nitrogen Solubility and Nitride Formation in Austenitic Fe—Ti Alloys. 815-822B
- Nitrogen, Sorption**  
The Kinetics of the Nitrogen Reaction With Liquid Iron—Sulfur Alloys. 551-559B

- Nitrogen compounds**  
See Nitrides
- Nodular iron, Mechanical properties**  
Effect of Carbon Content and Ferrite Grain Size on the Tensile Flow Stress of Ferritic Spheroidal Graphite Cast Iron. 667-673A  
Embrittlement of Austempered Nodular Irons: Grain Boundary Phosphorus Enrichment Resulting From Precipitate Decomposition. 797-805A
- Nonmetallic inclusions**  
Physical Refining of Steel Melts by Filtration. 725-742B
- Notch ductility**  
See Ductility
- Notch impact strength**  
See Impact strength
- Notch strength, Microstructural effects**  
Influence of Microstructure on Fatigue Crack Initiation in Fully Pearlitic Steels. 753-760A  
The Effects of Orientation and Thickness on the Notch—Tensile Creep Strength of Single Crystals of a Nickel-Base Superalloy. 1457-1466A
- Notch toughness, Heating effects**  
Modified Heat Treatment for Lower Temperature Improvement of the Mechanical Properties of Two Ultra-High-Strength Low-Alloy Steels. 83-91A  
Embrittlement of Austempered Nodular Irons: Grain Boundary Phosphorus Enrichment Resulting From Precipitate Decomposition. 797-805A
- Notch toughness, Microstructural effects**  
Influence of Microstructure on Fatigue Crack Initiation in Fully Pearlitic Steels. 753-760A
- Notched bar tensile test**  
See Tension tests
- Notched tensile strength**  
See Notch strength
- Nuclear binding energy**  
See Binding energy (nuclear)
- Nuclear forces**  
See Binding energy (nuclear)
- Nuclear fuel claddings**  
See Nuclear fuel elements
- Nuclear fuel elements, Coating**  
Microstructural Investigation of Intermediate Phase Formation in Uranium—Aluminum Diffusion Couples. 589-595A
- Nuclear reactor components**  
The Microstructural Response of Mill—Annealed and Solution—Annealed INCONEL 600 to Heat Treatment. 1225-1236A
- Nuclear reactors**  
See Boiling water reactors  
Tokamak devices
- Nucleation**  
Perspectives on Nucleation. 487-502A  
Estimation of Nucleation Rate and Growth Rate From Time Dependence of Global Microstructural Properties During Phase Transformations. 559-564A  
Experimental Observations on the Nucleation and Growth of  $\delta'$  (Al<sub>3</sub>Li) in Dilute Al—Li Alloys. 1203-1211A
- Nucleation, Field effects**  
A Novel Solidification Technique of Metals and Alloys: Under the Influence of Applied Potential. 1354-1355A
- Nuclei (transformation)**  
See Nucleation
- Numerical analysis**  
A Note on Grain Boundary Diffusion Controlled Cavity Growth During Elevated-Temperature Fatigue. 300-302A  
Numerical Calculation of Fluid Flow in a Continuous Casting Tundish. 497-504B
- Oil field equipment, Corrosion**  
Sulfide Stress Cracking of High Strength Modified Cr—Mo Steels. 935-944A
- Optical masers**  
See Lasers
- Order disorder**  
See also Long range order  
Short range order  
Decomposition of Rapidly Solidified Cu—Ti Solid Solutions. 1353-1354A  
Low Temperature Aging of the Freshly Formed Martensite in an Fe—Ni—C Alloy. 1745-1750A
- Ordering**  
See Order disorder
- Ores**  
See Bornite  
Chalcocite  
Chalcopyrite  
Copper ores  
Galena  
Hematite  
Pyrrhotite  
Sphalerite  
Titanium ores
- Orientation**  
See also Grain orientation  
Plastic Behavior of Dual Phase Steel Following Plane-Strain Deformation. 421-425A



- Orientation Relationship Between Alpha Prime Titanium and Silicide  $S_2$  in Alloy Ti—6Al—6Zr—0.5Mo—0.25Si.** 453-455A
- Oscillations**  
Grain Structure and Solidification Cracking in Oscillated Arc Welds of 5052 Aluminum Alloy. 1345-1352A
- OSM process**  
See Oxygen steel making
- Oxidation**  
See also Internal oxidation  
Fatigue Microcrack Initiation in Polycrystalline Alpha-Iron With Polished and Oxidized Surfaces. 641-649A
- Oxidation rate**  
Oxidation of Pyrrhotite Particles Falling Through a Vertical Tube. 627-638B
- Oxidation rate, Environmental effects**  
An Effect of Chemisorbing Surface Reaction Poisons on the Transition From Internal to External Oxidation. 133-136A  
The Effect of Chlorine on the Kinetics of Oxidation of Cobalt in Environments Containing 0.5 Atmosphere of Oxygen Between 900K and 1200K. 751-761B
- Oxide coatings**  
Examination of the Strength of Oxide Skins on Aluminum Alloy Melts. 47-51B
- Oxide coatings, Mechanical properties**  
Reactive Element—Sulfur Interaction and Oxide Scale Adherence. 1164-1166A
- Oxide films**  
See Oxide coatings
- Oxides**  
See Aluminum oxide  
Carbon dioxide  
Lime  
Magnesium oxide  
Silicon dioxide  
Sulfur dioxide  
Wustite
- Oxidizing**  
See Oxidation
- Oxygen, Chemical analysis**  
A New Type of Oxygen Analyzer Utilizing a Potentiostatic Coulometric Titration Technique. 113-119B
- Oxygen, Diffusion**  
Electronic and Ionic Transport in Liquid PbO—SiO<sub>2</sub> Systems. Short-Range Reordering of Heavy Interstitials in Ta, Nb, and Fe During Relaxation and Static Strain Aging. 77-82B  
361-366A
- Oxygen, Reactions (chemical)**  
Effect of Arsenic on the Activity of Oxygen Dissolved in Dilute Liquid Copper Solutions. 339-344B
- Oxygen, Ternary systems**  
Thermodynamics of the Ca—S—O, Mg—S—O, and La—S—O Systems at High Temperatures. 287-294B
- Oxygen conversion processes**  
See Oxygen steel making
- Oxygen probes**  
A New Type of Oxygen Analyzer Utilizing a Potentiostatic Coulometric Titration Technique. 113-119B
- Oxygen steel making**  
Characteristics of Round Vertical Gas Bubble Jets. 263-275B
- Packing (crystal density)**  
See Crystal structure
- Packing fraction**  
See Binding energy (nuclear)
- Palladium, Binary systems**  
Phase Relationships and Thermodynamic Properties of the Pd—S System. 143-148B
- Palladium, Sorption**  
The Use of Palladium to Obtain Reproducible Boundary Conditions for Permeability Measurements Using Galvanostatic Charging. 715-719A
- Parameters**  
See Lattice parameters
- Passivation**  
A Unified Mechanism of Stress Corrosion and Corrosion Fatigue Cracking. 1133-1141A
- Pearlite**  
Influence of Microstructure on Fatigue Crack Initiation in Fully Pearlitic Steels. 753-760A
- Pearlite, Crystal growth**  
The Effect of Alloying Elements on Pearlite Growth. 597-603A  
Entropy Criteria Applied to Pattern Selection in Systems With Free Boundaries. 1781-1797A
- Penetration**  
The Use of Palladium to Obtain Reproducible Boundary Conditions for Permeability Measurements Using Galvanostatic Charging. 715-719A
- Permanent magnets**  
Role of Alloying Elements in Phase Decomposition in Alnico Magnet Alloys. 179-185A
- Permeability**  
The Effect of Pressure Modulation on the Flow of Gas Through a Solid Membrane: Surface Inhibition and Internal Traps. 1013-1024A
- Permeation**  
See Penetration
- Phase boundary**  
The Contiguity of Liquid Phase Sintered Microstructures. 1247-1252A  
Mobility of Martensitic Interfaces. 1713-1722A  
Entropy Criteria Applied to Pattern Selection in Systems With Free Boundaries. 1781-1797A
- Phase decomposition**  
See also Spinodal decomposition  
Growth Kinetics and Morphology of Grain Boundary Ferrite Allotriomorphs in an Fe—C—V Alloy. 521-527A  
The Early Stages of the Decomposition of Alloys. 1173-1184A  
Microstructural and Microchemical Aspects of the Solid-State Decomposition of Delta Ferrite in Austenitic Stainless Steels. 1363-1369A
- Phase decomposition, Alloying effects**  
Ordering Reactions in Ni—Al—Mo—Ta and Ni—Al—Mo—W Superalloys. 1963-1995A  
Rhenium Additions to a Nickel-Base Superalloy: Effects on Microstructure. 1997-2005A
- Phase decomposition, Heating effects**  
Cellular Decomposition in a Cu—25Ni—15Co Side-Band Alloy. 1751-1757A
- Phase diagram reactions**  
See also Austenitizing  
Martensitic transformations  
Phase decomposition  
Spinodal decomposition  
Thermodynamics of Formation of Y—Co Alloys. 1195-1201A  
Thermodynamics of the Fe—Cr—C System at 985K. 1479-1490A  
Low Temperature Aging of the Freshly Formed Martensite in an Fe—Ni—C Alloy. 1745-1750A  
Phase Transformations During Aging of a Nitrogen-Strengthened Austenitic Stainless Steels. 1759-1771A
- Phase diagrams**  
The Correlation of the Thermodynamic Properties and Phase Diagram of the System Tin—Lead Using a Gaussian Plus Krupkowski Formalism. 91-96B  
On the Arrangement of Monovariant Lines in Two-Dimensional Potential Phase Diagrams. 137-139A  
Isothermal Para-Equilibrium Phase Diagrams for Ternary Systems. 139-142A  
Phase Relationships and Thermodynamic Properties of the Pd—S System. 143-148B  
Thermodynamics and Phase Relationships of Transition Metal—Sulfur Systems. V.—A Reevaluation of the Fe—S System Using an Associated Solution Model for the Liquid Phase. 277-285B  
Phase Equilibria in the Ni—Al—Ti System at 1173K. 319-322A  
Applicability of Central Atoms Models to Binary Silicate and Aluminate Melts. 325-331B  
Correction to "Phase Relationships in the Fe—Cr—C System at Solidification Temperatures". 652B  
Effect of Magnetic Transition on Solubility of Carbon in B.C.C. Iron and F.C.C. Co—Ni Alloys. 913-921A  
Orthogonal Coordinates for Systems of Many Components. 928-933A  
The Fe-Rich Corner of the Metastable C—Cr—Fe Liquidus Surface. 1541-1549A  
The Niobium (Columbium)—Platinum Constitution Diagram. 1943-1949A
- Phase stability**  
A Mössbauer Spectrometry Study of the Mechanical Transformation of Precipitated Austenite in 6Ni Steel. 173-177A  
Carbide Stability in Nimonic 80A Alloy. 511-520A
- Phase stability, Diffusion effects**  
An Instability in Fe—C—M Alloys. 1609-1611A
- Phase stability, Field effects**  
Magnetic Contributions to the Thermodynamic Functions of Pure Nickel, Cobalt and Iron. 153-165A
- Phase stability, Heating effects**  
The Stability of Precipitated Austenite and the Toughness of 9Ni Steel. 2237-2249A  
The Mechanical Stability of Precipitated Austenite in 9Ni Steel. 2251-2256A
- Phase transformations**  
See also Allotropic transformation  
Austenitizing  
Martensitic transformations  
Massive type transformation  
Estimation of Nucleation Rate and Growth Rate From Time Dependence of Global Microstructural Properties During Phase Transformations. 559-564A
- Phase transformations, Alloying effects**  
The Effect of Alloying Elements on Pearlite Growth. 597-603A
- Phase transformations, Cooling effects**  
Kinetics of Austenite—Ferrite and Austenite—Pearlite Transformations in a 1025 Carbon Steel. 565-578A
- Phase transformations, Diffusion effects**  
X-Ray Diffraction and Resistivity Studies of Titanium—Molybdenum Alloys. 187-195A
- Phases (state of matter)**  
See also Gas phases  
Intermetallic phases  
Sigma phase
- Phases (state of matter), Composition effects**  
Phase Constitution and Lattice Parameter Relationships in Rapidly Solidified (Fe<sub>0.85</sub>Mn<sub>0.35</sub>)<sub>0.83</sub>Al<sub>0.17</sub>—xC and Fe<sub>3</sub>Al—xC Pseudobinary Alloys. 5-10A

## Phases (state of matter)

### Phases (state of matter), Crystal growth

Estimation of Nucleation Rate and Growth Rate From Time Dependence of Global Microstructural Properties During Phase Transformations.

559-564A

### Phases (state of matter), Crystal lattices

An X-Ray Diffraction Line Profile of Cold-Worked Hexagonal Alloys Zn—Ag:  $\eta$  and  $\epsilon$  Phase.

1427-1435A

### Phosphor bronzes, Corrosion

Sulfidation Under Atmospheric Conditions of Cu—Ni, Cu—Sn and Cu—Zn Binary and Cu—Ni—Sn and Cu—Ni—Zn Ternary Systems.

275-284A

### Phosphorus, Diffusion

The Influence of Grain Boundary Precipitation on the Measurement of Chromium Redistribution and Phosphorus Segregation in Ni—18Cr—9Fe.

349-359A

Grain Boundary Segregation of Phosphorus in 304L Stainless Steel.

2061-2062A

### Phosphorus, Impurities

Carbide Precipitation, Grain Boundary Segregation, and Temper Embrittlement in NiCrMoV Rotor Steels.

721-737A

### Photo oxidation

See Oxidation

### Photodecomposition

See Decomposition reactions

### Physical metallurgy

Solute Interactions in Multicomponent Solutions.

807-813B

### Physical properties

See Adhesion

Compressibility

Cryogenic properties

Diffusivity

Heat of formation

Heat of fusion

Heat of mixing

Permeability

Porosity

Solid solubility

Solubility

Specific heat

Surface tension

Texture

Vapor pressure

### Piano wire, Casting

Microstructure and Mechanical Properties of Fe—Ni—Cr—Al Steel Wires Produced by In-Rotating-Water Spinning Method.

215-226A

### Pipe, Materials substitution

Mathematical Modeling of Thermal Stresses in Basic Oxygen Furnace Hood Tubes.

247-261B

### Pipe, Mechanical properties

Effects of Gaseous Hydrogen on Fatigue Crack Growth in Pipeline Steel.

115-122A

### Pitting (corrosion)

The Effect of Microstructural Changes on the Caustic Stress Corrosion Cracking Resistance of a NiCrMoV Rotor Steel.

1333-1344A

### Plasma arcs

Distribution of the Heat and Current Fluxes in Gas Tungsten Arcs.

841-848B

### Plasma oscillations

See Oscillations

### Plaster of Paris

See Calcium compounds

### Plastic deformation

High Strain Rate Deformation of Molybdenum and Mo—33Re by Shock Loading. II.—Rates of Defect Generation and Accumulation of Plastic Strain.

891-895A

### Plastic deformation, Microstructural effects

Time-Dependent Deformation of Metals.

2215-2226A

### Plastic flow, Microstructural effects

Plastic Flow in Dispersion Hardened Materials. Time-Dependent Deformation of Metals.

2191-2200A

2215-2226A

### Plastic strain

See Plastic deformation

### Plasticity

See Superplasticity

### Plate metal, Casting

Centerline Porosity in Plate Castings.

823-829B

### Plate metal, Welding

Chemical Reactions During Submerged Arc Welding With FeO—MnO—SiO<sub>2</sub> Fluxes.

237-245B

### Platinum, Binary systems

The Niobium (Columbium)—Platinum Constitution Diagram.

1943-1949A

### Platinum metals

See Palladium

Platinum

### Point defects

See also Interstitial impurities

### Point defects, Deformation effects

High Strain Rate Deformation of Molybdenum and Mo—33Re by Shock Loading. I.—Substructure Development.

881-890A

### Polarization (electrodes)

See Anodic polarization

### Pores

See Porosity

### Porosity

Mathematical Modeling of Porosity Formation in Solidification.

359-366B

Centerline Porosity in Plate Castings.

823-829B

Microporosity in Hot Isostatically Pressed Ti—6Al—4V Powder Compacts.

1831-1834A

The Influence of Strain Rate and Porosity on the Deformation and Fracture of Titanium and Nickel.

2273-2281A

### Porosity, High temperature effects

Thermally Induced Porosity in Ti—6Al—4V Prealloyed Powder Compacts.

1526-1531A

### Portevin-Le Chatelier effect

See Serrated yielding

### Powder compacts

See also Sintered compacts

### Powder compacts, Corrosion

Effect of Cobalt Content on the Stress-Corrosion Cracking Behavior of 7091-Type Aluminum Powder Alloys.

945-951A

### Powder compacts, Fabrication

Explosive Consolidation of Rapidly Solidified Aluminum Alloy Powders.

1445-1455A

### Powder compacts, Forging

Thermomechanical Processing of Microalloyed Powder Forged Steels and a Cast Vanadium Steel.

1599-1608A

### Powder compacts, Mechanical properties

Correlation of Microyield Behavior With Silicon in X-520 and HIP-50 Beryllium.

807-814A

Microstructural Development in High Volume Fraction Gamma Prime Ni-Base Oxide-Dispersion-Strengthened Superalloys.

1285-1294A

The Influence of Strain Rate and Porosity on the Deformation and Fracture of Titanium and Nickel.

2273-2281A

### Powder compacts, Microstructure

Thermally Induced Porosity in Ti—6Al—4V Prealloyed Powder Compacts.

1526-1531A

Microporosity in Hot Isostatically Pressed Ti—6Al—4V Powder Compacts.

1831-1834A

### Powder metallurgy

Discussion of "Practical Applications of Hot-Isostatic Pressing Diagrams: From Case Studies".

1903-1904A

### Powder metallurgy parts, Heat treatment

The Development of Two Texture Variants and Their Effect on the Mechanical Behavior of a High Strength P/M Aluminum Alloy, X7091.

1089-1103A

### Powder metallurgy parts, Materials substitution

The Substitution of Nickel for Cobalt in Hot Isostatically Pressed Powder Metallurgy UDIMET 700 Alloys.

993-1003A

### Powder metallurgy parts, Mechanical properties

High Temperature Deformation of Ultra-Fine-Grained Oxide Dispersion Strengthened Alloys.

777-787A

High Cycle Fatigue and Fatigue Crack Growth of the Oxide Dispersion Strengthened Alloy MA 754.

1437-1444A

### Powder metallurgy parts, Microstructure

Effect of Dihedral Angle on the Morphology of Grains in a Matrix Phase.

923-928A

The Contiguity of Liquid Phase Sintered Microstructures.

1247-1252A

### Powder technology

See Powder metallurgy

### Powdering

Laser-Melting/Spin-Atomization Method for the Production of Titanium Alloy Powders.

1897-1900A

### Powders

See also Alloy powders

Metal powders

A Unified Approach to Bubbling—Jetting Phenomena in Powder Injection Into Iron and Steel.

203-209B

### Power supplies

See Electric batteries

### Precious metal alloys

See Gold base alloys

### Precious metals

See Gold

Palladium

Platinum

Silver

### Precipitate free zone

Product Microstructures and Properties Induced by Hot Working at Pb—1.85%Sn Alloy.

1273-1285A

### Precipitates

Equilibrium Solute Concentration Surrounding Elastically Interacting Precipitates.

337-347A

Orientation Relationship Between Precipitated Al<sub>3</sub>(Fe,Ni)<sub>2</sub> Phase and Alpha-Aluminum.

683-686A

Microstructure and Crystallography of Unidirectionally Solidified Ni—W Eutectic Alloy.

1185-1193A

### Precipitates, Crystal growth

Driving Force for Discontinuous Coarsening in a Ni—Al—Mo Base Superalloy.

11-16A

Criterion for Predicting the Morphology of Crystalline Cubic Precipitates in a Cubic Matrix.

197-202A

Orientation Relationship Between Alpha Prime Titanium and Silicide S<sub>2</sub> in Alloy Ti—6Al—5Zr—0.5Mo—0.25Si.

453-455A



- Use of Stereological Measurements for the Study of Grain Boundary Diffusion Controlled Precipitate Growth Kinetics. Perspectives on Nucleation. 456-457A  
Growth Kinetics and Morphology of Grain Boundary Ferrite Allotriomorphs in an Fe—C—V Alloy. 521-527A  
Coarsening Rate of Beta Precipitates in Al—11Mg Alloy. 709-713A
- Precipitates, Crystal lattices**  
Atom-Probe Microanalysis of a Nickel-Base Superalloy. 1703-1711A
- Precipitates, Phase transformations**  
Phase Transformations During Aging of a Nitrogen-Strengthened Austenitic Stainless Steels. 1759-1771A
- Precipitates, Stress effects**  
The Development of  $\gamma$ — $\gamma'$  Lamellar Structures in a Nickel-Base Superalloy During Elevated Temperature Mechanical Testing. 1969-1982A
- Precipitation**  
Direct Copper Precipitation From a Loaded Chelating Extractant by Pressure Hydrogen Stripping. 13-22B  
Growth Kinetics and Morphology of Grain Boundary Ferrite Allotriomorphs in an Fe—C—V Alloy. 521-527A
- Precipitation, Composition effects**  
The Influence of Cobalt, Tantalum, and Tungsten on the Microstructure of Single Crystal Nickel-Base Superalloys. 1849-1862A
- Precipitation hardening**  
See also Aging (artificial)  
Strain aging  
Serrated Grain Boundary Formation Potential of Nickel-Based Superalloys and Its Implications. 17-28A  
Mechanical Properties of Nitrogen—Ferrite. 45-50A  
Orientation Relationship Between Alpha Prime Titanium and Silicide  $S_2$  in Alloy Ti—6Al—5Zr—0.5Mo—0.25Si. 453-455A  
Experimental Observations on the Nucleation and Growth of  $\delta'$  ( $Al_3Li$ ) in Dilute Al—Li Alloys. 1203-1211A  
Low Temperature Carbide Precipitation in a Nickel Base Superalloy. 1213-1223A  
Ordering Reactions in Ni—Al—Mo—Ta and Ni—Al—Mo—W Superalloys. 1983-1995A  
Discussion of "Effect of Retrogression and Reaging Treatments on the Microstructure of Al-7075-T651". 2068A  
Improvement of Strength and Electrical Conductivity of Copper Alloy by Means of Thermo-Mechanical Treatment. 2073-2077A  
Precipitation Hardening. 2131-2165A  
Plastic Flow in Dispersion Hardened Materials. 2191-2200A
- Precipitation hardening, Alloying effects**  
Rhenium Additions to a Nickel-Base Superalloy: Effects on Microstructure. 1997-2005A
- Precipitation hardening alloys, Mechanical properties**  
On the Development of Crack Closure and the Threshold Condition for Short and Long Fatigue Cracks in 7150 Aluminum Alloy. 1467-1477A  
The Development of  $\gamma$ — $\gamma'$  Lamellar Structures in a Nickel-Base Superalloy During Elevated Temperature Mechanical Testing. 1969-1982A  
Plastic Flow in Dispersion Hardened Materials. 2191-2200A
- Precipitation hardening alloys, Phases (state of matter)**  
Microanalytical Study of the Heterogeneous Phases in Commercial Al—Zn—Mg—Cu Alloys. 1925-1936A
- Precipitation hardening steels, Mechanical properties**  
Mathematical Modeling of Thermal Stresses in Basic Oxygen Furnace Hood Tubes. 247-261B
- Precipitation heat treatment**  
See also Aging (artificial)  
Precipitation hardening  
Coarsening Rate of Beta Precipitates in Al—11Mg Alloy. 709-713A  
On the Development of Crack Closure and the Threshold Condition for Short and Long Fatigue Cracks in 7150 Aluminum Alloy. 1467-1477A
- Preferential attack (corrosion)**  
See Intergranular corrosion
- Pregnant liquors, Chemical analysis**  
Determination of Cu(II) and Fe(III) in Chloride Solutions Concentrated in Both Copper and Iron. 403-404B
- Pressing**  
See Hot isostatic pressing  
Hot pressing
- Pressure**  
See Vapor pressure
- Pressure sintering**  
See Hot pressing
- Pressure vessels**  
Microstructural Changes in 1Cr—0.5Mo Steel After 20 Years of Service. 109-114A  
A Study of Fatigue Crack Propagation in Prior Hydrogen Attacked Pressure Vessel Steels. 1491-1501A
- Pressure welding**  
See Diffusion welding  
Explosive welding
- Prestressing**  
Effect of Cold Work on Stress Corrosion Cracking Behavior of Types 304 and 316 Stainless Steels. 285-289A
- Primary displacements**  
See Displacements (lattice)
- Probes**  
See Oxygen probes
- Projectiles, Mechanical properties**  
Adiabatic Shear Localization in Titanium and Ti—8Al—4V Alloy. 761-775A
- Propagation**  
See Crack propagation
- Properzi process**  
See Continuous casting
- Protective coatings, Corrosion**  
Sulfation of  $Y_2O_3$  and  $HfO_2$  in Relation to MCrAl Coatings. 303-306A
- Pyroceram**  
See Ceramics
- Pyrometallurgy**  
Thermodynamic Study of  $Na_2O$ — $SiO_2$  Melts at 1300 and 1400°C. 313-323B  
Cyclic Thermogravimetric Methods for the Study of the Decomposition of Carbonates— $CaCO_3$ . 743-749B
- Pyrrhotite, Oxidation**  
Oxidation of Pyrrhotite Particles Falling Through a Vertical Tube. 627-638B
- Quantitative metallography**  
The Contiguity of Liquid Phase Sintered Microstructures. 1247-1252A
- Quaternary systems, Diffusion**  
Quaternary Diffusion in the Cu—Ni—Zn—Mn System at 775°C. 1123-1132A
- Quench hardening**  
See Austempering
- Quenching (cooling)**  
See also Rapid solidification  
The Concept of an Effective Quench Temperature and Its Use in Studying Elevated-Temperature Microstructures. 1521-1523A
- Quenching stresses**  
See Residual stress
- Radiant heating**  
See Laser beam heating
- Radiocrystallography**  
See Crystallography
- Rail steels, Mechanical properties**  
Influence of Microstructure on Fatigue Crack Initiation in Fully Pearlitic Steels. 753-760A
- Rapid solidification**  
Orientation Relationship Between Precipitated  $Al_3(Fe,Ni)_2$  Phase and Alpha-Aluminum. 683-686A  
The Microstructure of Rapidly Solidified  $Al_3Mn$ . 1005-1012A  
Decomposition of Rapidly Solidified Cu—Ti Solid Solutions. 1353-1354A  
The Effect of Cooling Conditions on the Microstructure of Rapidly Solidified Ti—6Al—4V. 1951-1959A
- Rare earth metals**  
See also Lanthanum
- Rare earth metals, Binary systems**  
The Structure of  $R_{1-x}Ga_x$  ( $0 < x < 0.33$ ) and Its Relation to  $RGa_2$  ( $R$  = Rare Earth Element) and Gallium. 167-171A
- Rare earth metals, Reactions (chemical)**  
Equilibria Between Rare Earth Elements and Sulfur in Molten Iron. 785-792B
- Rare gases**  
See Argon  
Helium
- Reaction kinetics**  
The Leaching of Hematite in Acid Solutions. 23-30B  
Representation of the Kinetics of Leaching of Galena by Ferric Chloride in Concentrated Sodium Chloride Solutions by a Modified Mixed Kinetics Model. 31-39B  
Kinetics of the Reaction Between Hydrogen Sulfide and Lime Particles. 163-168B  
Intrinsic Kinetics of the Hydrogen Reduction of Copper Sulfate: Determination by a Nonisothermal Technique. 397-401B  
The Kinetics of Dissolution of Sphalerite in Ferric Chloride Solution. 413-424B  
Leaching of Chrysocolla With Ammonia—Ammonium Carbonate Solutions. 441-448B  
Kinetic Model for the Chemical Dissolution of Multiparticle Systems. 449-454B  
Direct Reduction of Lead Sulfide With Carbon and Lime; Effect of Catalysts: II.—Analytical Model. 477-488B  
Kinetics of the Zinc Slag-Fuming Process. I.—Industrial Measurements. 513-527B  
Kinetics of the Zinc Slag-Fuming Process. II.—Mathematical Model. 529-540B  
Kinetics of the Zinc Slag-Fuming Process. III.—Model Predictions and Analysis of Process Kinetics. 541-549B  
The Kinetics of the Nitrogen Reaction With Liquid Iron—Sulfur Alloys. 551-559B  
Successive Gas—Solid Reaction Model for the Hydrogen Reduction of Cuprous Sulfide in the Presence of Lime. 645-662B  
The Rate of Formation of  $SiO$  by the Reaction of CO or Hydrogen With Silica and Silicate Slags. 801-806B  
Intrinsic Kinetics of the Hydrogen Reduction of  $Cu_2S$ . 831-839B  
The Effect of Carbon Content on the Kinetics of Decarburization in Fe—C Alloys. 1180-1163A  
Displacement Reactions Between Chromium and  $MoO_2$  in a Nickel-Base Alloy Matrix. 1815-1830A
- Reactions (chemical)**  
See Carbothermic reactions  
Chlorination  
Decomposition reactions

## Reactions (chemical)

- Dehydrogenation
- Desulfurizing
- Desulfurizing
- Dezincification
- Hydrogen reduction
- Interface reactions
- Internal oxidation
- Oxidation
- Reactivity (chemical)**  
See Activity (chemical)
- Reactors**  
See Boiling water reactors  
Tokamak devices
- Recrystallization**  
See also Grain refinement  
Secondary recrystallization
- Recrystallization, Alloying effects**  
Dynamic Recrystallization During Creep in a 45% Ni—35% Fe—20% Cr Alloy System. 51-57A
- Recrystallization, Deformation effects**  
Effect of Cold Work on Recrystallization Behavior and Grain Size Distribution in Titanium. 703-708A
- Red hardness**  
See Hardness
- Reduction (chemical)**  
See Direct reduction  
Flash smelting  
Fluidized bed reduction  
Hydrogen reduction
- Reduction (electrolytic)**  
See Electrowinning
- Reduction (metal working)**  
See Cold rolling  
Deep drawing  
Wire drawing
- Refining**  
Thermodynamic Study of  $\text{Na}_2\text{O}$ — $\text{SiO}_2$  Melts at 1300 and 1400°C. 313-323B
- Refractory alloys**  
See Molybdenum base alloys  
Niobium base alloys  
Tungsten base alloys  
Vanadium base alloys
- Refractory metal compounds**  
See Molybdenum compounds  
Tungsten carbide  
Vanadium compounds
- Refractory metals**  
See Chromium  
Molybdenum  
Niobium  
Rhenium  
Tantalum  
Tungsten  
Vanadium
- Reinforcement**  
See Fiber composites
- Relaxation**  
See Stress relaxation
- Research**  
See Technology transfer
- Residual stress**  
Fatigue Crack Propagation in Carburized High Alloy Bearing Steels. 1253-1265A
- Residual stress, Heating effects**  
Fatigue Crack Propagation in Carburized X-2M Steel. 1267-1271A
- Residual stress, Impurity effects**  
Tetragonal Distortion Field of Hydrogen Atoms in Iron. 1649-1653A
- Resistance welds**  
See Welded joints
- Retained austenite**  
A Theoretical Model for the Flow Behavior of Commercial Dual-Phase Steels Containing Metastable Retained Austenite. I.—Derivation of Flow Curve Equations. 2013-2021A  
A Theoretical Model for the Flow Behavior of Commercial Dual-Phase Steels Containing Metastable Retained Austenite. II.—Calculation of Flow Curves. 2023-2029A
- Retained austenite, Composition effects**  
The Relationship Between Microstructure and Fracture Behavior of Fully Austenitic Type 316L Weldments at 4.2K. 1835-1848A
- Reviews**  
The Early Stages of the Decomposition of Alloys. 1173-1184A  
A Brief History of Dislocation Theory. 2085-2090A  
Theory of Workhardening 1934-1984. 2091-2108A  
Kinetics of Solution Hardening. 2109-2129A  
Precipitation Hardening. 2131-2165A  
Polycrystalline Strengthening. 2167-2190A  
Plastic Flow in Dispersed Hardened Materials. 2191-2200A  
Hardening Behavior in Fatigue. 2201-2214A  
Time-Dependent Deformation of Metals. 2215-2226A
- Rhenium, Alloying elements**  
Rhenium Additions to a Nickel-Base Superalloy: Effects on Microstructure. 1997-2005A
- Rheocasting**  
A Model for Deformation and Segregation of Solid—Liquid Mixtures. 1393-1403A
- Ribbons (metallic)**  
See Tapes (metallic)
- Riseling**  
See Gating and risering
- Rolling**  
See Cold rolling  
Controlled rolling
- Rolling contact**  
Fatigue Crack Propagation in Carburized High Alloy Bearing Steels. 1253-1265A
- Rotary kilns**  
See Kilns
- Rotor blades**  
Carbide Precipitation, Grain Boundary Segregation, and Temper Embrittlement in NiCrMoV Rotor Steels. 721-737A
- Roundness**  
See Shape
- Rupture strength**  
See Creep rupture strength
- S N diagrams, Deformation effects**  
The Effect of Cold Rolling on the Fatigue Properties of Ti—6Al—4V. 144-145A
- Salt (sodium chloride)**  
See Sodium chloride
- Salt water**  
See Sea water
- Salts (inorganic)**  
See Inorganic salts
- Sand casting**  
Modeling of Heat Flow in Sand Castings. II.—Applications of the Boundary Curvature Method. 203-209B
- Sand castings, Thermal properties**  
Modeling of Heat Flow in Sand Castings. I.—The Boundary Curvature Method. 195-202B  
Modeling of Heat Flow in Sand Castings. II.—Applications of the Boundary Curvature Method. 203-209B
- Sand molds, Thermal properties**  
Modeling of Heat Flow in Sand Castings. I.—The Boundary Curvature Method. 195-202B  
Modeling of Heat Flow in Sand Castings. II.—Applications of the Boundary Curvature Method. 203-209B
- Sap process**  
See Dispersion hardening
- Sapphire, Reactions (chemical)**  
Interfacial Phenomena Between Molten Metals and Sapphire Substrate. 567-575B
- Scale (corrosion)**  
Mechanical Properties of a Low Alloy Steel in a Molten Nitrate Salt Environment. 1031-1041A  
Reactive Element—Sulfur Interaction and Oxide Scale Adherence. 1164-1168A
- Scale (corrosion), Crystal growth**  
Formation of Aluminum Oxide Scales in Sulfur-Containing High Temperature Environments. 2051-2059A
- Sea water, Environment**  
Effect of Cobalt Content on the Stress-Corrosion Cracking Behavior of 7091-Type Aluminum Powder Alloys. 945-951A
- Season cracking**  
See Stress corrosion cracking
- Secondary displacements**  
See Displacements (lattice)
- Secondary recrystallization**  
The Effect of Initial Carbide Morphology on Abnormal Grain Growth in Decarburized Low Carbon Steel. 897-906A
- Secondary recrystallization, Deformation effects**  
Ferrite Recrystallization and Austenite Formation in Cold-Rolled Intercritically Annealed Steel. 1385-1392A
- Seeding**  
See Nucleation
- Segregations**  
Subcritical Intergranular Crack Growth Rates and Thresholds of Iron and Iron + Antimony. 123-131A  
Interaction of Iron Particles With a Solid/Liquid Interface in Lead and Lead Alloys. 367-375B  
Grain Boundary Fracture of L<sub>12</sub> Type Intermetallic Compound Ni<sub>3</sub>Al. 441-443A  
Inverse Segregation in Directionally Solidified Al—Cu—Ti Alloys With Equiaxed Grains. 579-587A  
Inverse Segregation. 595-604B  
Effect of Oscillation-Mark Formation on the Surface Quality of Continuously Cast Steel Slabs. 605-624B  
Discussion of "An Analytical Electron Microscope Study of the Kinetics of the Equilibrium Segregation of Bismuth in Copper" and Authors Reply. 686-690A  
An Experimental Study of Segregation in Rotary Kilns. 763-774B  
Embrittlement of Austempered Nodular Irons: Grain Boundary Phosphorus Enrichment Resulting From Precipitate Decomposition. 797-805A  
Correction to "Effect of Oscillation-Mark Formation on the Surface Quality of Continuously Cast Steel Slabs". 858B

- The Effect of Initial Carbide Morphology on Abnormal Grain Growth in Decarburized Low Carbon Steel. 897-906A
- Superalloy Microstructural Variations Induced by Gravity Level During Directional Solidification. 1683-1687A
- Measurement and Analysis of Distribution Coefficients in Fe—Ni Alloys Containing Sulfur and/or Phosphorus. II.— $K_F$ ,  $K_{GS}$ , and  $K_{GP}$ . 1871-1878A
- Grain Boundary Segregation of Phosphorus in 304L Stainless Steel. 2061-2062A
- Flow of Interdendritic Liquid and Permeability in Pb—20Sn Alloys. 2263-2271A
- Segregations, Alloying effects**  
The Influence of Grain Boundary Precipitation on the Measurement of Chromium Redistribution and Phosphorus Segregation in Ni—16Cr—9Fe. 349-359A
- Segregations, Crystal growth**  
Influence of Dendrite Network Defects on Channel Segregate Growth. 1687-1689A
- Segregations, Pressure effects**  
A Model for Deformation and Segregation of Solid—Liquid Mixtures. 1393-1403A
- Selenium, Impurities**  
Thermodynamics of Removing Selenium and Tellurium From Liquid Copper by Sodium Carbonate Slags. 171-172B
- Self diffusion**  
See Diffusion
- Semicontinuous casting**  
See Continuous casting
- Separators**  
See Filters (fluid)
- Serrated yielding**  
Temperature and Strain Rate Dependence of Stress—Strain Behavior in a Nickel-Base Superalloy. 1049-1067A
- Shaft kilns**  
See Kilns
- Shape, Stress effects**  
Criterion for Predicting the Morphology of Crystalline Cubic Precipitates in a Cubic Matrix. 197-202A
- Shear properties**  
See also Shear strength  
Observations of Adiabatic Shear Band Formation in 7039 Aluminum Alloy. 1900-1903A
- Shear strength, Deformation effects**  
Adiabatic Shear Localization in Titanium and Ti—6Al—4V Alloy. 761-775A
- Sheet metal, Mechanical properties**  
Thermal Gradients, Strain Rate and Ductility in Sheet Steel Tensile Specimens. 37-43A  
Hill's Plastic Strain Ratio of Sheet Metals. 1531-1535A  
A Simplified Numerical Analysis of the Sheet Tensile Test. 2291-2298A  
An Analysis of the Nonisothermal Tensile Test. 2299-2308A
- Sheet metal, Metal working**  
Plastic Behavior of Dual Phase Steel Following Plane-Strain Deformation. 421-425A  
Effects of Plastic Anisotropy and Yield Surface Shape on Sheet Metal Stretchability. 629-639A
- Shielded arc welding**  
See Gas tungsten arc welding  
Shielded metal arc welding  
Submerged arc welding
- Shielded metal arc welding**  
Hydrogen Attack Kinetics of 2.25 Cr—1 Mo Steel Weld Metals. 1143-1149A
- Shock loading**  
High Strain Rate Deformation of Molybdenum and Mo—33Re by Shock Loading. I.—Substructure Development. 881-890A  
High Strain Rate Deformation of Molybdenum and Mo—33Re by Shock Loading. II.—Rates of Defect Generation and Accumulation of Plastic Strain. 891-895A
- Short range order**  
Determination of the Coordination Number of Liquid Metals Near the Melting Point. 267-274A
- Shrinkage**  
Centerline Porosity in Plate Castings. 823-829B
- Sigma phase**  
The Structure of  $R_{(1-x)}Ga_{2(1+x)}$  ( $0 < x < 0.33$ ) and Its Relation to  $RGa_3$  ( $R$  = Rare Earth Element) and Gallium. 167-171A
- Sigma phase, Crystal growth**  
Phase Transformations During Aging of a Nitrogen-Strengthened Austenitic Stainless Steels. 1759-1771A
- Silica**  
See Silicon dioxide
- Silicates**  
Applicability of Central Atoms Models to Binary Silicate and Aluminate Melts. 325-331B
- Silicides, Crystal growth**  
Orientation Relationship Between Alpha Prime Titanium and Silicide  $S_2$  in Alloy Ti—6Al—5Zr—0.5Mo—0.25Si. 453-455A
- Silicon, Alloying additive**  
Effect of Silicide Precipitation on Tensile Properties and Fracture of Alloy Ti—6Al—5Zr—0.5Mo—0.25Si. 227-231A
- Silicon, Alloying elements**  
The Effect of Alloying Elements on Pearlite Growth. 597-603A
- Mössbauer Effect of Al—Fe—Si Intermetallic Compounds. 1937-1942A
- Silicon, Impurities**  
Impurity Effect on Cube Texture in Pure Aluminum Foils. 27-36A  
Correlation of Microyield Behavior With Silicon in X-520 and HIP-50 Beryllium. 807-814A
- Silicon base alloys, Thermal properties**  
New Eutectic Alloys and Their Heats of Transformation. 323-328A
- Silicon carbide, Composite materials**  
Analysis of Stress—Strain, Fracture, and Ductility Behavior of Aluminum Matrix Composites Containing Discontinuous Silicon Carbide Reinforcement. 1105-1115A
- Silicon compounds**  
See Silicon carbide  
Silicon dioxide
- Silicon dioxide, Reactions (chemical)**  
Kinetics of the Reaction of  $SiO_2(g)$  With Carbon Saturated Iron. 121-127B  
The Rate of Formation of  $SiO$  by the Reaction of  $CO$  or Hydrogen With Silica and Silicate Slags. 801-806B  
Correction to "Kinetics of the Reaction of  $SiO_2(g)$  With Carbon Saturated Iron". 857B
- Silicon iron**  
See Silicon steels
- Silicon manganese steels, Heat treatment**  
Austenitization During Intercritical Annealing of an Fe—C—Si—Mn Dual-Phase Steel. 1237-1245A
- Silicon steels**  
See also Electrical steels  
Silicon manganese steels
- Silicon steels, Mechanical properties**  
Microstructure—Mechanical Property Relationships of Dual-Phase Steel Wire. 831-840A
- Silicon steels, Phase transformations**  
Discussion of "The Bainite Transformation in a Silicon Steel" and Authors' Reply. 457-468A
- Silver, Extraction**  
Heterogeneous Equilibria in the Au—CN— $H_2O$  and Ag—CN— $H_2O$  Systems. 455-463B
- Silver, Reactions (chemical)**  
Interfacial Phenomena Between Molten Metals and Sapphire Substrate. 567-575B
- Silver, Recovering**  
Distribution of Gold and Silver Between Copper and Matte. 53-59B
- Simulation**  
See Computer simulation
- Single crystals, Mechanical properties**  
Elevated Temperature Creep-Rupture Behavior of the Single Crystal Nickel-Base Superalloy NASAIR 100. 427-439A  
Elastic Constants of a Monocrystalline Nickel-Base Superalloy. 661-665A  
The Effects of Orientation and Thickness on the Notch—Tensile Creep Strength of Single Crystals of a Nickel-Base Superalloy. 1457-1468A
- Single crystals, Microstructure**  
The Influence of Cobalt, Tantalum, and Tungsten on the Microstructure of Single Crystal Nickel-Base Superalloys. 1849-1862A
- Sintered compacts, Mechanical properties**  
Effect of Inclusions on LCF Life of HIP Plus Heat Treated Powder Metal René 95. 775-784B  
Effect of Strain Rate on the Flow Stress of Three Liquid Phase Sintered Tungsten Alloys. 2031-2037A  
The Influence of Strain Rate and Porosity on the Deformation and Fracture of Titanium and Nickel. 2273-2281A
- Sintering**  
Sintering Kinetics and Alumina Yield in Lime—Soda Sinter Process for Alumina From Coal Wastes. 385-395B
- Sintering (powder metallurgy)**  
See Liquid phase sintering
- Slag fuming**  
Kinetics of the Zinc Slag-Fuming Process. I.—Industrial Measurements. 513-527B  
Kinetics of the Zinc Slag-Fuming Process. II.—Mathematical Model. 529-540B  
Kinetics of the Zinc Slag-Fuming Process. III.—Model Predictions and Analysis of Process Kinetics. 541-549B
- Slags**  
See also Blast furnace slags  
Thermodynamic Study of  $Na_2O$ — $SiO_2$  Melts at 1300 and 1400°C. 313-323B  
Applicability of Central Atoms Models to Binary Silicate and Aluminate Melts. 325-331B
- Slags, Diffusion**  
Electronic and Ionic Transport in Liquid  $PbO$ — $SiO_2$  Systems. 77-82B
- Slags, Solubility**  
Determination and Prediction of Water Vapor Solubilities in  $CaO$ — $MgO$ — $SiO_2$  Slags. 61-66B  
Solubilities of Carbon Dioxide in Sodium Silicate Melts. 561-566B
- Slip**  
See Slip planes
- Slip planes**  
Mechanism for the Formation of High Cycle Fatigue Cracks at FCC Annealing Twin Boundaries. 873-880A

## Slip planes

- The Effect of Grain Size and Plastic Strain on Slip Length in 70-30 Brass. 1025-1029A
- An X-Ray Diffraction Line Profile of Cold-Worked Hexagonal Alloys Zn—Ag:  $\eta$  and  $\epsilon$  Phase. 1427-1435A
- Slip planes, Composition effects**
- Deformation Characteristics in Beta Phase Ti—Nb Alloys. 789-795A
- Slurries, Physical properties**
- A Model for Deformation and Segregation of Solid—Liquid Mixtures. 1393-1403A
- Smelting**
- See Flash smelting
- Sodium aluminum fluoride**
- See Cryolite
- Sodium chloride, Environment**
- Stress Corrosion Cracking of an Aluminum Alloy Under Compressive Stress. 1663-1670A
- Sodium compounds**
- See Sodium chloride
- Sodium hydroxide
- Sodium hydroxide, Environment**
- The Effect of Microstructural Changes on the Caustic Stress Corrosion Cracking Resistance of a NiCrMoV Rotor Steel. 1333-1344A
- Soft annealing**
- See Annealing
- Softening**
- See Strain softening
- Solar heating**
- Mechanical Properties of a Low Alloy Steel in a Molten Nitrate Salt Environment. 1031-1041A
- Solid solubility**
- Discussion of "Effects of Tempering on the Carbon Activity and Hydrogen Attack Kinetics of 2.25Cr—1Mo Steel" and Authors' Reply. 1355-1357A
- Thermodynamics of the Fe—Cr—C System at 985K. 1479-1490A
- Solid solubility, Field effects**
- Effect of Magnetic Transition on Solubility of Carbon in B.C.C. Iron and F.C.C. Co—Ni Alloys. 913-921A
- Solidification**
- See also Directional solidification
- Rapid solidification
- The Influence of Convection on Heat Transfer in Liquid Tin. Interaction of Iron Particles With a Solid/Liquid Interface in Lead and Lead Alloys. 367-375B
- Perspectives on Nucleation. 487-502A
- Metal/Mold Interfacial Heat Transfer. 585-594B
- On the Permeability of the Two-Phase Zone During Solidification of Alloys. 693A
- Influence of Dendrite Network Defects on Channel Segregate Growth. 1667-1689A
- Flow of Interdendritic Liquid and Permeability in Pb—20Sn Alloys. 2263-2271A
- Solubility**
- See also Solid solubility
- The Structure of  $R_{1-x}Ga_{2x}Al_{1-x}$  ( $0 < x < 0.33$ ) and Its Relation to  $RGa_2$  ( $R$  = Rare Earth Element) and Gallium. 167-171A
- Solubility, Alloying effects**
- Isotopic Solubility of Hydrogen in Vanadium Alloys at Low Temperatures. 367-374A
- Nitrogen Solubility and Nitride Formation in Austenitic Fe—Ti Alloys. 815-822B
- Solubility, Composition effects**
- Determination and Prediction of Water Vapor Solubilities in CaO—MgO—SiO<sub>2</sub> Slags. 61-66B
- Solubility, PH effects**
- The Solubility of Barium Arsenate: Sherritt's Barium Arsenate Process. 404-406B
- Solubilities of Carbon Dioxide in Sodium Silicate Melts. 561-566B
- Correction to "The Solubility of Barium Arsenate: Sherritt's Barium Arsenate Process". 662B
- Solutes, Microstructural effects**
- Equilibrium Solute Concentration Surrounding Elastically Interacting Precipitates. 337-347A
- Solution annealing**
- The Microstructural Response of Mill—Annealed and Solution—Annealed INCONEL 600 to Heat Treatment. 1225-1236A
- Solution hardening**
- See Solution strengthening
- Solution heat treatment**
- Carbide Stability in Nimonic 80A Alloy. 511-520A
- Solution strengthening**
- Kinetics of Solution Hardening. 2109-2129A
- Solvent extraction**
- Direct Copper Precipitation From a Loaded Chelating Extractant by Pressure Hydrogen Stripping. 13-22B
- Reductive Stripping of Fe(III)-Loaded D2EHPA With the Aqueous Solutions Containing Sulfur Dioxide. 187-194B
- Hydrolytic Stripping of Single and Mixed Metal—Versatic Solutions. 671-677B
- Solvus (metallurgical)**
- See Solid solubility
- Sorption**
- See Absorption (material)
- Sour gas, Environment**
- Sulfide Stress Cracking of High Strength Modified Cr—Mo Steels. 935-944A
- Space lattices**
- See Crystal lattices
- Specific heat, Field effects**
- Magnetic Contributions to the Thermodynamic Functions of Pure Nickel, Cobalt and Iron. 153-165A
- Spectrography**
- See Spectroscopy
- Spectrometry**
- See Spectroscopy
- Spectroscopy**
- See also Mass spectroscopy
- Mosbauer spectroscopy
- Determination of Cu(II) and Fe(III) in Chloride Solutions Concentrated in Both Copper and Iron. 403-404B
- Speller**
- See Zinc
- Sphalerite, Reduction (chemical)**
- The Kinetics of Dissolution of Sphalerite in Ferric Chloride Solution. 413-424B
- Kinetics of Bio-Chemical Leaching of Sphalerite Concentrate. 667-670B
- Reaction Mechanism for the Ferric Chloride Leaching of Sphalerite. 715-724B
- Sphericity**
- See Shape
- Spheroidal iron**
- See Nodular iron
- Spheroidizing**
- The Formation of Austenite at Low Intercritical Annealing Temperatures in a Normalized 0.08C—1.45Mn—0.21Si Steel. 1523-1526A
- Spinodal decomposition**
- Decomposition of Rapidly Solidified Cu—Ti Solid Solutions. 1353-1354A
- Spinodal decomposition, Alloying effects**
- Role of Alloying Elements in Phase Decomposition in Alnico Magnet Alloys. 179-185A
- Spinodal decomposition, Heating effects**
- Cellular Decomposition in a Cu—25Ni—15Co Side-Band Alloy. 1751-1757A
- Sponginess**
- See Porosity
- Squeeze casting**
- A Model for Deformation and Segregation of Solid—Liquid Mixtures. 1393-1403A
- Stability**
- See Phase stability
- Stacking fault energy, Deformation effects**
- An X-Ray Diffraction Line Profile of Cold-Worked Hexagonal Alloys Zn—Ag:  $\eta$  and  $\epsilon$  Phase. 1427-1435A
- Stacking faults**
- Lattice Image Studies on the Intervariant Boundary Structure and Substructure of Cu—Zn—Al 18R Martensite. 1551-1566A
- Stainless steels**
- See also Austenitic stainless steels
- Ferritic stainless steels
- Stainless steels, Composite materials**
- The Effects of Hot Pressing Parameters on the Strength of Aluminum/Stainless Steel Composites. 623-628A
- Stainless steels, Corrosion**
- Formation of Aluminum Oxide Scales in Sulfur-Containing High Temperature Environments. 2051-2059A
- Stainless steels, Refining**
- Turbulent Fluid Flow Phenomena in a Water Model of an AOD System. 67-75B
- Stamping**
- Plastic Behavior of Dual Phase Steel Following Plane-Strain Deformation. 421-425A
- Static fatigue**
- See Creep rupture strength
- Static tests**
- See Creep tests
- Steel constituents**
- See Austenite
- Bainite
- Ferrite
- Martensite
- Pearlite
- Retained austenite
- Steel converters**
- See Basic converters
- Steel making**
- See also Oxygen steel making
- Determination and Prediction of Water Vapor Solubilities in CaO—MgO—SiO<sub>2</sub> Slags. 61-66B
- Turbulent Fluid Flow Phenomena in a Water Model of an AOD System. 67-75B
- Hydrodynamic Modeling of Some Gas Injection Procedures in Ladle Metallurgy Operations. 83-90B



- Applicability of Central Atoms Models to Binary Silicate and Aluminate Melts. 325-331B
- Steels**  
 See also Austenitic stainless steels  
 Bearing steels  
 Carbon steels  
 Chromium molybdenum steels  
 Chromium steels  
 Die steels  
 Dual phase steels  
 Electrical steels  
 Ferritic stainless steels  
 High speed tool steels  
 High strength low alloy steels  
 High strength steels  
 Hot work tool steels  
 Low alloy steels  
 Manganese steels  
 Molybdenum steels  
 Nickel chromium molybdenum steels  
 Nickel chromium steels  
 Nickel molybdenum steels  
 Nickel steels  
 Precipitation hardening steels  
 Rail steels  
 Silicon manganese steels  
 Silicon steels  
 Stainless steels
- Steels, Casting**  
 Numerical Calculation of Fluid Flow in a Continuous Casting Tundish. 497-504B  
 Effect of Oscillation-Mark Formation on the Surface Quality of Continuously Cast Steel Slabs. 605-624B  
 Centerline Porosity in Plate Castings. 823-829B  
 Correction to "Effect of Oscillation-Mark Formation on the Surface Quality of Continuously Cast Steel Slabs". 858B
- Steels, Corrosion**  
 A Unified Mechanism of Stress Corrosion and Corrosion Fatigue Cracking. 1133-1141A
- Steels, Mechanical properties**  
 Measurement and Evaluation of the Anisothermal Softening of Austenite After Hot Deformation. 67-72A  
 On Macroscopic and Microscopic Analyses for Crack Initiation and Crack Growth Toughness in Ductile Alloys. 233-248A  
 Correction to "On Macroscopic and Microscopic Analyses for Crack Initiation and Crack Growth Toughness in Ductile Alloys". 1358A  
 Hill's Plastic Strain Ratio of Sheet Metals. 1531-1535A
- Steels, Refining**  
 Hydrodynamic Modeling of Some Gas Injection Procedures in Ladle Metallurgy Operations. 83-90B  
 A Unified Approach to Bubbling—Jetting Phenomena in Powder Injection Into Iron and Steel. 203-209B  
 Simultaneous Desulfurization and Dephosphorization Reactions of Molten Iron by Soda Ash Treatment. 303-312B  
 Physical Refining of Steel Melts by Filtration. 725-742B
- Stereomicroscopy**  
 Use of Stereological Measurements for the Study of Grain Boundary Diffusion Controlled Precipitate Growth Kinetics. 456-457A
- Stick electrode arc welding**  
 See Shielded metal arc welding
- Sticking (adhesion)**  
 See Adhesion
- Stirring**  
 See Electromagnetic stirring
- Stora Kaido process**  
 See Oxygen steel making
- Storage**  
 See Heat storage
- Strain aging**  
 Short-Range Reordering of Heavy Interstitials in Ta, Nb, and Fe During Relaxation and Static Strain Aging. 361-366A
- Strain hardenability**  
 The Effect of Grain Size and Plastic Strain on Slip Length in 70-30 Brass. 1025-1029A
- Strain hardening**  
 Thermal Gradients, Strain Rate and Ductility in Sheet Steel Tensile Specimens. 37-43A  
 Work Hardening Correlations Based on State Variables in Some F.C.C. Metals in Monotonic Loading. 411-420A  
 Tensile Stress—Strain Analysis of Cold Worked Metals and Steels and Dual-Phase Steels. 865-872A  
 Temperature and Strain Rate Dependence of Stress—Strain Behavior in a Nickel-Base Superalloy. 1049-1067A  
 Some Trends Observed in the Elevated-Temperature Kinematic and Isotropic Hardening of Type 304 Stainless Steel. 1069-1076A  
 Product Microstructures and Properties Induced by Hot Working at Pb—1.85% Sb Alloy. 1273-1285A  
 Theory of Workhardening 1934-1984. 2091-2108A  
 Polycrystalline Strengthening. 2167-2190A  
 Hardening Behavior in Fatigue. 2201-2214A  
 Time-Dependent Deformation of Metals. 2215-2226A
- Strain hardening, Microstructural effects**  
 The Dependence of Some Tensile and Fatigue Properties of a Dual-Phase Steel on Its Microstructure. 1405-1415A
- Strain rate**  
 Influence of Strain Rate and Temperature on the Deformation Behavior of a Metastable High Carbon Iron—Nickel Austenite. 445-452A
- Strain softening**  
 Measurement and Evaluation of the Anisothermal Softening of Austenite After Hot Deformation. 67-72A
- Strategic materials**  
 Of Perspectives, Issues, and Politics in Materials Technology. 5-11B  
 Of Perspectives, Issues, and Politics in Materials Technology. 311-317A
- Strength of materials**  
 See Mechanical properties
- Strengthening (solution)**  
 See Solution strengthening
- Stress aging**  
 See Strain aging
- Stress concentration**  
 The Effect of Grain Morphology on Longitudinal Creep Properties of INCONEL MA 754 at Elevated Temperatures. 1307-1324A
- Stress corrosion cracking**  
 Investigation of Stress Corrosion Crack Growth in Magnesium Alloys Using J-Integral Estimations. 101-108A  
 Effect of Cold Work on Stress Corrosion Cracking Behavior of Types 304 and 316 Stainless Steels. 285-289A  
 Sulfide Stress Cracking of High Strength Modified Cr—Mo Steels. 935-944A  
 Effect of Cobalt Content on the Stress-Corrosion Cracking Behavior of 7091-Type Aluminum Powder Alloys. 945-951A  
 Crack Size Effects on the Chemical Driving Force for Aqueous Corrosion Fatigue. 953-969A  
 Stress Corrosion Cracking of Alpha—Beta Brass in Distilled Water and Sodium Sulfate Solutions. 971-978A  
 Stress Corrosion Cracking of Carbon Steel in Caustic Aluminate Solutions—Crack Propagation Studies. 979-986A  
 A Unified Mechanism of Stress Corrosion and Corrosion Fatigue Cracking. 1133-1141A  
 The Embrittlement of Al—Zn—Mg and Al—Mg Alloys by Water Vapor. 1503-1514A  
 Stress Corrosion Cracking of an Aluminum Alloy Under Compressive Stress. 1663-1670A  
 Stress Corrosion Cracking of  $\alpha$ -Brass in Waters With and Without Additions. 1671-1681A  
 Stress Corrosion Cracking of Stainless Steels. 1909-1923A  
 A Plastic Flow Induced Fracture Theory for  $K_{ISCC}$ . 2333-2340A
- Stress corrosion cracking, Microstructural effects**  
 The Effect of Microstructural Changes on the Caustic Stress Corrosion Cracking Resistance of a NiCrMoV Rotor Steel. 1333-1344A
- Stress corrosion resistance**  
 See Corrosion resistance
- Stress corrosion tests**  
 Stress Corrosion Cracking of Alpha—Beta Brass in Distilled Water and Sodium Sulfate Solutions. 971-978A  
 Stress Corrosion Cracking of Carbon Steel in Caustic Aluminate Solutions—Crack Propagation Studies. 979-986A
- Stress distribution**  
 See Stress concentration
- Stress relaxation**  
 Effect of Hydrogen on the Young's Modulus of Iron. 1655-1662A
- Stress relieving**  
 See Grain refinement
- Stress rupture strength**  
 See Creep rupture strength
- Stress strain curves**  
 Work Hardening Correlations Based on State Variables in Some F.C.C. Metals in Monotonic Loading. 411-420A  
 High Temperature Deformation of Ultra-Fine-Grained Oxide Dispersion Strengthened Alloys. 777-787A  
 Tensile Stress—Strain Analysis of Cold Worked Metals and Steels and Dual-Phase Steels. 865-872A  
 Mechanical Properties of a Low Alloy Steel in a Molten Nitrate Salt Environment. 1031-1041A  
 Temperature and Strain Rate Dependence of Stress—Strain Behavior in a Nickel-Base Superalloy. 1049-1067A  
 Some Trends Observed in the Elevated-Temperature Kinematic and Isotropic Hardening of Type 304 Stainless Steel. 1069-1076A  
 Analysis of Stress—Strain, Fracture, and Ductility Behavior of Aluminum Matrix Composites Containing Discontinuous Silicon Carbide Reinforcement. 1105-1115A  
 Effect of Strain Rate on the Flow Stress of Three Liquid Phase Sintered Tungsten Alloys. 2031-2037A  
 Hardening Behavior in Fatigue. 2201-2214A  
 A Simplified Numerical Analysis of the Sheet Tensile Test. 2291-2298A
- Stress strain curves, Deformation effects**  
 Measurement and Evaluation of the Anisothermal Softening of Austenite After Hot Deformation. 67-72A
- Stress strain curves, Microstructural effects**  
 Mechanical Properties of 0.40% C—Ni—Cr—Mo High-Strength Steel Having a Mixed Structure of Martensite and Bainite. 73-82A  
 A Theoretical Model for the Flow Behavior of Commercial Dual-Phase Steels Containing Metastable Retained Austenite. II.—Calculation of Flow Curves. 2023-2029A
- Stresses**  
 See Residual stress
- Stressing**  
 See Prestressing
- Stretch forming**  
 Effects of Plastic Anisotropy and Yield Surface Shape on Sheet Metal Stretchability. 629-639A

## Stretchability

### Stretchability

Effects of Plastic Anisotropy and Yield Surface Shape on Sheet Metal Stretchability.

629-639A

### Stretching

See Stretch forming

### Strong liquor

See Pregnant liquors

### Structural hardening

See Aging (artificial)

Precipitation hardening

Strain aging

Strain hardening

### Structural steels

See Rail steels

### Structure (atomic)

See Atomic structure

### Structures (crystalline)

See Banded structure

Crystal structure

Dendritic structure

Grain structure

Intergranular structure

Intragranular structure

Lamellar structure

Microstructure

Widmanstätten structure

### Submerged arc welding

Chemical Reactions During Submerged Arc Welding With

FeO—MnO—SiO<sub>2</sub> Fluxes.

237-245B

Hydrogen Attack Kinetics of 2.25 Cr—1 Mo Steel Weld Metals.

1143-1149A

### Submerged arc welds

See Welded joints

### Sulfates, Reduction (chemical)

Intrinsic Kinetics of the Hydrogen Reduction of Copper Sulfate: Determination by a Nonisothermal Technique.

397-401B

### Sulfidation (corrosion)

See Sulfurization

### Sulfides, Environment

Sulfide Stress Cracking of High Strength Modified Cr—Mo Steels.

935-944A

### Sulfides, Reduction (chemical)

Kinetics of the Reaction Between Hydrogen Sulfide and Lime Particles.

163-168B

Direct Reduction of Lead Sulfide With Carbon and Lime; Effect of Catalysts: I.—Experimental.

465-475B

Direct Reduction of Lead Sulfide With Carbon and Lime; Effect of Catalysts: II.—Analytical Model.

477-488B

Successive Gas—Solid Reaction Model for the Hydrogen Reduction of Cuprous Sulfide in the Presence of Lime.

645-662B

Intrinsic Kinetics of the Hydrogen Reduction of Cu<sub>2</sub>S.

831-839B

Thermodynamic Properties of S—Fe—Co—Ni and Fe—Co—Ni Systems.

907-911A

### Sulfur, Alloying additive

Reactive Element—Sulfur Interaction and Oxide Scale Adherence.

1164-1166A

### Sulfur, Binary systems

Phase Relationships and Thermodynamic Properties of the Pd—S System.

143-148B

Thermodynamics and Phase Relationships of Transition Metal—Sulfur Systems. V.—A Reevaluation of the Fe—S System Using an Associated Solution Model for the Liquid Phase.

277-285B

### Sulfur, Impurities

Trapping of Hydrogen by Sulfur-Associated Defects in Steel.

401-409A

Thermodynamic Properties of S—Fe—Co—Ni and Fe—Co—Ni Systems.

907-911A

### Sulfur, Sorption

An Effect of Chemisorbing Surface Reaction Poisons on the Transition From Internal to External Oxidation.

133-136A

### Sulfur, Ternary systems

Thermodynamics of the Ca—S—O, Mg—S—O, and La—S—O Systems at High Temperatures.

287-294B

The Co—Cr—S Ternary System at 1223K and Applications to Corrosion.

503-510A

### Sulfur compounds

See Sulfur dioxide

### Sulfur dioxide, Environment

Stress Corrosion Cracking of  $\alpha$ -Brass in Waters With and Without Additions.

1671-1681A

### Sulfuric acid leaching

Effect of Suspension Potential on the Oxidation Rate of Copper Concentrate in a Sulfuric Acid Solution.

695-705B

### Sulfurization

Sulfidation Under Atmospheric Conditions of Cu—Ni, Cu—Sn and Cu—Zn Binary and Cu—Ni—Sn and Cu—Ni—Zn Ternary Systems.

275-284A

Hot Corrosion of B-1900 in CaSO<sub>4</sub>/Na<sub>2</sub>SO<sub>4</sub> Salt Mixtures in Reducing Atmospheres.

291-297A

The Co—Cr—S Ternary System at 1223K and Applications to Corrosion.

503-510A

### Sulfurization, Alloying effects

Sulfation of Y<sub>2</sub>O<sub>3</sub> and HfO<sub>2</sub> in Relation to MCrAl Coatings.

303-306A

### Sulphur

See Sulfur

## Superalloys, Alloy development

Microstructural Development in High Volume Fraction Gamma Prime Ni-Base Oxide-Dispersion-Strengthened Superalloys.

1285-1294A

## Superalloys, Composite materials

Interdiffusional Effects Between Tungsten Fibers and an Iron—Nickel-Base Alloy.

1961-1968A

## Superalloys, Corrosion

Hot Corrosion of B-1900 in CaSO<sub>4</sub>/Na<sub>2</sub>SO<sub>4</sub> Salt Mixtures in Reducing Atmospheres.

291-297A

Sulfation of Y<sub>2</sub>O<sub>3</sub> and HfO<sub>2</sub> in Relation to MCrAl Coatings.

303-306A

## Superalloys, Crystal growth

Driving Force for Discontinuous Coarsening in a Ni—Al—Mo Base Superalloy.

11-16A

Superalloy Microstructural Variations Induced by Gravity Level During Directional Solidification.

1683-1687A

Rapid Solidification Characteristics in Melt Spinning a Nickel-Base Superalloy.

1773-1779A

## Superalloys, Directional solidification

Mechanical Properties and Microstructure of Centrifugally Cast Alloy 718.

1295-1306A

## Superalloys, Heat treatment

Carbide Stability in Nimonic 80A Alloy.

511-520A

Effect of Single Aging on Microstructure and Impact Property of INCONEL X-750.

821-829A

The Microstructural Response of Mill—Annealed and Solution—Annealed INCONEL 600 to Heat Treatment.

1225-1236A

## Superalloys, Mechanical properties

Dynamic Recrystallization During Creep in a 45% Ni—35% Fe—20% Cr Alloy System.

51-57A

High-Cycle Fatigue Properties of the ODS-Alloy MA 6000 at 850°C.

393-399A

Elevated Temperature Creep-Rupture Behavior of the Single Crystal Nickel-Base Superalloy NASAIR 100.

427-439A

Elastic Constants of a Monocrystalline Nickel-Base Superalloy.

661-665A

Effect of Inclusions on LCF Life of HIP Plus Heat Treated Powder Metal René 95.

775-784B

High Temperature Deformation of Ultra-Fine-Grained Oxide Dispersion Strengthened Alloys.

777-787A

Temperature and Strain Rate Dependence of Stress—Strain Behavior in a Nickel-Base Superalloy.

1049-1067A

A Model for Anelastic Relaxation Controlled Cyclic Creep. The Effect of Grain Morphology on Longitudinal Creep Properties of INCONEL MA 754 at Elevated Temperatures.

1117-1122A

High Cycle Fatigue and Fatigue Crack Growth of the Oxide Dispersion Strengthened Alloy MA 754.

1307-1324A

The Effects of Orientation and Thickness on the Notch—Tensile Creep Strength of Single Crystals of a Nickel-Base Superalloy.

1437-1444A

The Effect of Environment on the Sustained Load Crack Growth Rates of Forged Waspalloy.

1457-1466A

The Influence of Cobalt, Tantalum, and Tungsten on the Elevated Temperature Mechanical Properties of Single Crystal Nickel-Base Superalloys.

1515-1521A

Small-Angle Neutron Scattering Investigation of Creep Damage in Type 304 Stainless Steel and Alloy 800.

1863-1870A

Superalloys, Microstructure

The Influence of Cobalt, Tantalum, and Tungsten on the Microstructure of Single Crystal Nickel-Base Superalloys.

2283-2289A

## Superalloys, Phases (state of matter)

Atom-Probe Microanalysis of a Nickel-Base Superalloy.

1703-1711A

## Superalloys, Powder technology

The Substitution of Nickel for Cobalt in Hot Isostatically Pressed Powder Metallurgy UDIMET 700 Alloys.

993-1003A

## Superalloys, Structural hardening

Serrated Grain Boundary Formation Potential of Nickel-Based Superalloys and Its Implications.

17-26A

Oxide Dispersion Strengthened Nickel-Base Heat Resistant Alloys by Means of the Spray-Dispersion Method.

1043-1048A

Low Temperature Carbide Precipitation in a Nickel Base Superalloy.

1213-1223A

The Development of  $\gamma$ — $\gamma'$  Lamellar Structures in a Nickel-Base Superalloy During Elevated Temperature Mechanical Testing.

1969-1982A

Rhenium Additions to a Nickel-Base Superalloy: Effects on Microstructure.

1997-2005A

Precipitation Hardening.

2131-2165A

## Superalloys, Surface properties

Effects of Temperature and Environment on Fatigue Crack Growth in Ordered (Fe, Ni)<sub>3</sub>V-Type Alloys.

815-820A

## Superalloys, Surface properties

Superplastic Al—Cu—Li—Mg—Zr Alloys.

2319-2332A

## Surface alloying

Microstructure of Rapidly Solidified Laser Molten Al—4.5 wt. % Cu Surfaces.

149-161B

## Surface diffusion

See Diffusion

## Surface energy

The Contiguity of Liquid Phase Sintered Microstructures.

1247-1252A

## Surface hardening

See Carburizing

## Surface properties

See Surface tension

## Surface tension, Composition effects

Interfacial Tension of Aluminum in Cryolite Melts.

333-338B

- Swaging**  
Effect of Cold Work on Recrystallization Behavior and Grain Size Distribution in Titanium. 703-708A
- Systems (metallurgical)**  
See also Binary systems  
Quaternary systems  
Ternary systems
- Systems (metallurgical), Phases (state of matter)**  
Orthogonal Coordinates for Systems of Many Components. 929-933A
- Tantalum, Alloying elements**  
The Influence of Cobalt, Tantalum, and Tungsten on the Microstructure of Single Crystal Nickel-Base Superalloys. 1849-1862A  
The Influence of Cobalt, Tantalum, and Tungsten on the Elevated Temperature Mechanical Properties of Single Crystal Nickel-Base Superalloys. 1863-1870A
- Tantalum, Structural hardening**  
Short-Range Reordering of Heavy Interstitials in Ta, Nb, and Fe During Relaxation and Static Strain Aging. 361-366A
- Tapes (metallic), Microstructure**  
Orientation Relationship Between Precipitated  $Al_3(Fe,Ni)_2$  Phase and Alpha-Aluminum. 683-686A
- Technology transfer**  
Of Perspectives, Issues, and Politics in Materials Technology. 5-11B  
Of Perspectives, Issues, and Politics in Materials Technology. 311-317A
- Tellurium, Impurities**  
Thermodynamics of Removing Selenium and Tellurium From Liquid Copper by Sodium Carbonate Slags. 171-172B
- Temper brittleness**  
Embrittlement of Austempered Nodular Irons: Grain Boundary Phosphorus Enrichment Resulting From Precipitate Decomposition. 797-805A  
Variation of the Fracture Mode in Temper Embrittled 2.25 Cr-1 Mo Steel. 1325-1331A  
The Stability of Precipitated Austenite and the Toughness of 9Ni Steel. 2237-2249A
- Temper brittleness, Impurity effects**  
Carbide Precipitation, Grain Boundary Segregation, and Temper Embrittlement in NiCrMoV Rotor Steels. 721-737A
- Temperature**  
See Temperature distribution
- Temperature distribution**  
Distribution of the Heat and Current Fluxes in Gas Tungsten Arcs. 841-846B
- Temperature field**  
See Temperature distribution
- Tempering**  
The Effect of Microstructural Changes on the Caustic Stress Corrosion Cracking Resistance of a NiCrMoV Rotor Steel. Crystallography and Tempering Behavior of Iron-Nitrogen Martensite. 1333-1344A  
The Mechanical Stability of Precipitated Austenite in 9Ni Steel. 1371-1384A  
2251-2256A
- Tenacity**  
See Tensile strength
- Tensile modulus**  
See Modulus of elasticity
- Tensile properties**  
See also Elongation  
Tensile strength  
Yield strength  
Discussion of "Deformation Kinetics of Commercial Ti-50A (0.5 at.% Oeq) at Low Temperatures ( $T < 0.3 T_m$ )" and Authors Reply. 694-697A  
Oxide Dispersion Strengthened Nickel-Base Heat Resistant Alloys by Means of the Spray-Dispersion Method. 1043-1048A  
Analysis of Stress-Strain, Fracture, and Ductility Behavior of Aluminum Matrix Composites Containing Discontinuous Silicon Carbide Reinforcement. 1105-1115A  
Correlation of Microstructure and Fracture Toughness in Two 4340 Steels. 1633-1648A
- Tensile properties, Alloying effects**  
Effect of Silicide Precipitation on Tensile Properties and Fracture of Alloy Ti-6Al-5Zr-0.5Mo-0.25Si. 227-231A  
The Substitution of Nickel for Cobalt in Hot Isostatically Pressed Powder Metallurgy UDIMET 700 Alloys. 993-1003A
- Tensile properties, Cooling effects**  
Mechanical Properties and Microstructure of Centrifugally Cast Alloy 718. 1295-1306A
- Tensile properties, Deformation effects**  
Effect of Finish Rolling Temperature on the Structure and Properties of Directly Quenched Nb Containing Low Steel. Product Microstructures and Properties Induced by Hot Working at Pb-1.85% Sb Alloy. 471-474A  
1273-1285A
- Tensile properties, Heating effects**  
The Development of Two Texture Variants and Their Effect on the Mechanical Behavior of a High Strength P/M Aluminum Alloy, X7091. 1089-1103A
- Tensile properties, Low temperature effects**  
Low Temperature Mechanical Behavior of Microalloyed and Controlled-Rolled Fe-Mn-Al-C-X Alloys. 1689-1693A
- Tensile properties, Microstructural effects**  
Mechanical Properties of 0.40% C-Ni-Cr-Mo High-Strength Steel Having a Mixed Structure of Martensite and Bainite. 73-82A
- Microstructure and Mechanical Properties of Fe-Ni-Cr-Al Steel Wires Produced by In-Rotating-Water Spinning Method. 215-226A  
The Dependence of Some Tensile and Fatigue Properties of a Dual-Phase Steel on its Microstructure. 1405-1415A  
Discussion of "Enhanced Tensile Strength for Electrodeposited Nickel-Copper Multilayer Composites". 1693A
- Tensile shear strength**  
See Shear strength
- Tensile strength**  
Mechanical Properties and Failure Characteristics of FP/Aluminum and W/Aluminum Composites. 853-864A
- Tensile strength, Composition effects**  
The Influence of Cobalt, Tantalum, and Tungsten on the Elevated Temperature Mechanical Properties of Single Crystal Nickel-Base Superalloys. 1863-1870A
- Tensile strength, Environmental effects**  
Stress Corrosion Cracking of Alpha-Beta Brass in Distilled Water and Sodium Sulfate Solutions. 971-978A  
Mechanical Properties of a Low Alloy Steel in a Molten Nitrate Salt Environment. 1031-1041A
- Tensile strength, Heating effects**  
Embrittlement of Austempered Nodular Irons: Grain Boundary Phosphorus Enrichment Resulting From Precipitate Decomposition. 797-805A
- Tensile strength, Microstructural effects**  
Effect of Carbon Content and Ferrite Grain Size on the Tensile Flow Stress of Ferritic Spheroidal Graphite Cast Iron. Effects of Temperature and Environment on Fatigue Crack Growth in Ordered (Fe, Ni)<sub>3</sub> V-Type Alloys. 815-820A  
Microstructure-Mechanical Property Relationships of Dual-Phase Steel Wire. 831-840A
- Tensile strength, Stress effects**  
Tensile Stress-Strain Analysis of Cold Worked Metals and Steels and Dual-Phase Steels. 965-972A
- Tensile tests**  
See Tension tests
- Tensile yield strength**  
See Yield strength
- Tension**  
See Surface tension
- Tension tests**  
Hill's Plastic Strain Ratio of Sheet Metals. 1531-1535A  
A Simplified Numerical Analysis of the Sheet Tensile Test. 2291-2298A  
An Analysis of the Nonisothermal Tensile Test. 2299-2308A
- Ternary systems**  
On the Arrangement of Monovariant Lines in Two-Dimensional Potential Phase Diagrams. 137-139A  
Isothermal Para-Equilibrium Phase Diagrams for Ternary Systems. 139-142A
- Ternary systems, Phases (state of matter)**  
Role of Alloying Elements in Phase Decomposition in Alnico Magnet Alloys. 179-185A  
Thermodynamics of the Ca-S-O, Mg-S-O, and La-S-O Systems at High Temperatures. 287-294B  
Phase Equilibria in the Ni-Al-Ti System at 1173K. 319-322A  
New Eutectic Alloys and Their Heats of Transformation. 323-328A  
The Co-Cr-S Ternary System at 1223K and Applications to Corrosion. 503-510A  
Correction to "Phase Relationships in the Fe-Cr-C System at Solidification Temperatures". 662B  
Effect of Magnetic Transition on Solubility of Carbon in B.C.C. Iron and F.C.C. Co-Ni Alloys. 913-921A  
Phases in Ni-Co-Ga Alloys Close to (Ni, Co)<sub>0.5</sub>Ga<sub>0.5</sub>. 1159-1160A  
Thermodynamics of the Fe-Cr-C System at 985K. 1479-1490A  
The Fe-Rich Corner of the Metastable C-Cr-Fe Liquidus Surface. 1541-1549A
- Tertiary displacements**  
See Displacements (lattice)
- Texture**  
A New Method for Determining the Defocusing Correction for Crystallographic Texture Measurement. 299-300A
- Texture, Heating effects**  
The Development of Two Texture Variants and Their Effect on the Mechanical Behavior of a High Strength P/M Aluminum Alloy, X7091. 1089-1103A
- Thermal capacity**  
See Specific heat
- Thermal flux**  
See Heat transmission
- Thermal properties**  
See Heat of formation  
Heat of fusion  
Heat of mixing  
Specific heat  
Vapor pressure
- Thermal reduction**  
See Flash smelting  
Fluidized bed reduction
- Thermochemistry**  
Thermochemistry of Binary Liquid Gold Alloys: the Systems (Gold + Chromium), (Gold + Vanadium), (Gold + Titanium) and (Gold + Scandium) at 1379K. 93-99A

## Thermodynamics

### Thermodynamics

- The Utilization of Galvanic Cells Using Ca Beta Double Prime—Alumina Solid Electrolytes in a Thermodynamic Investigation of the  $\text{CaO}-\text{Al}_2\text{O}_3$  System. 107-112B
- Thermodynamics of the  $\text{Ca}-\text{S}-\text{O}$ ,  $\text{Mg}-\text{S}-\text{O}$ , and  $\text{La}-\text{S}-\text{O}$  Systems at High Temperatures. 287-294B
- Thermodynamic Stabilities of Some Beta and Beta Double Prime Aluminas. 295-301B
- Water and Solute Activities of  $\text{H}_2\text{SO}_4-\text{Fe}_2(\text{SO}_4)_3-\text{H}_2\text{O}$  and  $\text{HCl}-\text{FeCl}_3-\text{H}_2\text{O}$  Solution Systems: I.—Activities of Water. 433-439B
- Solute Interactions in Multicomponent Solutions. 807-813B
- Thermodynamic Properties of  $\text{S}-\text{Fe}-\text{Co}-\text{Ni}$  and  $\text{Fe}-\text{Co}-\text{Ni}$  Systems. 907-911A
- Orthogonal Coordinates for Systems of Many Components. Thermodynamics of Formation of  $\text{Y}-\text{Co}$  Alloys. 929-933A
- Thermodynamics of the  $\text{Fe}-\text{Cr}-\text{C}$  System at 985K. 1195-1201A
- Discussion of "A Thermodynamic Analysis of the  $\text{Fe}-\text{C}$  and the  $\text{Fe}-\text{N}$  Phase Diagrams" and Author's Reply. 1479-1490A
- 2063-2065A
- Thermodynamics, Composition effects**  
A Two-Sublattice Model for Molten Solutions With Different Tendency for Ionization. 261-266A
- Thermodynamics, Field effects**  
Magnetic Contributions to the Thermodynamic Functions of Pure Nickel, Cobalt and Iron. 153-165A
- Thermomechanical treatment**  
See also Controlled rolling  
Effect of Finish Rolling Temperature on the Structure and Properties of Directly Quenched Nb Containing Low Steel. The Development of Two Texture Variants and Their Effect on the Mechanical Behavior of a High Strength P/M Aluminum Alloy, X7091. 471-474A
- 1089-1103A
- Thermomechanical Processing of Microalloyed Powder Forged Steels and a Cast Vanadium Steel. 1599-1606A
- Improvement of Strength and Electrical Conductivity of Copper Alloy by Means of Thermo-Mechanical Treatment. 2073-2077A
- Thin films, Crystal growth**  
Isotope Separation During Thin Film Compound Growth. 142-144A
- Tig arc welding**  
See Gas tungsten arc welding
- Tilting furnaces**  
See Basic converters
- Tin, Alloying elements**  
Sulfidation Under Atmospheric Conditions of  $\text{Cu}-\text{Ni}$ ,  $\text{Cu}-\text{Sn}$  and  $\text{Cu}-\text{Zn}$  Binary and  $\text{Cu}-\text{Ni}-\text{Sn}$  and  $\text{Cu}-\text{Ni}-\text{Zn}$  Ternary Systems. 275-284A
- Tin, Binary systems**  
The Correlation of the Thermodynamic Properties and Phase Diagram of the System  $\text{Ti}-\text{Lead}$  Using a Gaussian Plus Krupkowski Formalism. 91-96B
- Tin, Chemical analysis**  
A New Type of Oxygen Analyzer Utilizing a Potentiostatic Coulometric Titration Technique. 113-119B
- Tin, Crystal growth**  
The Influence of Convection on Heat Transfer in Liquid Tin. 355-357B
- Tin, Impurities**  
Carbide Precipitation, Grain Boundary Segregation, and Temper Embrittlement in  $\text{NiCrMoV}$  Rotor Steels. 721-737A
- Tin bronzes**  
See Phosphor bronzes
- Tin plate, Sorption**  
The Use of Palladium to Obtain Reproducible Boundary Conditions for Permeability Measurements Using Galvanostatic Charging. 715-719A
- Titanium, Alloying additive**  
Sulfide Stress Cracking of High Strength Modified  $\text{Cr}-\text{Mo}$  Steels. 935-944A
- Correlation of Microstructure and Fracture Toughness in Two 4340 Steels. 1633-1648A
- Titanium, Alloying elements**  
Effects of Hydrogen on Some Mechanical Properties of Vanadium—Titanium Alloys. 59-66A
- Isopiestic Solubility of Hydrogen in Vanadium Alloys at Low Temperatures. 387-374A
- Nitrogen Solubility and Nitride Formation in Austenitic  $\text{Fe}-\text{Ti}$  Alloys. 815-822B
- Titanium, Crystal growth**  
Effect of Cold Work on Recrystallization Behavior and Grain Size Distribution in Titanium. 703-708A
- Titanium, Crystal lattices**  
On the Relation Between Grain Size and Grain Topology. 2007-2011A
- Titanium, Diffusion**  
Inverse Segregation in Directionally Solidified  $\text{Al}-\text{Cu}-\text{Ti}$  Alloys With Equiaxed Grains. 579-587A
- Titanium, Mechanical properties**  
Adiabatic Shear Localization in Titanium and  $\text{Ti}-6\text{Al}-4\text{V}$  Alloy. 761-775A
- Hill's Plastic Strain Ratio of Sheet Metals. 1531-1535A
- Titanium, Powder technology**  
The Influence of Strain Rate and Porosity on the Deformation and Fracture of Titanium and Nickel. 2273-2281A
- Titanium, Ternary systems**  
Phase Equilibria in the  $\text{Ni}-\text{Al}-\text{Ti}$  System at 1173K. 319-322A
- Titanium, Welding**  
Fundamental Aspects of Formation and Stability of Explosive Welds. 841-852A

### Titanium base alloys, Mechanical properties

- The Effect of Cold Rolling on the Fatigue Properties of  $\text{Ti}-6\text{Al}-4\text{V}$ . 144-145A
- Effect of Silicide Precipitation on Tensile Properties and Fracture of Alloy  $\text{Ti}-6\text{Al}-5\text{Zr}-0.5\text{Mo}-0.25\text{Si}$ . 227-231A
- Discussion of "Deformation Kinetics of Commercial  $\text{Ti}-50\text{A}$  (0.5 at.% Oeq) at Low Temperatures ( $T < 0.3 T_m$ )" and Authors Reply. 694-697A
- Microstructural Influences on Fatigue Crack Propagation in  $\text{Ti}-10\text{V}-2\text{Fe}-3\text{Al}$ . 739-751A
- Adiabatic Shear Localization in Titanium and  $\text{Ti}-6\text{Al}-4\text{V}$  Alloy. 761-775A
- Deformation Characteristics in Beta Phase  $\text{Ti}-\text{Nb}$  Alloys. 789-795A
- The Effect of Hydrogen as a Temporary Alloying Element on the Microstructure and Tensile Properties of  $\text{Ti}-6\text{Al}-4\text{V}$ . 1077-1087A
- Titanium base alloys, Metal working**  
Effects of Plastic Anisotropy and Yield Surface Shape on Sheet Metal Stretchability. 629-639A
- Titanium base alloys, Microstructure**  
The Effect of Cooling Conditions on the Microstructure of Rapidly Solidified  $\text{Ti}-6\text{Al}-4\text{V}$ . 1951-1959A
- Titanium base alloys, Phase transformations**  
X-Ray Diffraction and Resistivity Studies of Titanium—Molybdenum Alloys. 187-195A
- Titanium base alloys, Powder technology**  
Thermally Induced Porosity in  $\text{Ti}-6\text{Al}-4\text{V}$  Prealloyed Powder Compacts. 1526-1531A
- Microporosity in Hot Isostatically Pressed  $\text{Ti}-6\text{Al}-4\text{V}$  Powder Compacts. 1831-1834A
- Laser-Melting/Spin-Atomization Method for the Production of Titanium Alloy Powders. 1897-1900A
- Titanium base alloys, Structural hardening**  
Orientation Relationship Between Alpha Prime Titanium and Silicide  $\text{S}_2$  in Alloy  $\text{Ti}-6\text{Al}-5\text{Zr}-0.5\text{Mo}-0.25\text{Si}$ . 453-455A
- Polycrystalline Strengthening. 2167-2190A
- Titanium base alloys, Welding**  
Discussion of "Microstructural and Mechanical Properties of a Welded Titanium Alloy" and Authors' Reply. 987A
- Titanium ores, Reduction (chemical)**  
Formation of Chlorinated Carbon Products During Carbochlorination Reactions. 847-849B
- Tokamak devices**  
The Effect of Pressure Modulation on the Flow of Gas Through a Solid Membrane: Surface Inhibition and Internal Traps. 1013-1024A
- Tool steels**  
See Die steels  
High speed tool steels  
Hot work tool steels
- Tools**  
See High speed tool steels
- Torsional strength**  
See Shear strength
- Toughness**  
See Fracture toughness  
Notch toughness
- Transferring**  
See Heat transfer
- Transformation entropy**  
See Entropy of transformation
- Transformations (materials)**  
See Allotropic transformation  
Martensitic transformations  
Massive type transformation  
Phase transformations
- Transformer steels**  
See Electrical steels
- Transition metal alloys**  
See Cobalt base alloys  
Ferrous alloys  
Manganese base alloys  
Molybdenum base alloys  
Nickel base alloys  
Niobium base alloys  
Titanium base alloys  
Tungsten base alloys  
Vanadium base alloys  
Zirconium base alloys
- Transition metal compounds**  
See Molybdenum compounds  
Nickel compounds  
Tungsten carbide  
Vanadium compounds  
Zirconium compounds
- Transition metals**  
See also Chromium  
Cobalt  
Hafnium  
Iron  
Manganese  
Molybdenum  
Nickel  
Niobium  
Palladium  
Platinum  
Rhenium



- Tantalum  
Titanium  
Tungsten  
Vanadium  
Yttrium  
Zirconium
- Transition metals, Extraction**  
Hydrolytic Stripping of Single and Mixed Metal—Versatile Solutions. 671-677B
- Transition metals, Structural hardening**  
Polycrystalline Strengthening. 2167-2190A
- Transmission**  
See Heat transmission
- Transmission electron microscopy**  
The Microstructure of Rapidly Solidified  $Al_6Mn$ . 1005-1012A  
Dislocation Structures of Monocrystalline Copper During Corrosion Fatigue in 0.1 M Perchloric Acid. 1151-1157A
- Transmission gears**  
See Gears
- Traps**  
Identification of Defects Generated During Cathodic Charging in Pure Iron by Thermal Analysis Technique. 468-471A
- Tubes, Mechanical properties**  
Mechanical Properties and Failure Characteristics of FP/Aluminum and W/Aluminum Composites. 853-864A
- Tubing (metal), Materials substitution**  
Mathematical Modeling of Thermal Stresses in Basic Oxygen Furnace Hood Tubes. 247-261B
- Tubular goods**  
See Pipe  
Tubes  
Tubing (metal)
- Tungsten, Alloying elements**  
The Influence of Cobalt, Tantalum, and Tungsten on the Microstructure of Single Crystal Nickel-Base Superalloys. 1849-1862A  
The Influence of Cobalt, Tantalum, and Tungsten on the Elevated Temperature Mechanical Properties of Single Crystal Nickel-Base Superalloys. 1863-1870A
- Tungsten, Composite materials**  
Mechanical Properties and Failure Characteristics of FP/Aluminum and W/Aluminum Composites. 853-864A  
Interdiffusional Effects Between Tungsten Fibers and an Iron—Nickel-Base Alloy. 1961-1968A
- Tungsten arc welding**  
See Gas tungsten arc welding
- Tungsten base alloys, Mechanical properties**  
Effect of Strain Rate on the Flow Stress of Three Liquid Phase Sintered Tungsten Alloys. 2031-2037A
- Tungsten base alloys, Powder technology**  
Effect of Dihedral Angle on the Morphology of Grains in a Matrix Phase. 923-928A
- Tungsten carbide, Composite materials**  
Binder Deformation in WC—(Co, Ni) Cemented Carbide Composites. 2309-2317A
- Tungsten compounds**  
See Tungsten carbide
- Turbine blades**  
Elastic Constants of a Monocrystalline Nickel-Base Superalloy. 661-665A  
The Effect of Grain Morphology on Longitudinal Creep Properties of INCONEL MA 754 at Elevated Temperatures. 1307-1324A  
The Effects of Orientation and Thickness on the Notch-Tensile Creep Strength of Single Crystals of a Nickel-Base Superalloy. 1457-1466A
- Turbine blades, Corrosion**  
Sulfation of  $Y_2O_3$  and  $HfO_2$  in Relation to MCrAl Coatings. 303-306A
- Turbine disks, Materials selection**  
The Substitution of Nickel for Cobalt in Hot Isostatically Pressed Powder Metallurgy UDIMET 700 Alloys. 993-1003A
- Turbine disks, Service life**  
The Effect of Environment on the Sustained Load Crack Growth Rates of Forged Waspaloy. 1515-1521A
- Turbines**  
See Gas turbines
- Turbulent flow**  
Turbulent Fluid Flow Phenomena in a Water Model of an AOD System. 67-75B  
Hydrodynamic Modeling of Some Gas Injection Procedures in Ladle Metallurgy Operations. 83-90B
- Twinning**  
Heterogeneous Nucleation Model of Twinned Crystal Growth From the Melt. 690-692A  
Transformation Behavior of Nearly Stoichiometric Ni—Mn Alloys. 1567-1579A  
Electron Microscopic Study of  $\beta$ -Phase Martensite in Ni—Mn Alloys. 1581-1597A
- Twinning, Composition effects**  
Deformation Characteristics in Beta Phase Ti—Nb Alloys. 789-795A
- Ultimate shear strength**  
See Shear strength
- Ultimate tensile strength**  
See Tensile strength
- Uranium, Bonding**  
Pressure Effects in Multiphase Binary Diffusion Couples. 605-611A
- Uranium, Diffusion**  
Microstructural Investigation of Intermediate Phase Formation in Uranium—Aluminum Diffusion Couples. 589-595A
- Uranium, Extraction**  
Catalytic Decomposition of Hydrogen Peroxide by Ferric Ion in Dilute Sulfuric Acid Solutions. 181-186B  
The Solubility of Barium Arsenate: Sherritt's Barium Arsenate Process. 404-406B  
Correction to "The Solubility of Barium Arsenate: Sherritt's Barium Arsenate Process". 662B
- Vanadium, Alloying additive**  
Sulfide Stress Cracking of High Strength Modified Cr—Mo Steels. 935-944A
- Vanadium, Alloying elements**  
Carbide Precipitation, Grain Boundary Segregation, and Temper Embrittlement in NiCrMoV Rotor Steels. 721-737A  
Low Temperature Mechanical Behavior of Microalloyed and Controlled-Rolled Fe—Mn—Al—C—X Alloys. 1689-1693A
- Vanadium base alloys, Mechanical properties**  
Effects of Hydrogen on Some Mechanical Properties of Vanadium—Titanium Alloys. 59-66A
- Vanadium base alloys, Solubility**  
Isopiestic Solubility of Hydrogen in Vanadium Alloys at Low Temperatures. 367-374A
- Vanadium compounds, Crystal growth**  
Growth Kinetics and Morphology of Grain Boundary Ferrite Allotriomorphs in an Fe—C—V Alloy. 521-527A
- Vapor deposition**  
The Ga—As—H—Cl Vapor Phase Epitaxial Growth System. 97-105B
- Vapor pressure**  
Thermodynamic Study of  $Na_2O$ — $SiO_2$  Melts at 1300 and 1400°C. 313-323B
- Vaporizing**  
See Coal gasification
- Vapors**  
See Water vapor
- Vessels**  
See Pressure vessels
- Water**  
See also Sea water
- Water, Environment**  
Stress Corrosion Cracking of  $\alpha$ -Brass in Waters With and Without Additions. 1671-1681A
- Water vapor, Environment**  
The Embrittlement of Al—Zn—Mg and Al—Mg Alloys by Water Vapor. 1503-1514A
- Water vapor, Solubility**  
Determination and Prediction of Water Vapor Solubilities in CaO—MgO— $SiO_2$  Slags. 61-66B
- Wear**  
See Hot gas corrosion
- Weld defects**  
Grain Structure and Solidification Cracking in Oscillated Arc Welds of 5052 Aluminum Alloy. 1345-1352A  
Alternating Grain Orientation and Weld Solidification Cracking. 1867-1896A
- Weld metal**  
Fluid Flow and Weld Penetration in Stationary Arc Welds. 203-213A
- Weld metal, Reactions (chemical)**  
Chemical Reactions During Submerged Arc Welding With FeO—MnO— $SiO_2$  Fluxes. 237-245B
- Weldability**  
Alternating Grain Orientation and Weld Solidification Cracking. 1867-1896A
- Weldability, Composition effects**  
Fundamental Aspects of Formation and Stability of Explosive Welds. 841-852A
- Welded joints, Corrosion**  
Hydrogen Attack Kinetics of 2.25 Cr—1 Mo Steel Weld Metals. 1143-1149A
- Welded joints, Mechanical properties**  
Alternating Grain Orientation and Weld Solidification Cracking. 1867-1896A
- Welded joints, Metallography**  
The Concept of an Effective Quench Temperature and Its Use in Studying Elevated-Temperature Microstructures. 1521-1523A
- Welded joints, Microstructure**  
Discussion of "Microstructural and Mechanical Properties of a Welded Titanium Alloy" and Authors' Reply. 967A
- Welding**  
See Diffusion welding  
Explosive welding  
Gas tungsten arc welding  
Laser beam welding  
Shielded metal arc welding  
Submerged arc welding
- Welding fluxes, Reactions (chemical)**  
Chemical Reactions During Submerged Arc Welding With FeO—MnO— $SiO_2$  Fluxes. 237-245B

## Welds

### Welds

See Welded joints

### Widmanstätten structure

Coarsening Rate of Beta Precipitates in Al—11Mg Alloy. 709-713A  
Austenitization During Intercritical Annealing of an Fe—C—Si—Mn Dual-Phase Steel. 1237-1245A

### Widmanstätten structure, Cooling effects

Microstructural and Microchemical Aspects of the Solid-State Decomposition of Delta Ferrite in Austenitic Stainless Steels. 1363-1369A

### Wire

See also Piano wire

### Wire, Mechanical properties

Microstructure—Mechanical Property Relationships of Dual-Phase Steel Wire. 831-840A

### Wire drawing

Microstructure—Mechanical Property Relationships of Dual-Phase Steel Wire. 831-840A

### Wire products

See Piano wire

### Wolfram

See Tungsten

### Work hardenability

See Strain hardenability

### Work hardening

See Strain hardening

### Work softening

See Strain softening

### Work strengthening

See Strain hardening

### Workability

See Formability

### Wustite, Reduction (chemical)

Correction to "The Breakdown of Dense Iron Layers on Wustite in CO/CO<sub>2</sub> and H<sub>2</sub>/H<sub>2</sub>O Systems". 857B  
Correction to "Establishment of Product Morphology During the Initial Stages of Wustite Reduction". 857B

### X ray analysis

See X ray diffraction  
X ray powder diffraction

### X ray diffraction

See also X ray powder diffraction  
A New Method for Determining the Defocusing Correction for Crystallographic Texture Measurement. 299-300A

### X ray diffractometer

See X ray diffraction

### X ray powder analysis

See X ray powder diffraction

### X ray powder diffraction

Phases in Ni—Co—Ga Alloys Close to (Ni, Co)<sub>0.5</sub>Ga<sub>0.5</sub>. 1159-1160A

### X ray powder diffraction, Crystal lattices

An X-Ray Diffraction Line Profile of Cold-Worked Hexagonal Alloys Zn—Ag: η and ε Phase. 1427-1435A

### X ray powder photography

See X ray powder diffraction

### Yield strength

Mechanical Properties and Failure Characteristics of FP/Aluminum and W/Aluminum Composites. 853-864A  
Some Trends Observed in the Elevated-Temperature Kinematic and Isotropic Hardening of Type 304 Stainless Steel. 1069-1076A  
Effect of Strain Rate on the Flow Stress of Three Liquid Phase Sintered Tungsten Alloys. 2031-2037A

### Yield strength, Composition effects

Effect of Carbon Content and Ferrite Grain Size on the Tensile Flow Stress of Ferritic Spheroidal Graphite Cast Iron. 667-673A

### Yield strength, Deformation effects

Measurement and Evaluation of the Anisothermal Softening of Austenite After Hot Deformation. 67-72A

### Yield strength, Diffusion effects

Hydrogen Degradation of Spheroidized AISI 1090 Steel. 1417-1425A

### Yield strength, Heating effects

Modified Heat Treatment for Lower Temperature Improvement of the Mechanical Properties of Two Ultra-High-Strength Low-Alloy Steels. 83-91A  
Embrittlement of Austempered Nodular Irons: Grain Boundary Phosphorus Enrichment Resulting From Precipitate Decomposition. 797-805A  
Discussion of "Effect of Retrogression and Reaging Treatments on the Microstructure of Al-7075-T651". 2068A

### Yield strength, Impurity effects

Correlation of Microyield Behavior With Silicon in X-520 and HP-50 Beryllium. 807-814A

### Yield strength, Microstructural effects

Microstructural Influences on Fatigue Crack Propagation in Ti—10V—2Fe—3Al. 739-751A  
Influence of Microstructure on Fatigue Crack Initiation in Fully Pearlitic Steels. 753-760A  
Effects of Temperature and Environment on Fatigue Crack Growth in Ordered (Fe, Ni)<sub>2</sub>V-Type Alloys. 815-820A  
Microstructure—Mechanical Property Relationships of Dual-Phase Steel Wire. 831-840A

The Effect of Hydrogen as a Temporary Alloying Element on the Microstructure and Tensile Properties of Ti—6Al—4V. 1077-1087A

A Theoretical Model for the Flow Behavior of Commercial Dual-Phase Steels Containing Metastable Retained Austenite. I.—Derivation of Flow Curve Equations. 2013-2021A

A Theoretical Model for the Flow Behavior of Commercial Dual-Phase Steels Containing Metastable Retained Austenite. II.—Calculation of Flow Curves. 2023-2029A

The Influence of Strain Rate and Porosity on the Deformation and Fracture of Titanium and Nickel. 2273-2281A

### Yield strength, Stress effects

Tensile Stress—Strain Analysis of Cold Worked Metals and Steels and Dual-Phase Steels. 865-872A

### Yield strength, Temperature effects

Temperature and Strain Rate Dependence of Stress—Strain Behavior in a Nickel-Base Superalloy. 1049-1067A

### Yield stress

See Yield strength

### Young's modulus

See Modulus of elasticity

### Yttrium, Alloying additive

Reactive Element—Sulfur Interaction and Oxide Scale Adherence. 1164-1166A

### Yttrium, Alloying elements

Sulfation of Y<sub>2</sub>O<sub>3</sub> and HfO<sub>2</sub> in Relation to MCrAl Coatings. 303-306A

### Yttrium, Binary systems

Thermodynamics of Formation of Y—Ni Alloys. 577-584B  
Thermodynamics of Formation of Y—Co Alloys. 1195-1201A

### Zinc, Alloying elements

Sulfidation Under Atmospheric Conditions of Cu—Ni, Cu—Sn and Cu—Zn Binary and Cu—Ni—Sn and Cu—Ni—Zn Ternary Systems. 275-284A

### Zinc, Diffusion

Quaternary Diffusion in the Cu—Ni—Zn—Mn System at 775°C. 1123-1132A

### Zinc, Extraction

The Kinetics of Dissolution of Sphalerite in Ferric Chloride Solution. 413-424B  
Kinetics of the Zinc Slag-Fuming Process. I.—Industrial Measurements. 513-527B  
Kinetics of the Zinc Slag-Fuming Process. II.—Mathematical Model. 529-540B  
Kinetics of the Zinc Slag-Fuming Process. III.—Model Predictions and Analysis of Process Kinetics. 541-549B  
Kinetics of Bio-Chemical Leaching of Sphalerite Concentrate. 667-670B  
Reaction Mechanism for the Ferric Chloride Leaching of Sphalerite. 715-724B

### Zinc base alloys, Crystal lattices

An X-Ray Diffraction Line Profile of Cold-Worked Hexagonal Alloys Zn—Ag: η and ε Phase. 1427-1435A

### Zinc ores

See Sphalerite

### Zirconium, Alloying additive

On the Improvement of Creep Strength and Ductility of Ni—20% Cr by Small Zirconium Additions. 651-660A

### Zirconium, Alloying elements

Superplastic Al—Cu—Li—Mg—Zr Alloys. 2319-2332A

### Zirconium base alloys, Crystal lattices

A New Method for Determining the Defocusing Correction for Crystallographic Texture Measurement. 299-300A

### Zirconium base alloys, Mechanical properties

The Influence of Multiaxial States of Stress on the Hydrogen Embrittlement of Zirconium Alloy Sheet. 675-681A  
Discussion of "Deformation Kinetics of Commercial Ti-50A (0.5 at.% Oeq) at Low Temperatures (T < 0.3 T<sub>m</sub>)" and Authors Reply. 694-697A

### Zirconium compounds, Reduction (chemical)

Formation of Chlorinated Carbon Products During Carbochlorination Reactions. 847-849B

